TRAJECTORY DESIGN FOR SOLAR SAILING FROM LOW-EARTH ORBIT TO THE MOON

by

Thomas A. Fekete
Ingénieur de L' Ecole Nationale Supérieure de L' Aéronautique et
de L' Espace
(1990)

Submitted to the Department of Aeronautics and Astronautics in
Partial Fulfillment of the Requirements for the Degree of

MASTER OF SCIENCE
in Aeronautics and Astronautics

at the

Massachusetts Institute of Technology

September 1991

Signature of Author _____
Department of Aeronautics and Astronautics
September 6, 1991

Approved by _____
Lester L. Sackett
Technical supervisor, The Charles Stark Draper Laboratory, Inc.

Certified by _____
Professor Andreas von Flotow
Thesis supervisor, Deparment of Aeronautics and Astronautics

Accepted by _____
Professor Harold Y. Wachman
Chairman, Department Graduate Committee

TRAJECTORY DESIGN FOR SOLAR SAILING FROM LOW-EARTH ORBIT TO THE MOON

by

Thomas A. Fekete

Submitted to the Department of Aeronautics and Astronautics on September 6, 1991 in partial fulfillment of the requirements for the degree of Master of Science.

ABSTRACT

This thesis presents a trajectory design for a solar sail journey from low-Earth orbit to an intercept location behind the Moon. The very weak thrust level (6. 10^{-5} g_0) induces extremely slow variations of the orbital parameters near the Earth.

In a first part, it is intended to leave the Earth's vicinity where the solar thrust/Earth attraction ratio is very small (less than 0.05). Averaging methods and basic orbital dynamics are used to define an efficient strategy to increase the semi major axis and bring the sail's trajectory into the Moon's orbital plane.

In a second part, unaveraged dynamics of the sail are considered to define an optimal control problem: minimize the time to bring the sail from a high-Earth orbit to a given intercept position behind the Moon.

Suboptimal trajectories are computed for various initial positions of the Moon and several simulations show the design performances.

Thesis Supervisor: Dr. Andreas von Flotow
Title: Associate Professor of Aeronautics and Astronautics

ACKNOWLEDGEMENTS

I would like to express my deep appreciation to Professor Andreas von Flotow for his guidance through-out the course of this study. His original ideas on orbital dynamics prevented this thesis from being a large and somewhat cumbersome numerical work. I wish to thank him for his kindness and help in hiring me as a research assistant on this project.

I am also especially grateful to Mr. Lester L. Sackett from the Charles Stark Draper Laboratory Inc. for his continuous interest in my work. The many questions and arguments he advanced helped me make my first steps in the field of trajectory optimization.

My final thanks go to MIT for the experience I have lived during this year.

TABLE OF CONTENTS

Appendices

Figures

Tables

Tables

INTRODUCTION

CHAPTER I

SOLAR SAILING BASICS

1.1. Historical review of solar sailing

Solar pressure is an effect of the Sun radiation on surfaces of materials. In space, this phenomenon induces significant forces that have been studied since the earliest days of space exploration.

At that time, the National Aeronautics and Space Administration (NASA) had small needles of metal launched in the ionosphere in order to study wave transmission in space environment. Whether or not solar pressure would push the needles down to Earth and make them burn in the atmosphere was a quite controversial issue at the time. When this actually happened, the effects of solar pressure were confirmed and practical evidence of this new force was provided.

As early as in the 1920's, two soviet pioneers of Astronautics: Konstantin Tsiolkovsky and Fridrich Arturovich Tsander had fancied "spacecrafts with large mirrors being driven by the pressure of sunlight" (reference [1] and [2]). However, until the mid 1950's, most papers dealing with solar sails were considered in the realm of science-fiction and the

subject had not yet found enough credibility to allow serious studies to be undertaken.

NASA began examining specific designs and technology issues related to solar sails in the mid 1960's, when the Apollo missions were diverting huge budgets to the space agency. However, after the tremendous success of the first human exploration of the Moon, the space program began to shrink and so did research projects on solar sailing.

In the late 1970's, a mission was planned to rendez-vous with Halley's comet. Jerome Wright found this was a good opportunity for a solar sail trajectory and hence the first mission analysis was undertaken (reference [3]). At the time (1976-1977), Dr. Bruce Murray was director of the Jet Propulsion Laboratory (JPL) and created a study team to put together a project plan for a rendez-vous with the comet. Louis Friedman, author of Star sailing:solar sails and interstellar travel (reference [4]) was in charge of the study. In 1977-1978, the JPL team conducted a preliminary design study that showed evidence of the feasibility of this solar sailing mission (reference [5]). However, NASA feared that the actual development and construction of the sail could not be achieved before 1981, which was the deadline for the launch since the rendez-vous was scheduled in 1986. A solar-electric propulsion project was preferred at the time but was never approved for a Halley mission. Eventually, the United States ended up with no comet mission at all.

Today, groups of scientists in the U.S., Europe, the Soviet Union and Japan are still working on solar sailing. In the United States, the World Space Foundation gathered engineers eager to develop a future solar sail (reference [6]) whereas in France, the Union Pour la Propulsion Photonique (U3P) has been conducting research with scientists from the Centre National d'Etudes Spatiales and other aerospace companies (reference [7]). In the United Kingdom, Cambridge Consultants Ltd is conceiving a sail for a Mars journey and for other future missions of the 1990's.

1.2. Solar sailing: the physics

1.2.1. Solar pressure

The issue in question through-out all this study is the capability of using solar radiation pressure to produce thrust. A given piece of material that is lit by a parallel beam of solar photons receives a power given by:

$$W = \frac{A}{d^2} \Phi \qquad (1.1)$$

Where: A is the area of this piece of material that is normal to the solar radiation.

d is the distance between the piece of material and the Sun.

$\Phi = 3.02\ 10^{25}$ Watt/steradian, which is the power of the solar radiation.

The momentum P of a parallel beam of photons with energy E is

$$P = \frac{E}{c} \tag{1.2}$$

Where: c is the speed of light.

The exerted force is:

$$\frac{dP}{dt} = \frac{W}{c}$$

which defines the absorbed momentum rate by unit area:

$$\frac{1}{A}\frac{dP}{dt} = K\left\{\frac{d_0}{d}\right\}^2 \tag{1.3}$$

Where: $K = 4.5\ 10^{-6}\ N/m^2$

d_0 is the distance from the Sun to the Earth, or one astronomical unit, or $149.6\ 10^6$ km.

d is the distance from the Sun to the solar sail.

A good solar sail is a very light mirror. This means that it will reflect the incoming light according to Descartes's law of optical reflection. By

doing so, a momentum will be transmitted to the sail. If during a period of time Δt, a momentum ΔP arrives perpendicularly on a mirror, it will transmit a momentum $2\Delta P$ to this mirror.

Lightness of the sail is required so that, despite the low level of thrust produced by the reflection of solar radiation, the acceleration level is maximized. To characterize the ability of the sail to create an acceleration, a parameter was defined: the lightness number. It is usually denoted by λ and is the ratio of the solar thrust that pushes the sail when it is oriented normally to the Sun radiation, to the gravitational attraction of the Sun on the sail.

$$\lambda = 2\frac{A K \left\{\frac{d_0}{d}\right\}^2}{m_{SS} G \frac{m_S}{d^2}} \qquad (1.4)$$

Replacing K by $\frac{\Phi}{c\, d_0^2}$ and introducing the Sun's gravitational constant $\mu_S = G\, m_S$, where m_S is the Sun's mass and G is the universal gravitational constant, we have the following expression of the lightness number in terms of the sail's mass (m_{SS}) and area (A):

$$\lambda = 2\,\frac{A}{m_{SS}}\,\frac{\Phi}{c\mu_S} \qquad (1.5)$$

Where: $\frac{\Phi}{c\mu_S} = 7.585\ 10^{-4}\ kg/m^2$.

m_{SS} is given in kilograms.

A is given in square meters.

For example: today's technology makes it possible to build a sail in Kapton that would have a lightness number of 0.1 (Kapton is aluminized to become a reflective material). This is equivalent to a mass per area coefficient of 17 g/m^2. This coefficient corresponds to an aluminized Kapton film of 7 μm thickness, which is commercially available in large quantities, and to a non-sail weight fraction of 25% (see reference [8]). With these characteristics, the maximum acceleration that can be induced by solar pressure is 6. 10^{-5} g_0, where $g_0 = 9.81$ m/s^2.

1.2.2. Orienting the sail

In order to control the trajectory of the sail, one must rotate the thrust vector and orient it along the desired acceleration direction. However, by rotating the sail, one changes the area of the reflecting surface that is normal to the solar radiation. Hence, changes in the orientation of the sail are associated with changes in the thrust direction and magnitude.

1.2.3. Model of the sail reflecting properties

We are only going to present a model of a perfectly reflecting flat sail. For details about more sophisticated kinds of solar sails such as non flat sails or for the heliogyro (to be presented in chapter II), it is interesting to read L. Sackett's report on solar sail escape trajectories (reference [9]). This model is the following: if θ is the angle between the normal to the

sail in the direction of the thrust and the Sun to solar sail direction, and if F_0 is the thrust due to solar pressure when the reflective side of the sail is normal to the solar radiation, then:

$$F(\theta) = F_0 \cos^2\theta \qquad (1.6)$$

$$F_0 = \lambda G \frac{m_{SS} m_S}{d^2}$$

Where: $F(\theta)$ is the thrust due to solar pressure when the Sun to solar sail direction and the thrust vector form an angle of θ radians.

1.3. Assets of photonic propulsion

Photonic propulsion is provided by the use of solar sails. Its main asset is that Sun radiation is available in free "unrestricted" quantities. As long as the Sun shines, solar sails will be able to navigate through-out space.

Practically, this feature allows one to plan longer missions than in the past, because propellant will never be lacking. It also facilitates the transportation of large payloads for which conventional spacecrafts would have to carry huge amounts of propellant. In theory, the technology developed in the 70's for the Halley's comet rendez-vous mission would enable the transport of a payload of 42 tons to Mercury in

less than 4 years (reference [10]). Furthermore, after each mission the solar sail could return to Earth to be refurbished on a parking orbit.

Solar sails can also achieve exotic orbits, some of which were unthinkable with conventional spacecrafts. Colin McInnes, a PhD student at the University of Glasgow, Scotland, wrote several papers on various kinds of trajectories made possible by solar sailing (see reference [11] and [12]). Among these new trajectories, which are unique to solar sails, are halo orbits centered on the Sun and out of the plane of the ecliptic. Observations of the Sun poles would then become possible without the difficulties that a conventional spacecraft must overcome to leave the plane of the ecliptic (e.g.,swing-by of Jupiter as was done with the Ulysses scientific spacecraft, see reference [13] and [14]).

Another interesting application of the solar sail is solar-eruption warning for Earth-based astronomical surveillance stations. By locating a conventional spacecraft at the Lagragian point L_1 of the Earth-Sun system, signals could be sent to Earth when unusual amounts of particles are detected. With a solar sail, the location of the spacecraft could be moved from the L_1 point to a point closer to the Sun. The bigger the lightness number of the sail, the closer to the Sun the sail can be located. Hence, earlier warnings can be sent to Earth and a preliminary study showed that the amount of warning time doubles and would reach two hours if a solar sail having a lightness number of 0.1 were to be used.

1.4. Two major designs of solar sails

The two configurations that have received the most attention over the years of solar sails short history are: the square sail, and
the heliogyro.

1.4.1. The square sail

Originally, when the JPL was working on a Halley's comet rendez-vous mission, the apparent simplicity of a square sail made it the only design to be considered. However, when NASA examined the square-sail design in more detail, several problems emerged. First, folding and packing a 640,000 square meters thin layer of Kapton in the shuttle's payload bay seemed to be quite impractical. Then came the problem of deployment with the fear of causing damage to the sail. Finally, dynamics of the sail are subject to its ability to be tightened on a supporting structure and to remain in a given shape. Uncertainty on the shape of the sail makes it hard to predict the location of the center of pressure and the thrust direction. These problems can be partly reduced by increasing the stiffness of the supporting structure but this also increases the weight of the solar sail and makes its lightness number decrease. Furthermore, one of the most unpleasant aspects of the square

sail design is the dimensions of the actuators that are required to rotate the sail and control the thrust orientation. Considering a square sail of 10,000 square meters, and considering that the center of pressure location is known within 1 meter, the actuators, which are "small" reflecting areas located at the corners of the sail, must be at least 200 square meters in area (reference [8]). The extravagant dimensions of such devices which are originally meant to steer the sail without adding too much weight, brought Richard MacNeal to introduce the following design.

1.4.2. The heliogyro

MacNeal's idea was to divide the sail into several blades. Then, the sail looked like a helicopter and this resulted in the name: heliogyro. With this design, the packaging problem turns into a much more tractable one since the blades rolled-up for storage, spaced symmetrically about a central core. The deployment issue also simplifies: the entire spacecraft is spun up when it leaves the rocket that takes it into its initial orbit, and the blades unroll freely under the action of the centrifugal force. This happens without the need of any supporting structure. At first glance, it might seem hard to believe that very thin and long sheets of plastic (Kapton is somewhat similar to plastic) can be controlled. Indeed, the orientation of the thrust is done by pointing the spin axis, which is achieved by pitching the blades. Richard

MacNeal carried out an experiment in 1971, where a sample blade 80 microns thick, 5 centimeters wide and 1.95 meters long was successfully put through pitch maneuvers in a rotating room (reference [15]). Avoiding the need of steering surfaces to orientate the sail, the heliogyro appears to be a more realistic spacecraft to control than the square sail.

1.5. Today's two major solar sailing events

Two solar sailing races are scheduled for 1992.

First, a race to Mars should take place to commemorate the quincentenary of Colombus' voyage to the new world. Each participant would carry a plaque weighting 1 kg. The winner would be the first of the entrants to pass within 10,000 kilometers of Mars. The race organizers hope to have one entrant from Europe from where Colombus set sail, one from America where he ended up and one from Asia to where he thought he was going (reference [10]).

The other solar sailing event is a race from the Earth to the Moon. This is intended to mark the international space year in 1992. It was originated by the French organization U3P, which persuaded Midi-Pyrennées, a regional government in France to sponsor a race to the Moon and to offer a prize. The race to the Moon, however, does offer one problem: the sail is best operated in interplanetary space, not near

Earth, where it must make many maneuvers to raise its altitude. The race will be quite demanding and will require a sophisticated sail, navigation, guidance and attitude control. For this reason, this study deals with the design of a trajectory from the Earth to the Moon, thus attempting to solve the trajectory issue of this race.

1.6. Basic ideas on an Earth-Moon trajectory for a solar sail

The departure will take place from a relatively low-Earth orbit. This orbit will either be a Geosynchronous Transfer Orbit (G.T.O.) or the geostationary orbit (reference [7]). The first one is characterized by a perigee altitude of about 7,500 km and an apogee altitude of about 42,000 km (both distances are referenced to the center of the Earth). The initial altitude with respect to the Earth's surface will thus range between 2,000 km and 36,000 km. At these altitudes, the Earth attraction is 500 times larger than the maximum thrust available through solar pressure on a sail having a lightness number of 0.1. Hence, the effect of solar radiation on the sail's orbit will be very tiny and if the steering law orientating the sail is chosen so as to increase altitude, the trajectory is going to slowly spiral away from the Earth.

Except under an extraordinary coincidence, the initial trajectory will not be in the Moon's orbital plane. For this reason, we must find a way to rotate the sail's orbital plane while increasing its altitude.

Due to the very slow variation of the orbit during the first months after departure, numerical simulations as well as analytical approaches can be greatly simplified by the use of averaging methods. These methods get rid of the very short term effects of the perturbations in order to enhance the variations of the solar sail orbit over large periods of time, such as several orbits. We will describe averaging techniques in the first part of the trajectory design, where we will make an extensive use of them.

Once the sail reaches distances equivalent to 60% of the distance from the Earth to the Moon, parameters characterizing the orbit begin to vary greatly in the period of one orbit and averaging methods are no longer valid. Furthermore, at such altitudes and provided that the sail orbit will then be coplanar with the Moon's orbit, phasing with the Moon will become a major issue. The overall goal is to pass behind the Moon, potentially for a gravity assist onto an interplanetary trajectory. This second part of the trajectory design will be approached from an optimal control point of view, in order to match an intercept position behind the Moon while minimizing the amount of time needed to reach this location.

When this study started, the design of the whole trajectory was considered in two ways. A first approach was to define a general

optimization problem: minimizing time from the initial low-Earth orbit to the final location behind the Moon; another possibility was to follow a more practical and less numerically intensive approach, based on the physics of the problem. This latter approach would make use of averaged and simplified dynamics of the solar sail's orbit.

General optimization of an Earth-Moon trajectory had already been done with propulsion systems developing higher levels of continuous thrust. For example, the study made by Breakwell and Rauch (reference [16], [17] and [18]) shows an elegant approach to solving this optimization problem, but their level of acceleration is $10^{-3}g_0$ whereas ours is only $10^{-5}g_0$. In their case, the spacecraft propulsion is electric and the thrust magnitude is independent of its orientation. In our case, it is numerically impractical to simulate a solar sail trajectory from low Earth altitude to a location close to the Moon without using numerical averaging techniques. That was not the case with a thrust magnitude of $10^{-3}g_0$. However, as stated earlier, the validity of these averaging techniques diminishes far from Earth, where the orbital parameters start to change by large amounts over a single orbit. For this reason, averaging appears as a need in the first part of the trajectory design, when the solar sail is spiralling away from the Earth. On the other hand, these techniques will not be used during the "phasing" part of the trajectory, when it is desired to catch up with the Moon's motion and disappear behind it.

Considering these practical facts, we have been led to approach the first part of the trajectory design from a physical point of view, more precisely we will derive steering laws from basic considerations on the dynamic equations of the orbital parameters. Conversely, the lack of simple physical approach for the phasing and intercept problem led to a more theoretical and numerical approach to the second part of the trajectory design. Finally, the goal of this study is to find a trajectory design for the solar sails race to the Moon and to present simulation examples showing its efficiency.

PART1

SPIRALING AWAY FROM THE EARTH AND MATCHING THE MOON'S ORBITAL PLANE

CHAPTER II

PREVIOUS WORKS AND UNDERLYING CONCEPTS

2.1. Overview of some major references

Numerous studies have been made and several papers were published on various ways of using solar sails to escape from planetary gravitational fields or travel through-out the solar system. Two types of trajectory designs can be noticed.

The first kind of studies involves most of the early research projects on solar sailing, often dating back to the 1960's. They deal with the design of heuristic maneuvers taking advantage of simplified situations such as planar problems where the trajectory is in the plane of the ecliptic, or particular initial orbits for which the physics of the solar sail motion are simplified (reference [19]). These studies are interesting because of the easy physical interpretation of the orientation laws that are presented. For example, in reference [20], Norman Sands develops a steering law that enables the solar sail spacecraft to escape from planetary gravitational fields by spinning the sail around its axis at half

the orbital rate. Sands concluded by stating that " it is found that for a practical case of escape from the Earth's gravitational field, solar sailing could accelerate a payload to escape conditions in a period of time of the order of several months, during which time it would pass the vicinity of the Moon's orbit about Earth".

However, Sands also concluded on the lack of efficiency of this extraordinary simple steering law and suggested taking advantage of the sail position on its elliptical orbit to select the locations where the rate of gain of total energy is the largest.

Another approach to escape trajectory design was made in 1977 by C. Uphoff in a JPL memo to Jerome Wright, the same person who had proposed a Halley's comet rendez-vous trajectory a few years before (reference [21]). This study shows two interesting features: first, the idea of increasing the total energy is the main driving concept in this research of an escaping trajectory. The energy of an orbit is:

$$E = -\frac{\mu}{2a} \qquad (2.1)$$

Where μ is the gravitational constant of the planet ($\mu = G M$ G is the universal gravitational constant and M is the mass of the planet.)

a is the major axis of the orbit.

The differential equation governing the rate of change of the total energy was used by Uphoff and we will introduce it later since it is also going to be the cornerstone of our "spiralling away strategy". The other interesting feature of Uphoff's approach is the use of averaging methods in order to foresee the changes ΔE over an arc of trajectory. As mentioned earlier, we are going to make an extensive use of averaging techniques in the first part of our Earth-Moon trajectory design.

The second kind of studies on solar sail trajectories deals with the calculus of variations approach in order to design minimum-time journeys between given orbits or given planets of the solar system. Despite several earlier works such as those of Cavoti (reference [22]) or Zhukov and Lebedev (reference [23]) who were applying the calculus of variations to the optimization of solar sail trajectories, Carl G. Sauer presented in 1976, one of the earliest optimization study on three dimensional interplanetary solar sail trajectories.

Although the problem that he was considering (Rendez-vous missions between various planets of the solar system) is quite different from our Earth-Moon trajectory problem, some of the formulation that he derived will find counterparts through-out this study, either in the first part for the derivation of sub-optimal steering laws, or in the second part in the formulation of the minimum time problem. Actually, Sauer's publication on Optimum solar-sail interplanetary trajectories (reference [24]) remains as an important reference for most optimization studies of

solar sail trajectories. The reason is that the optimal orientation of the sail can always be defined as the orientation that maximizes the component of the thrust vector along a given vector. Hence the orientation of the sail is given by a general expression that is independent of the criteria to be optimized (see maximizing the rate of change of the semi major axis, minimizing the inclination or minimizing the time of flight in the last part). This general expression is presented in Sauer's paper and takes the form:

$$\alpha = -\,\mathrm{Atan}\left[\frac{3\cos^2\zeta + \sqrt{8 + \cos^2\zeta}}{4\sin\zeta}\right] \qquad (2.2)$$

Where: α is an angle defining the thrust orientation.

ζ is an angle defining the orientation of the vector, which characterizes the criteria to be optimized.

Details about this major formula will be presented on several occasions in this document, and it will be derived clearly in the next chapter.

One of the latest works referencing Sauer's paper is Theodore Edelbaum and Lester Sackett's study of Optimal solar sail planetocentric trajectories (reference [25]). This work presents a fully optimized Earth-centered trajectory between a low-Earth-orbit and a given sub-escape orbit. With the help of Mr Sackett, various features of this work were gathered and applied to our problem. Namely, averaging formulations,

as well as the choice of particular orbital elements are inspired from this reference.

We are now going to present miscellaneous topics that were necessary for the design of the first part of the trajectory. More precisely, we will present the orbital elements that were used to describe the trajectory and the model of the dynamics that seemed to be a good compromise between reasonable accuracy and simplicity. An important issue in the simulation of space trajectories is the choice of units, which may decide of the numerical behavior of the simulator and this will also be presented in the next section.

2.2. The equinoctial elements

For orbits of zero inclination angle, the line of nodes does not exist. For orbits of zero eccentricity, the line of apsides is meaningless. Hence, the classical orbital elements, whose definition relies on the ascending node or on the pericenter, show singularities in their variational equations. These elements are ω: the argument of pericenter, Ω: the longitude of the ascending node as well as any anomaly defining the position of the body on its orbit.

New orbital elements were introduced in order to describe the dynamics of orbits which are circular or have zero inclination. One set of non-singular elements is the set of so-called equinoctial elements, which are studied extensively in reference [26] by Paul Cefola. These elements (a,h,k,p,q,F) are defined by the following expressions referring to the classical orbital elements (a,e,i,Ω,ω,E):

$$\begin{aligned} a &= a & F &= E + \Omega + \omega \\ h &= e \sin(\Omega + \omega) & k &= e \cos(\Omega + \omega) \\ p &= \tan(\tfrac{i}{2}) \sin \Omega & q &= \tan(\tfrac{i}{2}) \cos \Omega \end{aligned} \qquad (2.3)$$

The parameter F is called the eccentric longitude and it defines the position of the body on its orbit.

Note: by using "retrograde" equinoctial elements, inclinations near 180 degrees can be considered but this will not be necessary in our study.

The inverse relation giving the classical elements in terms of the equinoctial elements is not as straightforward. However classical elements can always be calculated from the equinoctial ones, whereas they fail to define values of the equinoctial elements in zero inclination and zero eccentricity cases.

Equinoctial to classical elements transformation:

First step: if p=q=0,

then i=0, Ω is not defined and can be set to 0.

else

Ω = Atan2(p,q)

i=2 Atan($\sqrt{p^2 + q^2}$)

Second step: if h=k=0,

then e=0, ω is not defined and can be set to 0.

else

ω = Atan2(h,k) - Ω

$e = \sqrt{h^2 + k^2}$

Associated with the equinoctial elements is an equinoctial frame. This frame is used to write the dynamical equations governing the variations of the equinoctial elements. If $\underline{Z}$ denotes the five component vector $[a,h,k,p,q]^T$, these equations can be written in matrix form :

$$\dot{\underline{Z}} = \underline{M}(\underline{Z},F) \cdot \underline{u} \qquad (2.4)$$

Where: $\underline{M}$ is a 5 by 3 matrix.

$\underline{u}$ is the three component vector of perturbations,

expressed in the equinoctial frame.

The equinoctial frame is defined by its three unit vectors ($\hat{f}$, $\hat{g}$, $\hat{w}$). $\hat{w}$ is along the kinetic momentum vector (and thus perpendicular to the orbital plane, in the orbital sense of rotation). $\hat{f}$ and $\hat{g}$ are described in figure 1 and the components of all three vectors in the Earth equatorial frame are:

$$\hat{f} = \frac{1}{1+p^2+q^2}\begin{bmatrix} 1-p^2+q^2 \\ 2pq \\ -2p \end{bmatrix}$$

$$\hat{g} = \frac{1}{1+p^2+q^2}\begin{bmatrix} 2pq \\ 1+p^2-q^2 \\ 2q \end{bmatrix} \qquad (2.5)$$

$$\hat{w} = \frac{1}{1+p^2+q^2}\begin{bmatrix} 2p \\ -2q \\ 1-p^2-q^2 \end{bmatrix}$$

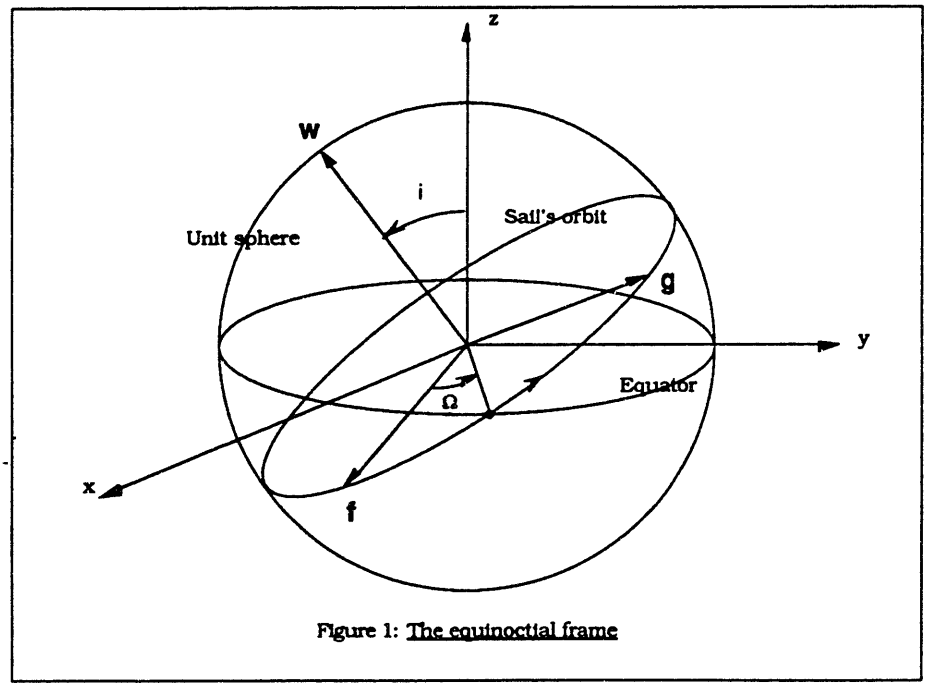

Figure 1: The equinoctial frame

Other useful relations involving the equinoctial elements were provided in reference [26] by Cefola:

$$\text{Position vector:} \quad \underline{r} = X_1 \hat{f} + Y_1 \hat{g}$$

$$\text{Velocity vector:} \quad \underline{v} = \dot{X}_1 \hat{f} + \dot{Y}_1 \hat{g} \tag{2.6}$$

Where:

$$X_1 = a\,[(1 - h^2\beta)\cos F + hk\beta \sin F - k)]$$

$$Y_1 = a\,[(1 - k^2\beta)\sin F + hk\beta \cos F - h)]$$

$$\dot{X}_1 = \frac{na^2}{r}\,[\,hk\beta \cos F - (1 - h^2\beta)\sin F] \tag{2.7}$$

$$\dot{Y}_1 = \frac{na^2}{r}\,[(1 - k^2\beta)\cos F - hk\beta \sin F]$$

and:

$$n = \sqrt{\frac{\mu}{a^2}}$$

$$\frac{r}{a} = 1 - k\cos F - h \sin F \tag{2.8}$$

$$\beta = \frac{1}{1 + \sqrt{1 - h^2 - k^2}}$$

The acceleration $\underline{u}$ is the sum of all perturbations acting on the spacecraft that are included in our model of the dynamics. This model is now going to be presented.

2.3. Model of the solar sail's dynamics

In this part of the trajectory, the presence of the Moon will be neglected with respect to the other sources of perturbations. This assumption is valid and a detailed approach of the dynamics of the second part of the trajectory (when the sail phases with the Moon) shows evidence that accuracy is not jeopardized by assuming so. Using an Earth-centered frame introduces a Sun gravity gradient acceleration, which is also going to be neglected since it is at least 100 times smaller than the solar thrust in the vicinity of the Earth .

Finally, the only two perturbation sources that are going to be taken into account in the dynamics of the solar sail orbit are :

The solar pressure on the sail.

The oblateness of the Earth (J_2 term only).

Actually, another perturbation of the orbit will be considered but it is not a source of acceleration as the two other ones: it is the effect of the Earth shadow on the sail which sometimes annihilates the effect of solar radiation.

The J_2 term of the Earth's gravitational potential induces an acceleration which is proportional to $\frac{1}{r^4}$ where r is the distance from the Earth's center to the sail and is thus decreasing quite rapidly while the

solar pressure magnitude remains roughly constant along the path from the Earth to the Moon. At a distance r = 27,000 km of the Earth's center, the accelerations due to the oblateness and to solar pressure are of comparable magnitudes: $6.10^{-5}g_0$. At geosynchronous altitude: r = 42,000 km, solar pressure can induce accelerations 70 times greater than the effects due to oblateness. Hence, considering the effects of the J_2 term of the Earth's gravitational field is more important at low altitudes and, in particular, in the case of an initial Geosynchronous Transfer Orbit.

As mentioned above, the other feature of our model of the dynamics is the consideration of Earth shadowing. We will define shadow situations by the following formulations: if $\underline{i}_S$ is the unit vector pointing from the Sun to the Earth, and if $\underline{i}_{ST}$ is a unit vector perpendicular to the previous one, the sail will be in the Earth's shadow when both of the following statements are true:

$$\begin{cases} \underline{r} \cdot \underline{i}_S > 0 \\ \| \underline{r} - (\underline{r} \cdot \underline{i}_S)\underline{i}_S \| > R_{Earth} \end{cases} \qquad (2.9)$$

R_{Earth} is the Earth radius and it will be taken as the Earth's equatorial radius: 6,378 km.

Our goal, in this first part is to define the orientation of the sail and consequently the thrust history $\underline{u}(t)$ to raise the apoge of the orbit and decrease its inclination with respect to the Moon's orbital plane.

2.4. Notions of cone and clock angles

To characterize the sail orientation and consequently the direction of the thrust due to solar pressure, we are going to use two particular angles, which are referred to as the cone and clock angles (these angles where introduced in Zukhov and Lebedev's paper, see reference [23])

More generally, we are going to define the cone and clock angles as a means to specify the orientation of any unit vector $\hat{i}_X$. Associated with these two angles, are two reference directions, which can be chosen arbitrarily as long as they are not parallel to each other. In our case, the two reference directions are : the Sun to solar sail direction, characterized by its unit vector $\hat{i}_S$, and the normal to the ecliptic pointing towards the North with its unit vector $\hat{i}_N$. It is assumed through-out this document that these two unit vectors are orthogonal.

The cone angle of $\hat{i}_X$ is defined with respect to $\hat{i}_S$ only, it is referred to by θ_X and its definition is given by

$$\theta_X = \text{Acos}\,(\hat{i}_X \cdot \hat{i}_S) \qquad (2.10)$$

The clock angle is defined with respect to $\hat{i}_S$ and $\hat{i}_N$ and is referred to by Ψ_X. It is the angle between the two half planes $(\hat{i}_S , \hat{i}_N)$ and $(\hat{i}_S , \hat{i}_X)$.

Ψ_X is given by:

$$\begin{cases} \sin \Psi_X = - \hat{i}_1 \cdot \hat{i}_2 \\ \cos \Psi_X = \hat{i}_N \cdot \hat{i}_2 \end{cases} \qquad (2.10)$$

Where:

$$\hat{i}_1 = \hat{i}_N \times \hat{i}_S$$

$$\hat{i}_2 = \hat{i}_S \times \frac{(\hat{i}_X \times \hat{i}_S)}{\| (\hat{i}_X \times \hat{i}_S) \|}$$

Given the values of θ_X and Ψ_X, $\hat{i}_X$ is completely characterized and can be expressed in terms of $\hat{i}_N$ and $\hat{i}_S$ according to :

$$\hat{i}_X = \cos\theta_X \, \hat{i}_S + \sin\theta_X \, (\cos\Psi_X \, \hat{i}_N - \sin\Psi_X \, \hat{i}_N \times \hat{i}_S) \qquad (2.10)$$

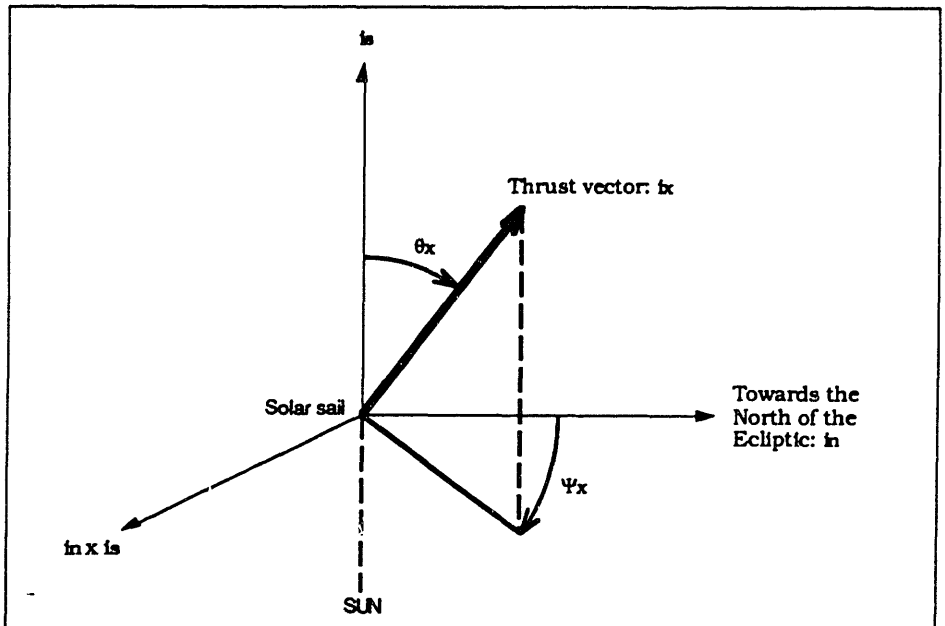

Figure 2: the cone (θ_X) and clock (Ψ_X) angles of the thrust vector.

Steering laws for the solar sail are given as cone and clock angle histories: $(\theta(t), \Psi(t))$, $t_0 < t < t_f$. These two functions of time determine the thrust vector pointing direction. To evaluate the performances of these control laws on the evolution of the orbital parameters, we will simulate the dynamics of the solar sail orbit by numerically integrating the 5 equations giving the variations of the equinoctial elements that define the size, shape and orientation of the orbit.

However, simulations are typically done over time periods of 150 days, which is roughly the time that will be required to reach 50 to 60% of the distance to the Moon's altitude. During these long periods of time, and especially when the sail is in the vicinity of the Earth, the orbital parameters vary slowly (a few percent over 100 orbits). This remark suggests the use of averaging methods to speed up the simulation program.

2.5. The averaging methods

There are two kinds of averaging methods: one is analytical and the other one is numerical. Both of these methods enable long term orbit predictions when knowledge of the short term variations of the orbital elements is not required (reference [27] and [28]) .

The main idea is to replace the instantaneous rates of change of each orbital element by averaged rates that take into account the size, shape and orientation of the orbit, but not the spacecraft position on the orbit. Here again, several possibilities occur: rates of change can be averaged with respect to each kind of anomaly. If α denotes a given orbital element, $\overline{\dot{\alpha}}$ is the averaged rate of change of α and can be defined by at least three different expressions (each of these is associated with a different anomaly).

$$\overline{\dot{\alpha}} = \frac{1}{2\pi}\int_0^{2\pi} \dot{\alpha}\, df \qquad \overline{\dot{\alpha}} = \frac{1}{2\pi}\int_0^{2\pi} \dot{\alpha}\, dE \qquad \overline{\dot{\alpha}} = \frac{1}{2\pi}\int_0^{2\pi} \dot{\alpha}\, dM \qquad (2.11)$$

Where: f is the true anomaly, E is the eccentric anomaly and M is the mean anomaly.

Most of the references use the last expression, which defines an average with respect to time since the mean anomaly is proportional to time. Hence, the most commonly used averaged rate of change is defined as:

$$\overline{\dot{\alpha}} = \frac{1}{2\pi}\int_0^{2\pi} \dot{\alpha}\, dM = \frac{1}{T}\int_0^{T} \dot{\alpha}\, dt \qquad (2.12)$$

Where T is the orbital period $T = 2\pi\sqrt{\frac{a^3}{\mu}}$.

The evaluation of the average rate $\overline{\dot{\alpha}}$ requires a quadrature. Depending on the complexity of the perturbation, i.e. of the expression of

$\dot{\alpha}$, this quadrature is done analytically (analytical averaging) or numerically (numerical averaging). In both cases, $\dot{\alpha}$ is a function of the 6 orbital elements. Among these 6 parameters, 5 characterize the size, shape and orientation of the orbit and they are held constant during the quadrature (for example a, e i, Ω, ω or a, h, k, p and q), the 6^{th} element characterizes the position on the orbit and the evaluation of the integral makes it disappear. The only assumption required to perform averaging methods is that the orbital elements do not change drastically (less than 5% for example) during one revolution of the satellite on its orbit. As far as accuracy is concerned, a rule of thumb was introduced in reference [25]. The error induced by simulating averaged dynamics of a solar sail in the vicinity of a planet was approximated by the ratio of the acceleration due to solar pressure to the acceleration due to the planet's gravitational field. This ratio is a function of the distance to the center of attraction; for a sail with a lightness coefficient of 0.1 orbiting around the Earth, it takes the following form: $\frac{\text{Solar pressure}}{\text{Earth attraction}} = 0.218\ r^2$ where r is the distance between the sail and the Earth's center (r = 1 if the sail is at the Moon's altitude: 384,400 kilometers). Table 1 shows that averaging methods bring about less than 5.5 percent errors as long as the sail's altitude is less than half of the Moon's altitude.

Altitude	0.2	0.3	0.4	0.5
Error (%)	0.872	1.96	3.5	5.45

Table 1: Validity of the averaging methods

For the purpose of our solar sail trajectories simulations, both analytical and numerical averaging were used.

2.5.1. Analytical averaging : effects of the Earth's oblateness

The effects of the J_2 term in the Earth gravitational potential concern the four equinoctial elements: h, k, p and q. Indeed, no variations of the semi-major axis are induced by this gravitational perturbation. From reference [26], we have the following closed form expressions of the averaged rates of change for h, k, p and q.

$$\begin{aligned}
\dot{\bar{h}}_{J_2} &= \frac{3\,\mu\,R_{eq}^2\,J_2\,k\,[1 - 6\,(p^2+q^2) + 3\,(p^2+q^2)^2]}{2\,n\,a^5\,(1-h^2-k^2)^2\;(1+p^2+q^2)^2} \\
\dot{\bar{k}}_{J_2} &= \frac{-3\,\mu\,R_{eq}^2\,J_2\,h\,[1 - 6\,(p^2+q^2) + 3\,(p^2+q^2)^2]}{2\,n\,a^5\,(1-h^2-k^2)^2\;(1+p^2+q^2)^2} \\
\dot{\bar{p}}_{J_2} &= \frac{-3\,\mu\,R_{eq}^2\,J_2\,q\,(1-p^2-q^2)}{2\,n\,a^5\,(1-h^2-k^2)^2\;(1+p^2+q^2)} \\
\dot{\bar{q}}_{J_2} &= \frac{3\,\mu\,R_{eq}^2\,J_2\,p\,(1-p^2-q^2)}{2\,n\,a^5\,(1-h^2-k^2)^2\;(1+p^2+q^2)}
\end{aligned} \qquad (2.13)$$

Where: R_{eq} is the Earth's equatorial radius.

Analytical averaging will also be considered to foresee the range of variations of the semi major axis or of the inclination when particular orientation schemes will be tried. Analytical averaging methods are well suited for preliminary studies because of the lack of computational overhead that is associated with them, however for various kinds of perturbation sources, analytical quadrature may become cumbersome or even impossible (e.g. elliptic integrals).

2.5.2. Numerical averaging

Numerical algorithms for quadrature are discussed in Numerical Averaging in Orbit Prediction by C. Uphoff (reference [27]). A Gaussian integration algorithm was used as recommended in this reference. The averaging interval can be broken up into several sub-intervals if more information about the behavior of the integrand $\dot{\alpha}$ is required. The number of intervals and the order of the quadrature formula for each interval are variables that can be adjusted to bring about a compromise between numerical overhead and accuracy. In our case, we chose to use a single interval (one revolution) and the number of points could be chosen freely and 16 points or 32 points were usually defined. Gaussian quadrature theory and algorithms were based on Numerical Recipes in C by William H. Press (reference [29]). The advantage of numerical averaging is that any kind of perturbation can be incorporated: shadowing is as easy to consider as the oblateness of the Earth. Hence,

fairly sophisticated models can be built as long as perturbations can be deterministically described.

Eventually, averaging methods remove the high frequency (higher or equal to once per orbit) variations from the perturbation equations. It is then possible to use large computing intervals in the numerical integration of the differential equations governing the equinoctial elements variations. Fast simulations of 150 days low-altitude-trajectories become possible (typically 2 to 5 minutes of C.P.U. time on a Sun Sparkstation).

2.6. Units

The last of our general considerations is the choice of units to be used to describe the trajectories. It is quite important to scale lengths and time. Using meters and seconds in astrodynamics studies can lead to numerical problems despite the use of very efficient algorithms. For this reason, we chose to use the following fairly intuitive units.

The unit of length will be the mean distance from the Earth to the Moon:

$$\begin{cases} 1 \text{ unit of length} = 384400 \text{ km} \\ 1 \text{ unit of time} = 1 \text{ day} = 86400 \text{ seconds} \end{cases} \tag{2.14}$$

Then the unit of acceleration is defined as:

1 unit of acceleration $= 1$ unit of length/(unit of time)^2

$= 5.14\ 10^{-2}$ m/s^2

$= 5.25\ 10^{-3}\ g_0$ with $g_0 = 9.81$ m/s^2

In these units, gravitational constants of the three celestial bodies that are relevant to this study have the following numerical values:

Gravitational constants:	(in (unit of length)^3/(unit of time)^2)
Earth	$\mu_E = 0.05238601$
Moon	$\mu_M = \mu_E / 81.31$
Sun	$\mu_S = 333432\ \mu_E$

Finally, the maximum acceleration due to solar pressure on a solar sail having a lightness number of 0.1 is: $A_0 = 0.0117$ unit of length/(unit of time)^2.

CHAPTER III

STEERING LAW DESIGN

3.1. A strategy to increase the energy

In the two body problem, the energy of an orbit is given by its semi major axis, as it was already presented in the previous chapter:

$$E = -\frac{\mu}{2a} \tag{3.1}$$

The energy is negative when the orbit is an ellipse (a>0). In that case, the spacecraft, or more generally the orbiting object, is captured by the gravitational field. The energy is split in two parts: the kinetic energy and the potential energy. The relation governing this partitioning of the energy is the vis-viva integral:

$$\frac{v^2}{2} - \frac{\mu}{r} = -\frac{\mu}{2a} \tag{3.2}$$

Where: r is the distance between the orbiting object and the center of attraction.

v is the velocity of the orbiting object with respect to the center of attraction.

As stated earlier, our first goal is to increase the solar sail altitude with respect to the Earth. One of the most obvious thing to try is to increase the semi major axis of the orbit. One could have thought of increasing the apogee altitude (which is given by a(1+e) where e is the orbit eccentricity) but it would then be tempting to increase the eccentricity and this would lead to lower and lower perigee altitudes, which is not desirable because of the threat of atmospheric drag (the perigee altitude is a(1-e)). Hence, we are first interested in increasing the semi major axis or equivalently, in increasing the orbital energy.

The variation of parameter equations are given by expressions of the form:

$$\frac{dEl}{dt} = \left.\frac{\partial El}{\partial \underline{v}}\right|_{\underline{r}} \cdot \underline{a}_d \qquad (3.3)$$

Where: El is a given orbital element.

$\underline{a}_d$ is the perturbing acceleration vector.

Here, $\left.\frac{\partial a}{\partial \underline{v}}\right|_{\underline{r}}$ is derived from the vis-viva integral:

$$\left\{\frac{v^2}{2} - \frac{\mu}{r} = -\frac{\mu}{2a}\right\} \quad \Rightarrow \quad \left\{\frac{\mu}{a^2}\left.\frac{\partial a}{\partial \underline{v}}\right|_{\underline{r}} = 2\underline{v}^T\right\} \qquad (3.4)$$

Finally, we have Gauss's form of the variational equation for the semi major axis:

$$\frac{da}{dt} = \frac{2\,a^2}{\mu}\, \underline{v} \cdot \underline{a}_d \qquad (3.5)$$

Hence, our first conclusion is that : **"to increase the instantaneous semi major axis, one must maximize the dot product: $\underline{v} \cdot \underline{a}_d$"**. This leads to two considerations:

First, it will be interesting to have a maximum component of the perturbing acceleration along the velocity vector.

Second, changes in the semi major axis will be more efficient when the magnitude of the velocity vector is large i.e. around the perigee.

The idea of maximizing the projection of the thrust on a given vector will be used in each part of the trajectory design. Hence, we will develop it in details in the next section.

3.1.1. Maximizing the projection of the thrust on a given unit vector

Let $\hat{\underline{i}}_V$ be a unit vector along which one wishes to maximize the projection of the solar thrust. We will use the notions of cone and clock angles that were introduced earlier in this document.

With $\hat{\underline{i}}_N$ being a unit vector perpendicular to the ecliptic and pointing to the North and $\hat{\underline{i}}_S$ being a unit vector pointing from the Sun to the solar

sail, we can define the cone and clock angles for both $\hat{i}_V$ (θ_V, Ψ_V) and the thrust unit vector $\hat{i}_U$ (θ_U, Ψ_U).

$$\hat{i}_V = \cos\theta_V \ \hat{i}_S + \sin\theta_V (\cos\Psi_V \ \hat{i}_N - \sin\Psi_V \ \hat{i}_1)$$

$$\hat{i}_U = \cos\theta_U \ \hat{i}_S + \sin\theta_U (\cos\Psi_U \ \hat{i}_N - \sin\Psi_U \ \hat{i}_1)$$

Where: $\hat{i}_1 = \hat{i}_N \times \hat{i}_S$

The thrust vector is given by : $\underline{u} = A_0 \cos^2\theta_U \ \hat{i}_U$ (3.6)

Maximizing the projection of the thrust on $\hat{i}_V$ is equivalent to maximizing: $\cos^2\theta_U \ \hat{i}_U \cdot i_V$. We are now facing the following problem:

$$\underset{\theta_U \text{ and } \Psi_U}{\text{Max}} \left\{\cos^2\theta_U [\cos\theta_V \cos\theta_U + \sin\theta_V \ \sin\theta_U \cos(\Psi_V - \Psi_U)]\right\}$$

Cone angles are always between 0 and 180 degrees, hence $\sin\theta_V \sin\theta_U$ is always positive and the term:

$$\cos^2\theta_U \sin\theta_V \sin\theta_U (\cos\Psi_V \ \cos\Psi_U + \sin\Psi_V \sin\Psi_U)$$

will be maximized if Ψ_U is chosen to be equal to Ψ_V.

We are now reduced to a one parameter optimization problem:

$$\underset{0<\theta_U<\pi}{\text{Max}} \left\{\cos^2\theta_U [\cos\theta_V \cos\theta_U + \sin\theta_V \ \sin\theta_U]\right\}$$

Calling this expression $F(\theta_U, \theta_V)$, we want to maximize it with respect to θ_U.

$$\frac{\partial F}{\partial \theta_U} = -2 \sin\theta_U \cos\theta_U (\cos\theta_V \cos\theta_U + \sin\theta_V \sin\theta_U) + \cos^2\theta_U \sin(\theta_V - \theta_U)$$

If $\cos\theta_U = 0$, we are not maximizing the projection of the thrust since its magnitude is then zero. Hence, we may divide the whole above expression by $\cos^3\theta_U$, which implies the following equivalence:

$$\left\{\frac{\partial F}{\partial \theta_U} = 0\right\} \quad \Leftrightarrow \quad \{-2 \sin\theta_V \tan^2\theta_U - 3 \cos\theta_V \tan\theta_U + \sin\theta_V = 0\}$$

The latter equation has two solutions in $\tan\theta_U$:

$$\tan\theta_U = \frac{-3\cos\theta_V \pm \sqrt{8 + \cos^2\theta_V}}{4\sin\theta_V} \tag{3.7}$$

In order to get rid of the indetermination, let us consider the following particular case: if $\theta_V = \frac{\pi}{2}$, then $F(\theta_U, \frac{\pi}{2}) = \sin\theta_U \cos^2\theta_U$ so that $\tan\theta_U = \pm\frac{\sqrt{8}}{4}$. $F(\theta_U, \frac{\pi}{2})$ will be maximized if $\tan\theta_U = \frac{\sqrt{8}}{4}$. We have thus derived the closed form solution:

$$\begin{cases} \Psi_U = \Psi_V \\ \theta_U = \text{Atan}\left[\dfrac{-3\cos\theta_V + \sqrt{8 + \cos^2\theta_V}}{4\sin\theta_V}\right] \end{cases} \tag{3.8}$$

These two relations completely specify the orientation of the thrust vector in terms of its cone and clock angles (θ_U, Ψ_U). This formulation maximizes the projection of the thrust vector on a given unit vector

specified by its cone and clock angles (θ_V,Ψ_V), the slight difference between this expression and formula 2.2 is due to the fact that cone angles are defined in the opposite sense than those in Sauer's paper.

It is interesting to notice that the relation defining the cone angle θ_U automatically constraints it to be in the (0, 90 degrees) range which is physically reasonable. Indeed, the cone angle θ_V of the vector $\hat{i}_V$ is, by definition between 0 and 180 degrees, implying that $\sin\theta_V$ is positive. Then, it is easy to verify that the expression

$$- 3 \cos x + \sqrt{8 + \cos^2 x}$$

is always positive when x belongs to $[0,\pi]$. Hence, the thrust vector cone angle is always between 0 and 90 degrees thus complying with the fact that no thrust can be oriented towards the Sun.

3.1.2. Analytical evaluation of the increasing energy strategy

Before simulating a steering law based on maximizing the projection of the solar thrust on the velocity vector, we are going to evaluate its performance. More precisely, we want to have an estimate of the averaged value of the rate of change of the semi major axis: $\overline{\dot{a}}$.

From Gauss's variational equation:

$$\dot{a} = \frac{2\,a^2}{\mu}\, \underline{v} \cdot \underline{a}_d \qquad (3.9)$$

We have the averaged equation:

$$\dot{\bar{a}} = \frac{2\,a^2}{\mu}\,\overline{\underline{v}\cdot\underline{a}_d} \qquad (3.10)$$

We will approximate $\overline{\underline{v}\cdot\underline{a}_d}$ by $V_{circ}\cdot\bar{a}_d$, where V_{circ} is the velocity of an object orbiting on a circular trajectory of radius a:

$$V_{circ} = \sqrt{\frac{\mu}{a}} \qquad (3.11)$$

$\bar{a}_d$ denotes the averaged level of acceleration along the velocity vector. It can be characterized as a fraction of the maximum acceleration:

$$\bar{a}_d = \frac{k}{100}\,u_{Max} \quad \text{with} \quad u_{Max} = 6.\,10^{-5}\,g_0. \qquad (3.12)$$

We are now going to try to estimate a reasonable value for k. k does obviously depend on the shape and inclination of the orbit: if the orbital plane is normal to the Sun-Earth line, the acceleration along the velocity vector is constant since the angle between the Sun to solar sail line and the velocity vector is always 90 degrees; for an orbit in the plane of the ecliptic, this angle takes all values between 0 and 360 degrees during one revolution around the Earth. Despite this dependence on the orbital characteristics, we want to find a value of k for near equatorial orbits (i.e. between -30 and +30 degrees of inclination with respect to the ecliptic).

The amount of acceleration along the velocity vector is a function of the cone angle of the velocity vector: θ_V.

$$\frac{\underline{u} \cdot \underline{i}_r}{u_{Max}} = \cos^2\theta_U \cos(\theta_V - \theta_U) \qquad (3.13)$$

Where: $$\theta_U = \text{Atan}\left[\frac{-3\cos\theta_V + \sqrt{8 + \cos^2\theta_V}}{4\sin\theta_V}\right]$$

This relation is plotted on figure 3 and shows that for velocity vector cone angles that are less than 120 degrees, the acceleration is greater than 15% of the maximum acceleration level.

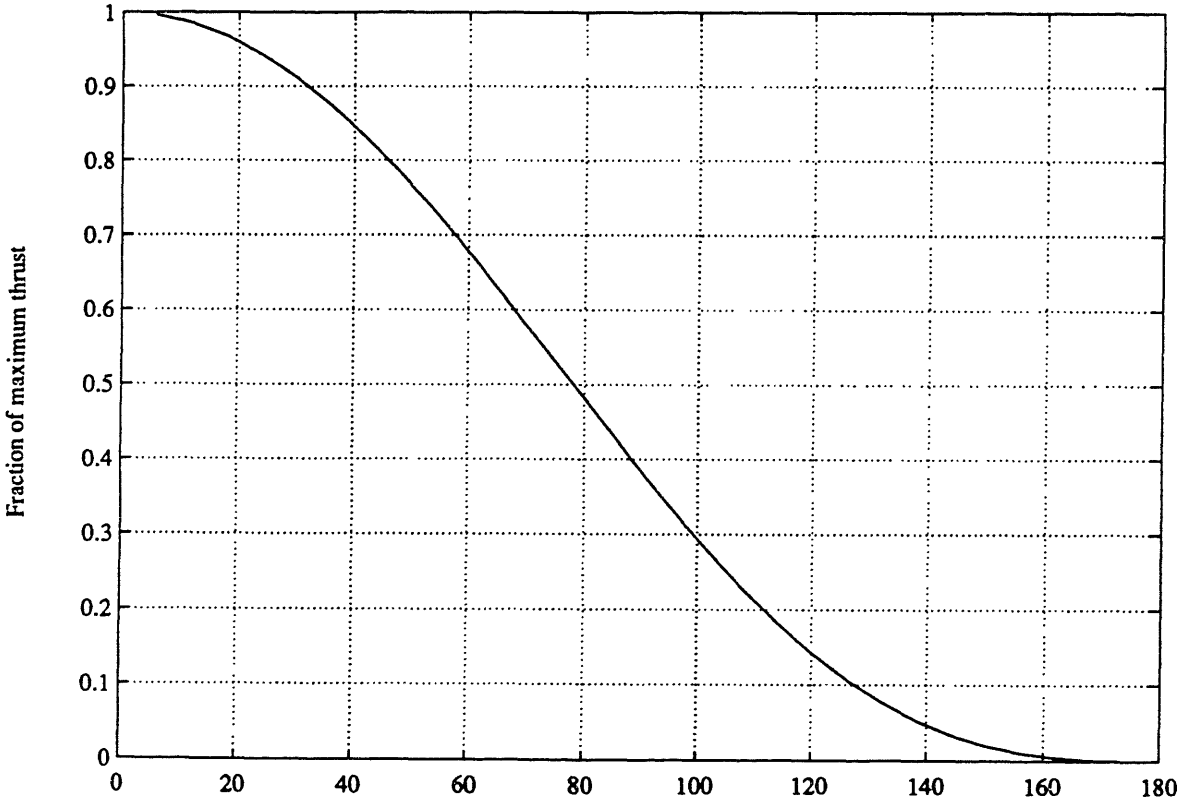

Figure 3: Thrust along the velocity vector vs velocity cone angle

Around 100 degrees, this fraction is more than 30% and this value is going to be selected to define the average amount of acceleration along the velocity vector. There is no rigorous mathematical reason for this choice but for orbits that are not normal to the solar radiation, the velocity vector cone angle can take on all values between 0 and 180 degrees. Selecting 100 degrees for an average value of the sail's cone angle seems to define a reasonable value of the average level of thrust. Having selected this evaluation of the averaged amount of acceleration along the velocity vector, we now have the semi major axis average rate of change as a function of the semi major axis itself:

$$\bar{\dot{a}} = \left[\frac{2}{\sqrt{\mu}} 0.3 \; u_{Max}\right] a^{1.5} \qquad (3.14)$$

Typical values of $\bar{\dot{a}}$ are presented in table 2:

a: in % of the Earth-Moon distance	0.05	0.1	0.2	0.4
$\bar{\dot{a}}$: in km/day	130	360	1030	2900
$\bar{\dot{a}}$: in 10^{-3} Earth-Moon distance/orbit	0.1	0.8	6.6	52

Table 2: Efficiency of the "increasing energy strategy".

This table shows that orientating the solar thrust along the velocity vector is an efficient way to increase the semi major axis, moreover, the

simplified expression of $\bar{\dot{a}}$ (3.14) enables us to have a first estimate of the time needed to reach a given value of the semi major axis.

$$\left\{ \bar{\dot{a}} = \left[\frac{2}{\sqrt{\mu}} 0.3\, u_{Max} \right] a^{1.5} \right\} \quad \Rightarrow \left\{ t_f - t_0 = \frac{\sqrt{\mu}}{0.3\, u_{Max}} \left[\frac{1}{\sqrt{a_0}} - \frac{1}{\sqrt{a_f}} \right] \right\} \qquad (3.15)$$

For example, starting from a geosynchronous transfer orbit (semi major axis = 0.065 unit of length) and reaching a semi major axis of half the distance to the Moon (a_f = 0.5 unit of length) requires a travel time of :

$$t_f - t_0 = 164 \text{ days.}$$

If the initial orbit is the geostationnary orbit (a_0 = 0.11 unit of length), the travel time becomes:

$$t_f - t_0 = 105 \text{ days.}$$

3.1.3. Numerical simulation of increasing energy trajectories

Now that the steering law has been specified ("maximize the thrust along the velocity vector") and that its efficiency has been established, particular trajectories are going to be computed to show how this strategy enables a solar sail to spiral away from the Earth and how particular initial orientations of the orbital plane may contribute to its efficiency or dramatically ruin its performances.

All the following simulations share several joint features:

semi major axis: a = 0.065 Earth-Moon distance.

eccentricity: e=0.7.

argument of perigee: ω = -90 degrees.

inclination with respect to the ecliptic: i = 28 degrees.

At t=0, the Sun position is always the same: it is on the vernal axis which is directed along the positive x-axis of the trajectory plots (see Appendix 1). Finally, only the longitude of the ascending node distinguishes all the following simulations. Practically, this allows to set the initial orientation of the apsidal line (perigee-apogee) with respect to the Earth-Sun line. Trajectories have been computed in cases where these two lines define angles of : 0, 45, 90, 135, 180, 225, 270 and 315 degrees, each of them lasts 120 days.

Conclusions about this increasing energy strategy can be drawn from the following table which summarizes the set of numerical simulations.

Angle α	-90	-45	0	45	90	135	180	225
a_f	0.44	0.50	0.47	0.37	0.28	0.25	0.28	0.36
$a(1+e)_f$	0.78	0.82	0.72	0.63	0.52	0.48	0.55	0.65
e_f	0.74	0.66	0.60	0.66	0.83	0.93	0.97	0.84

Table 3: Effects of the apsidal line initial orientation.

The angle α is given in degrees and specifies the orientation of the apsidal line, a_f is the final value of the semi major axis, $a(1+e)_f$ is the final apogee altitude and e_f is the final value of the eccentricity.

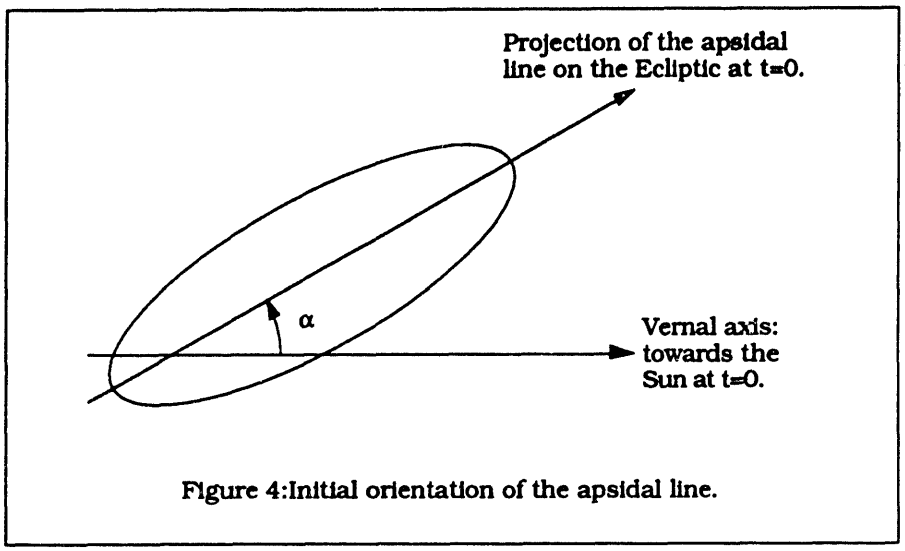

Figure 4:Initial orientation of the apsidal line.

Keeping in mind that our goal is to reach as high an apogee altitude as possible without too much decreasing the perigee altitude to prevent the sail from the effects of atmospheric drag, it readily appears that some particular initial orientations of the apsidal line with respect to the Earth-Sun line are more favorable than others.

Namely, the best case seems to be associated with an initial orientation between -45 and 0 degrees (values of the angle α), i.e. with the Sun slightly ahead of the perigee in its apparent circular motion around the Earth.

In this case, a semi major axis of 0.5 Earth-Moon distance is reached in 120 days thus proving that our previous analytical flight-time estimate (164 days) was not too optimistic in an average case. This "best case" is presented on the next pages: initial and final values of the main orbital elements are provided, as well as time histories of some particular parameters such as the perigee altitude and the inclination with respect to the ecliptic. The 7 other simulations are included in Appendix 1, they show how particular initial orientations of the apsidal line may induce large eccentricities and thus jeopardize the sail's mission.

It is interesting to notice that this inclination is varying under the action of solar pressure and the perturbation due to the J_2 term of the Earth gravitational potential. Bringing the sail in the vicinity of the Moon is going to require control on the locations where the sail's trajectory intersects the Moon's orbital plane. This emphasizes the notions of node of the sail's trajectory with the Moon's orbital plane as well as the inclination of the sail's trajectory with respect to the Moon's orbital plane. The next section is going to present a modified version of the previously developed "increasing energy strategy" which intends to solve this inclination versus node issue.

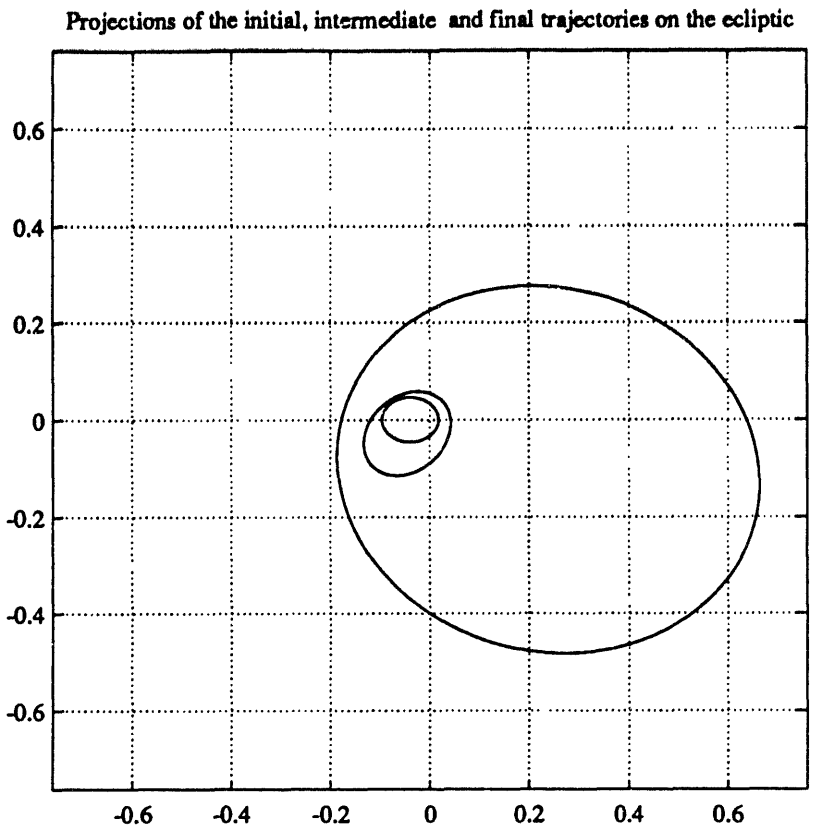

ORBITAL ELEMENTS

	INITIAL VALUES	FINAL VALUES
Semi major axis	0.065	0.4735
Excentricity	0.7	0.6067

The following elements are referenced to the Ecliptic:

Inclination	28	25.51
Ascending node	90	55.23
Argument of perigee	-90	100.2

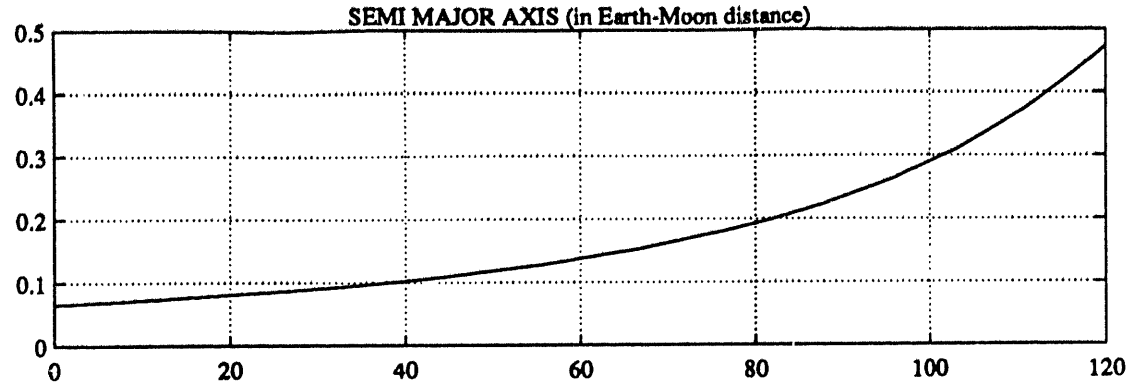
SEMI MAJOR AXIS (in Earth-Moon distance)
0.5
0.4
0.3
0.2
0.1
0
0
20
40
60
80
100
120

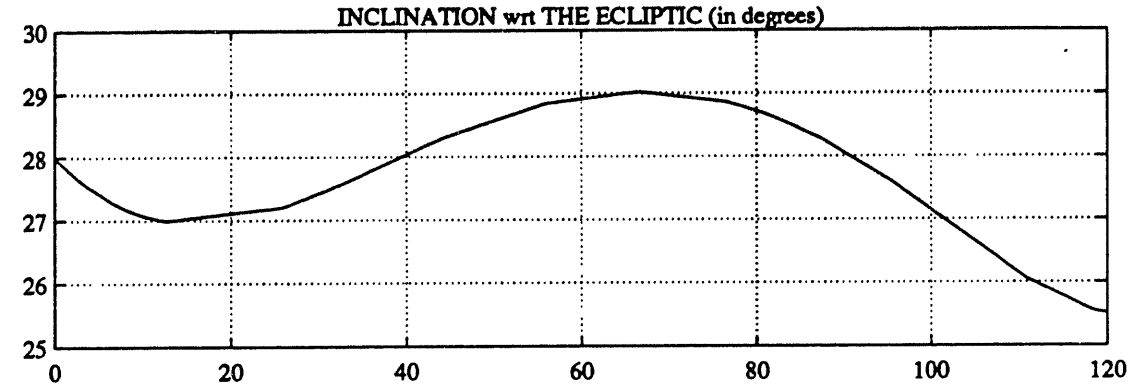
INCLINATION wrt THE ECLIPTIC (in degrees)
30
29
28
27
26
25
0
20
40
60
80
100
120

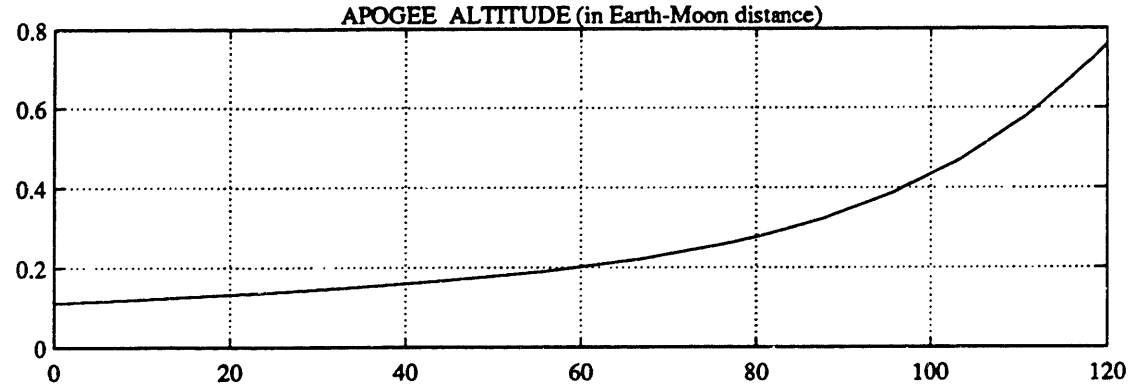
APOGEE ALTITUDE (in Earth-Moon distance)
0.8
0.6
0.4
0.2
0
0
20
40
60
80
100
120

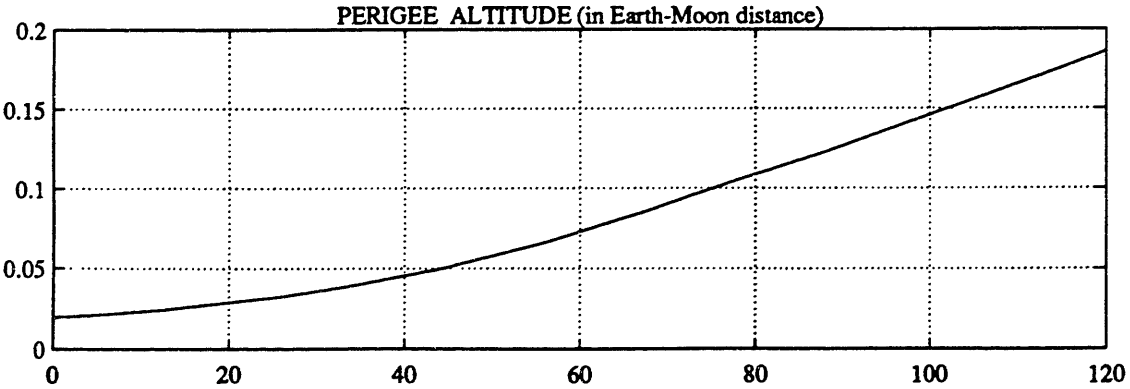
PERIGEE ALTITUDE (in Earth-Moon distance)
0.2
0.15
0.1
0.05
0
0
20
40
60
80
100
120

3.2. Inclination change strategy

The previously developed "increasing energy strategy" provides an efficient way of spiralling away from the Earth by means of solar pressure. However, as can be seen on simulation examples, the inclination, and more generally, the orientation of the sail's orbital plane is not controlled and varies freely as a consequence of the application of this steering law.

In this section, we want to develop a strategy that will provide control on the orientation of the orbital kinetic momentum in order to bring the sail's orbital plane in an adequate position for a later intercept of a near-lunar location.

Two possibilities were first envisioned. The first one, was to schedule an intercept at one of the nodes of the solar sail trajectory with the orbital plane of the Moon. This idea had already been used and developed in James S. Miller's thesis (reference [30]) for a low-thrust lunar reconnaissance trajectory, and is the basis of navigation schemes developed by Dr Richard Battin in his book Astronautical Guidance (reference [31]). Despite the good performances of such trajectories, it was decided to look for another type of strategy. This decision was motivated by the fact that intercepts at the node of the trajectory put the emphasis

on two short periods of time around the passage at the nodes. Any error during these short phases must be rapidly corrected, a solution conceivable with the electric propulsion considered in Miller's thesis, but, in our case, the very low level of acceleration coupled with the orientation of the sail make fast orbital corrections impossible. Hence, it was preferred to focus on a plane change maneuver, which would bring the sail's orbital plane in the Moon's orbital plane.

This second possibility offers the advantage that future intercept will be possible in all directions of the sail's orbital plane and not only at two specific locations. Furthermore, this will allow looking for an intercept at apogee, whereas in the previous scheme, the apogee was not necessarily located at one of the nodes.

3.2.1. Matching the Moon's orbital plane

If classical orbital elements are used (or equinoctial elements based on the classical ones), two parameters must be matched with two elements of the Moon's orbital parameters. Namely, the inclination (i) and the longitude of the ascending node (Ω) of both orbits must have the same value for the two orbital planes to coincide. These orbital elements are referenced to the Earth equatorial plane. We thus have at least three planes to consider: the equator, the Moon's orbital plane and the solar sail's orbital plane.

An interesting simplification occurs when the equatorial plane is no longer used as a reference. Instead, the Moon's orbital plane is considered to define new orbital elements of the solar sail trajectory. When considering only the solar sail trajectory and the Moon's orbital plane, it is clear that matching the two planes is equivalent to bringing to zero the inclination of the solar sail orbit with respect to the Moon's orbital plane. Instead of matching two sets of two orbital elements it is only necessary to bring one parameter to zero.

3.2.2. Inclination with respect to the Moon's orbital plane

The Moon's orbit is not fixed in an Earth centered inertial frame, its motion has long been a research topic. In 1920, E.W. Brown published a quite complete set of tables of the Moon's motion. Mean elements of the Moon's orbit are given in Dr Battin's book Astronautical Guidance. In particular, the mean inclination of the Moon's orbit with respect to the ecliptic is 5.15 degrees. We also learn in this reference that the line of nodes rotates with a period of 6,798 days. These two features of the Moon's orbit, associated with the value of the longitude of the node Ω_0 at a given epoch, enable one to define i_M and Ω_M: the inclination with respect to the ecliptic and the longitude of the ascending node of the Moon's orbit.

We now want to derive an expression for the inclination of the solar sail orbit with respect to the Moon's orbital plane. Assuming values of i and Ω for the solar sail orbit inclination and longitude of the ascending node with respect to the equator, we are able to compute the components of the unit vector along the kinetic momentum of the solar sail orbit in the classical geocentric inertial frame:

$$\hat{\underline{i}}_{\underline{h}\ \text{Solar sail}} = \begin{bmatrix} \sin i \sin\Omega \\ -\sin i \cos\Omega \\ \cos i \end{bmatrix} \tag{3.16}$$

Since the ecliptic is inclined at an angle $\alpha = 23.45$ degrees with respect to the equator, the components of $\hat{\underline{i}}_{\underline{h}}$ in the ecliptic inertial frame are:

$$\hat{\underline{i}}_{\underline{h}\ \text{Solar sail}} = \begin{bmatrix} 1 & 0 & 0 \\ 0 & \cos\alpha & \sin\alpha \\ 0 & -\sin\alpha & \cos\alpha \end{bmatrix} \cdot \begin{bmatrix} \sin i \sin\Omega \\ -\sin i \cos\Omega \\ \cos i \end{bmatrix} \tag{3.17}$$

In the ecliptic inertial frame, the components of the unit vector along the kinetic momentum of the Moon's orbit are:

$$\hat{\underline{i}}_{\underline{h}\ \text{Moon}} = \begin{bmatrix} \sin i_M \sin\Omega_M \\ -\sin i_M \cos\Omega_M \\ \cos i_M \end{bmatrix} \tag{3.18}$$

Given these two unit vectors, the inclination of the solar sail's orbit with respect to the Moon's orbital plane is given by:

$$i' = \text{Acos}\left\{ \hat{\underline{i}}_{\underline{h}\ \text{Solar sail}} \cdot \hat{\underline{i}}_{\underline{h}\ \text{Moon}} \right\} \tag{3.19}$$

Note: We can also easily compute the direction of the ascending node of the solar sail trajectory in the Moon's orbital plane: this direction is pointed to by the vector:

$$\hat{\underline{i}}_{Node} = \hat{\underline{i}}_{h\ Moon} \times \hat{\underline{i}}_{h\ Solar\ sail} \qquad (3.20)$$

3.2.3. Strategy to decrease the inclination with respect to the Moon's orbital plane

The equatorial plane does not play any physical role in the derivation of the variation of parameters equations for the classical orbital elements. If another reference plane is chosen, the form of these equations will remain the same but the parameters involved in these new equations will all be referenced to the new plane.

In particular, the variational equation governing the evolution of the inclination angle is:

$$\frac{di}{dt} = \frac{r\cos\theta}{h} a_{dh} \qquad (3.21)$$

Where: θ is the sum of the argument of perigee (ω) and of the true anomaly (f).

h is the norm of the kinetic momentum (does not depend on the reference plane).

a_{dh} is the component of the disturbing acceleration along the kinetic momentum of the orbit.

An interesting way of looking at this variational equation is to consider the orbit as a rigid body. Then, the rate of change of the kinetic momentum is given by the sum of the torques applied to the orbit.

In our case, we want to rotate the kinetic momentum around the line of nodes. We thus have to generate a torque, whose axis will be perpendicular to the line of nodes. This torque can be generated by orientating the thrust perpendicularly to the solar sail's orbital plane and in a direction opposite to the kinetic momentum when the sail is near the ascending node and along the kinetic momentum when it passes in the vicinity of the descending node.

This approach of the orbit's dynamics is quite simple and is in agreement with the variational equation of the inclination angle.

Hence, the inclination decreasing strategy can be stated as follows:

Maximize the thrust component along $-\hat{i}_{\underline{h}}$ Solar sail in the vicinity of the ascending node.

Maximize the thrust component along $+\hat{i}_{\underline{h}}$ Solar sail in the vicinity of the descending node.

The steering laws associated with this strategy are easily derived since they are characterized by the maximization of the thrust along a vector. Once more, we will use the expressions of the cone and clock angles of the thrust vector, that were derived earlier. This time, we will

need to compute the cone and clock angles of the kinetic momentum unit vector $\hat{i}_{\underline{h}}$ Solar sail and of its opposite - $\hat{i}_{\underline{h}}$ Solar sail.

Before showing some numerical simulations of these orientation schemes, we are going to evaluate their performances by a simplified analytical approach.

3.2.4. Analytical evaluation of the efficiency of the inclination decreasing strategy

The so-called inclination decreasing strategy is actually an improved version of the "increasing energy strategy". On most of the orbit, the thrust vector is oriented so as to maximize its component along the velocity vector. Only in the vicinity of the nodes, is the thrust oriented according to the above inclination decreasing strategy. Moreover, depending on each case, the latter strategy is applied only after a given value of the semi major axis is reached. The region around the nodes, where inclination control is applied, also needs to be defined experimentally.

For the sake of this analytical evaluation, we will consider that the inclination strategy does not perturb the increase of the semi major axis and we will apply it from the initial orbit to our goal: a semi major axis equal to half of the Earth-Moon distance. The region on which inclination control is active, is defined by an angular range of $\pm \frac{\pi}{6}$

around each node (this value will later be selected as an efficient one in the light of various numerical simulations).

From Gauss's variational equation for the inclination, we have:

$$\frac{di}{dt} = \frac{r\cos\theta}{h} \cdot a_{dh}$$

In order to simplify the analysis, we consider a circular orbit of radius r=a and $\cos\theta$ is taken to be equal to 0.95 which is its average value on the interval $[-\frac{\pi}{6}, +\frac{\pi}{6}]$. As in the case of the energy strategy, $\overline{a_{dh}}$ is chosen to be equal to 0.3 u_{Max}. Finally we have an approximated averaged equation:

$$\frac{\overline{di}}{dt} = \frac{-1}{3} 0.95 \frac{0.3\, u_{Max}}{\sqrt{\mu}} \cdot \sqrt{a} \qquad \text{in rad/day} \qquad (3.22)$$

Where: the $\frac{1}{3}$ factor accounts for the fact that this steering law is only applied on a third of the length of the orbit (one region around each node, each region being $\frac{\pi}{3}$ wide)

The time-averaged rate of change of the inclination turns out to be a function of the semi major axis. We are now interested in getting an estimate of the inclination changes that are possible during the first phase of the trajectory i.e. during the spiralling away from the Earth.

From the previous section, we have the time averaged rate of change of the semi major axis:

$$\overline{\frac{da}{dt}} = \frac{2}{\sqrt{\mu}} 0.3 \; u_{Max} \; a^{1.5}$$

Combining these two equations, we can estimate the range of the inclination changes that can be achieved along a trajectory leading from an initial value of the semi major axis a_0 to a final value of the semi major axis a_f.

$$\Delta i = \int_{t_0}^{t_f} \overline{\frac{di}{dt}} \, dt = \int_{a_0}^{a_f} \overline{\frac{di}{dt}} \; \overline{\frac{dt}{da}} \, da = \int_{a_0}^{a_f} \frac{\overline{di/dt}}{\overline{da/dt}} \, da \qquad (3.23)$$

This leads to the following expression for the inclination change:

$$\Delta i = \frac{-0.95}{6} \mathrm{Ln} \left[\frac{a_f}{a_0} \right] \qquad (3.24)$$

For $a_0 = 0.065$ (G.T.O.) and $a_f = 0.5$, we obtain $\Delta i \sim -19$ degrees.

For $a_0 = 0.11$ (geostationnary initial orbit), we get $\Delta i \sim -14$ degrees.

This analysis shows that our inclination decreasing strategy is efficient and that it is reasonable to base our trajectory design on an orbital plane change that will occur simultaneously with the semi major axis increase.

However, this approach does not pretend to foresee actual values of the inclination changes nor did the analytical evaluation of the changes in the semi major axis. The values that were obtained in these two

preliminary evaluations were just intended to bring about confidence in strategies that were derived from basic equations of the orbital dynamics.

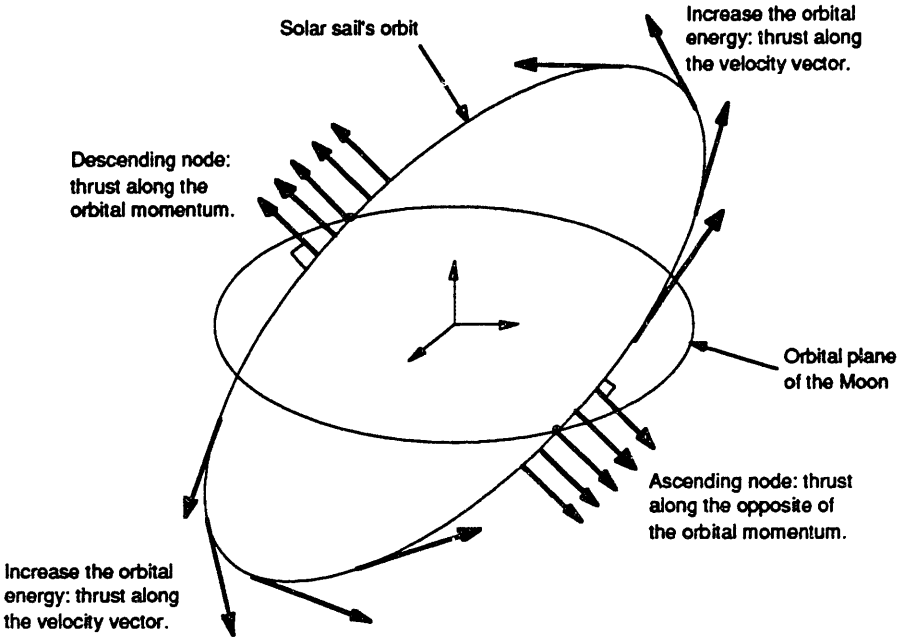

Figure 5: The "general strategy"

3.2.5. Numerical simulations of the general strategy: increasing energy and decreasing inclination

As presented in the above figure the general strategy to orientate the sail during the first part of the trajectory is a combination of three different steering laws. The first scheme was developed in section 3.1. and intends to raise the apogee of the sail's orbit by maximizing the component of the thrust along the velocity vector. The two other schemes are designed for the same goal: decreasing the inclination of the sail's orbital plane with respect to the Moon's orbital plane. One of them maximizes the component of the thrust along the kinetic momentum of the sail's orbit and takes place around the descending node of the sail's trajectory with respect to the Moon's orbital plane, whereas the other scheme takes place around the ascending node and minimizes the component of the thrust along the orbital kinetic momentum.

Simulating trajectories with this kind of steering laws requires the definition of regions around each node where the inclination change schemes are to be applied. These regions were found to be always less than $\frac{\pi}{3}$ wide around each node. However, depending on the initial orientation of the sail's orbit with respect to the Sun, particular values were selected to obtain the greatest change in inclination without loosing too much performance on the semi major axis increase that was

provided by the "increasing energy strategy". Numerical examples are included in Appendix 2 but one of the most efficient cases is presented hereafter. It was shown that for different orientations of the apsidal line with respect to the Earth-Sun direction, the "increasing energy strategy" was more or less efficient, best initial situations were defined when these two lines were separated by angles ranging between -45 and 0 degrees (see section 3.1.3.). It is pleasant to see that these cases are also suitable for the inclination change strategy. Indeed, little loss is induced on the semi major axis increase that was provided by the "increasing energy strategy". Table 4 shows a comparison of both strategies:

α	-45		0		45	
Δi?	no	yes	no	yes	no	yes
a_f	0.498	0.35	0.47	0.42	0.38	0.34
i_f	32	0	25	0	35	0
ap_f	0.82	0.66	0.72	0.7	0.62	0.58

Table 4: Efficiency of the "general strategy".

α is the angle (in degrees) defining the relative orientation of the apsidal line and the Sun-Earth direction (see section 3.1.3.).

$\Delta i?$ states whether the "increasing energy strategy" was applied alone ($\Delta i?$=no) or if the "general strategy" was applied in order to provide inclination control ($\Delta i?$=yes). It is important to know that the trajectories generated by the "increasing energy strategy" last 120 days whereas those generated with the "general strategy" require an additional 50-60 days.

a_f is the final value of the semi major axis in Earth-Moon distance.

i_f is the final value of the inclination with respect to the Moon's orbital plane. For simplicity, this plane was considered to be coplanar with the Ecliptic since its inclination is only 5.15 degrees and its orientation varies in an inertial frame. However this inclination control strategy can be applied to decrease the inclination of an orbit with respect to any well defined plane (i.e. as long as the components of the normal to the plane are known as functions of time).

ap_f is the final value of the apogee altitude in Earth-Moon distance.

In every case it appears that matching the sail's orbital plane with the Moon's orbital plane (which has been approximated by the Ecliptic in these simulations) is possible and that it does not conflict with the semi major axis increase. Following, is the simulation of a solar sail trajectory from low-Earth orbit to a high-Earth orbit with zero final inclination with respect to the Ecliptic. At initial time, the apsidal line and the Sun-Earth direction coincide since, according to the above table this seems to define one of the most favorable case. However, as it may be seen on other cases which are included in Appendix 2, it is possible to

reach high-Earth orbit with zero final inclination with respect to the Ecliptic with other initial orientations of the apsidal line.

Projections of the initial, intermediate and final trajectories on the ecliptic

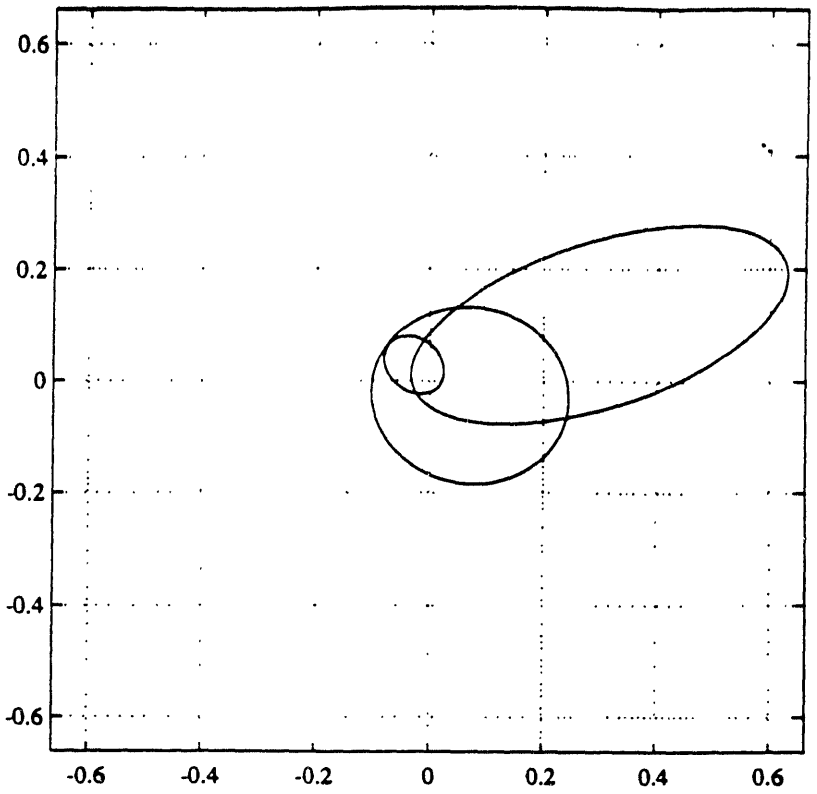

ORBITAL ELEMENTS

	INITIAL VALUES	FINAL VALUES
Semi major axis	0.065	0.3472
Excentricity	0.7	0.9065

The following elements are referenced to the Ecliptic:

Inclination	28	0.141
Ascending node	45	35.38
Argument of perigee	-90	163.2

Inclination control if: $a < 0.2$ and theta < 30 degrees, or

$a > 0.2$ and theta <18 degrees

where theta is the sail's angular position with respect to the nearest node.

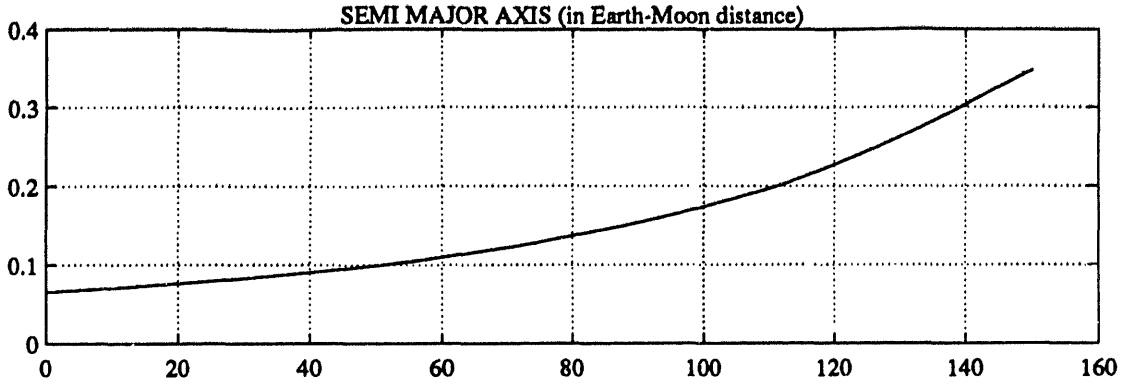
SEMI MAJOR AXIS (in Earth-Moon distance)
0.4
0.3
0.2
0.1
0
0
20
40
60
80
100
120
140
160

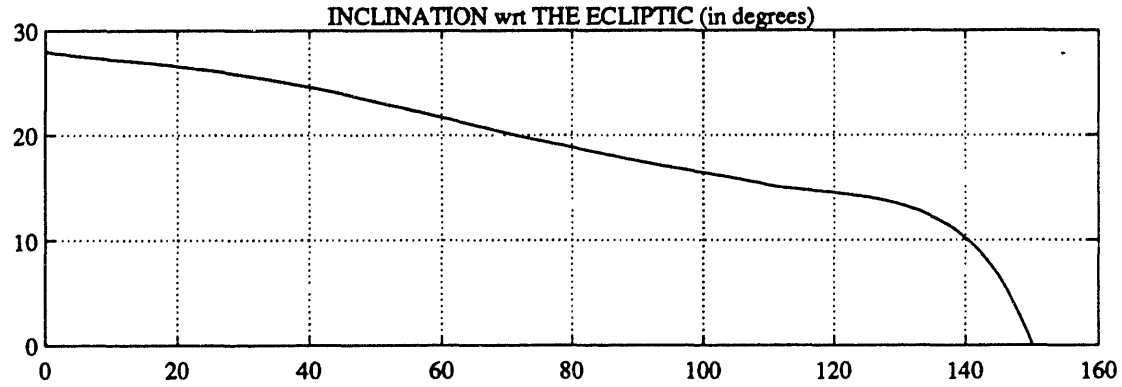
INCLINATION wrt THE ECLIPTIC (in degrees)
30
20
10
0
0
20
40
60
80
100
120
140
160

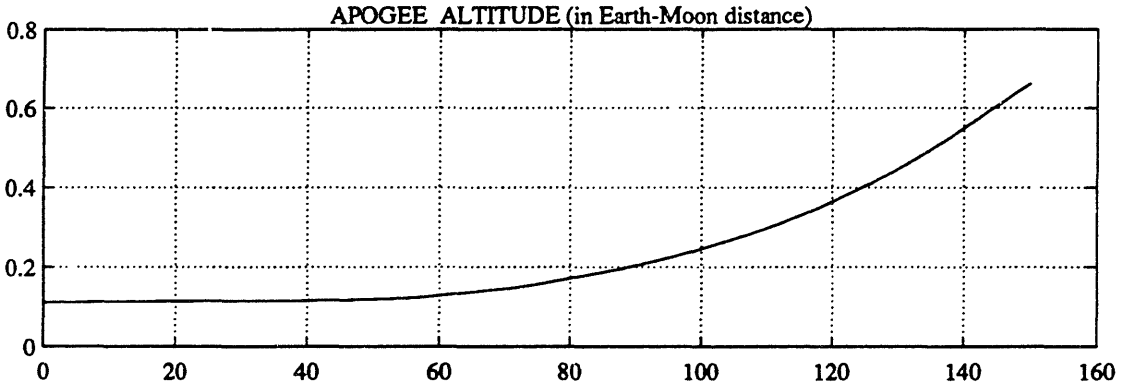
APOGEE ALTITUDE (in Earth-Moon distance)
0.8
0.6
0.4
0.2
0
0
20
40
60
80
100
120
140
160

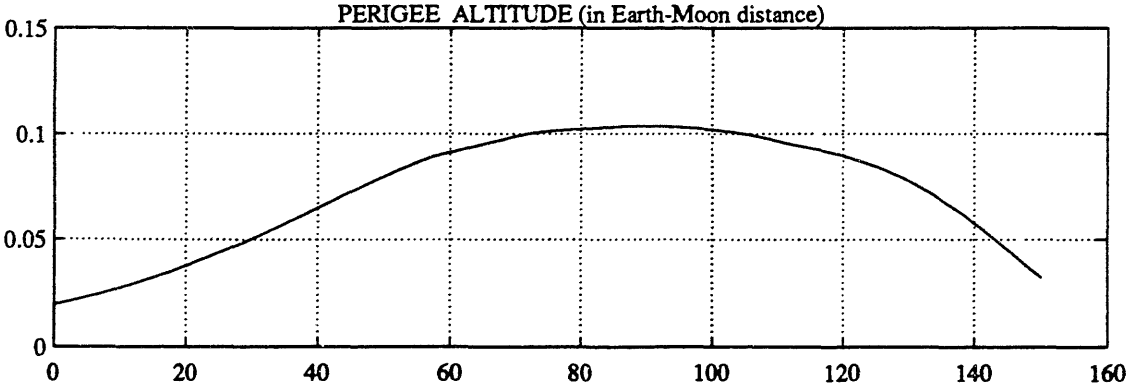
PERIGEE ALTITUDE (in Earth-Moon distance)
0.15
0.1
0.05
0
0
20
40
60
80
100
120
140
160

To conclude this first part, a characterization of the global strategy performances can be stated as follows: typical flight times of 160 days from an initial orbit characterized by a semi major axis of 0.065 Earth-Moon distance and 28 degrees of inclination with respect to the Ecliptic, enable to reach an orbit with zero-inclination and a semi major axis of 0.42 Earth-Moon distance (apogee at 0.62 Earth-Moon distance).

PART 2

THE MINIMUM TIME INTERCEPT PROBLEM

CHAPTER IV

THE OPTIMAL CONTROL PROBLEM

4.1. Assumptions

The second part of this study deals with intercepting a chosen location in the vicinity of the Moon (an intercept is characterized by reaching a given position without specifying the terminal velocity). As it was defined in the framework of the future Earth- Moon "race", a target point behind the Moon was chosen.

Until now, we have assumed that the gravitational attraction of the Moon could be neglected in the equations of the solar sail's dynamics. In this last phase of the Earth-Moon journey, dynamics must be re-established to account for perturbations of the Keplerian orbit (solar sail around the Earth) other than solar pressure and the effects of the Earth's oblateness.

Due to our previous inclination control results, the rendez-vous problem is going to be studied in the planar case. This introduces an approximation into our model since the Moon's orbital plane is slightly inclined with respect to the ecliptic (5.15 degrees). This is acceptable for

two reasons. First it would just be a matter of computer and mathematical overhead to develop a three dimensional approach for the intercept problem, deriving it would not introduce any new difficulties in comparison to the planar case although numerical convergence may become harder to achieve. Second, given the limited actual knowledge about the behavior of a solar sail in space environment, it is not worth developing a highly accurate model of the perturbations when we are not able to assert with equal accuracy the model of the sail's dynamics.

Reducing our problem to a planar one enables us to avoid including a model of the Moon's motion and decreases the number of variables in the optimal control problem. Four state components are needed instead of six, as well as four costate components (Lagrange multipliers) instead of six and finally one control parameter (angle characterizing the setting of the sail) instead of two in the three dimensional problem (cone and clock angles). These variables will be described more carefully in the formulation of the minimum time intercept problem.

4.2. Dynamics of the solar sail

We first write the equations of motion of the Earth, Moon and solar sail in a Sun centered inertial frame. The x- axis of this frame is pointing to a given star or as usually used, towards the γ direction (or vernal

direction, which is defined as the line from Earth towards the point of intersection of the ecliptic and the equator where the Sun crosses the equator from South to North in its apparent annual motion along the ecliptic). The y- axis is chosen to define a direct orthonormal frame in the sense of rotation of the Earth's trajectory.

Let : $\underline{r}_E$ denote the Earth's position vector.

$\underline{r}_M$ denote the Moon's position vector.

$\underline{r}_{SS}$ denote the solar sail's position vector.

μ_E, μ_M and μ_S denote the gravitational constants of the Earth, Moon and Sun.

The equations of motion of the three bodies with respect to the Sun are:

$$\frac{d^2 \underline{r}_E}{dt^2} = -\mu_S \frac{\underline{r}_E}{||\underline{r}_E||^3} - \mu_M \frac{\underline{r}_E - \underline{r}_M}{||\underline{r}_E - \underline{r}_M||^3} \tag{4.1}$$

$$\frac{d^2 \underline{r}_M}{dt^2} = -\mu_S \frac{\underline{r}_M}{||\underline{r}_M||^3} - \mu_E \frac{\underline{r}_M - \underline{r}_E}{||\underline{r}_M - \underline{r}_E||^3} \tag{4.2}$$

$$\frac{d^2 \underline{r}_{SS}}{dt^2} = -\mu_S \frac{\underline{r}_{SS}}{||\underline{r}_{SS}||^3} - \mu_E \frac{\underline{r}_{SS} - \underline{r}_E}{||\underline{r}_{SS} - \underline{r}_E||^3} - \mu_M \frac{\underline{r}_{SS} - \underline{r}_M}{||\underline{r}_{SS} - \underline{r}_M||^3} +$$

acceleration due to solar pressure + effect of J_2. (4.3)

Our vector of interest is $\underline{r} = \underline{r}_{SS} - \underline{r}_E$, the position vector of the solar sail with respect to the Earth. Its dynamics are given by the equation:

$$\frac{d^2(\underline{r}_{SS} - \underline{r}_E)}{dt^2} = -\mu_S\left(\frac{\underline{r}_{SS}}{||\underline{r}_{SS}||^3} - \frac{\underline{r}_E}{||\underline{r}_E||^3}\right)$$

$$-\mu_M\left(\frac{\underline{r}_{SS} - \underline{r}_M}{||\underline{r}_{SS} - \underline{r}_M||^3} - \frac{\underline{r}_E - \underline{r}_M}{||\underline{r}_E - \underline{r}_M||^3}\right) \qquad (4.4)$$

$$-\mu_E\frac{\underline{r}_{SS} - \underline{r}_E}{||\underline{r}_{SS} - \underline{r}_E||^3}$$

+ acceleration due to solar pressure

+ effect of J_2.

The solar sail is submitted to:

1/ Solar gravity gradient: $\underline{a}_1 = -\mu_S\left(\frac{\underline{r}_{SS}}{||\underline{r}_{SS}||^3} - \frac{\underline{r}_E}{||\underline{r}_E||^3}\right)$

2/ Moon gravity: $\underline{a}_2 = -\mu_M\left(\frac{\underline{r}_{SS} - \underline{r}_M}{||\underline{r}_{SS} - \underline{r}_M||^3} - \frac{\underline{r}_E - \underline{r}_M}{||\underline{r}_E - \underline{r}_M||^3}\right)$

3/ Earth gravity: $\underline{a}_3 = -\mu_E\frac{\underline{r}_{SS} - \underline{r}_E}{||\underline{r}_{SS} - \underline{r}_E||^3}$

4/ Solar pressure: $\underline{a}_4 = \lambda\frac{\mu_S}{r_{SS}^2}\cos^2\theta\ \hat{\underline{u}}(\theta)$

Where: λ is the lightness number of the solar sail ($\lambda = 0.1$).

θ is the angle between the Sun to solar sail line and the normal to the sail in the direction of the thrust.

$\hat{\underline{u}}(\theta)$ is the unit vector along the thrust.

5/ Effect of J_2.

4.2.1. Approximate ranges of the different accelerations

Solar gravity gradient: $$\underline{a}_1 = -\mu_S \left(\frac{\underline{r}_{SS}}{||\underline{r}_{SS}||^3} - \frac{\underline{r}_E}{||\underline{r}_E||^3} \right)$$

We want to give an upper bound to this source of acceleration. The "worst case" happens when the Sun, the Earth and the solar sail are aligned with the Earth between the two others. Then, the magnitude of this acceleration is maximum when the solar sail is in the vicinity of the Moon, and its value reaches $1.6\ 10^{-6}\ g_0$.

$$|a_1| \leq 1.6\ 10^{-6}\ g_0. \tag{4.5}$$

Moon gravity: $$|a_2| \approx \mu_M \left(\frac{1}{||\underline{r}_{SS} - \underline{r}_M||^2} \pm 1 \right) \tag{4.6}$$

Earth gravity: $$|a_3| \approx \mu_E \frac{1}{(1 - ||\underline{r}_{SS} - \underline{r}_M||)^2} \tag{4.7}$$

Solar pressure: $$|a_4| \approx 6.\ 10^{-5}\ g_0 \tag{4.8}$$

Oblateness: From reference [31] the acceleration due to the J_2 term of the Earth's gravitational potential is given by:

$$\begin{bmatrix} a_{dr} \\ a_{d\theta} \\ a_{dh} \end{bmatrix} = -\frac{3\ \mu_E\ J_2\ R_{eq}^2}{2\ ||\underline{r}_{SS} - \underline{r}_E||^4} \begin{bmatrix} 1 - 3\ \sin^2\theta\ \sin^2 i \\ \sin 2\theta\ \sin^2 i \\ \sin\theta\ \sin 2i \end{bmatrix} \tag{4.9}$$

Where: a_{dr}, $a_{d\theta}$ and a_{dh} are the components of the acceleration in the classical orthoradial orbital frame (a_{dr} along the position vector,

a_{dh} along the kinetic momentum of the orbit and $a_{d\theta}$ so that $(a_{dr}, a_{d\theta}, a_{dh})$ defines a direct frame).

The magnitude of this acceleration can then be approximated by:

$$|a_5| \approx \frac{3\,\mu_E\,J_2\,R_{eq}^2}{2(1 - \|\underline{r}_{SS} - \underline{r}_M\|^4)} \quad \text{with:} \begin{cases} J_2 = 1.08228\ 10^{-3} \\ R_{eq} = 1.66\ 10^{-2} \text{ unit of length} \end{cases}$$

$$|a_5| \approx \frac{1.229\ 10^{-10}}{(1 - \|\underline{r}_{SS} - \underline{r}_M\|)^4}\, g_0 \quad \text{with: } g_0 = \begin{cases} 9.81 \text{ m/s}^2 \\ 190.47 \text{ unit of length / day}^2 \end{cases}$$

We can summarize these results by the following table:

Sun's gravity gradient	$\approx 1.5\ 10^{-6}\, g_0$
Moon's gravity	$\approx (\frac{1}{r^2} - 1)\, 3.4\ 10^{-6}\, g_0$
Earth's gravity	$\approx \frac{2.75\ 10^{-4}}{(1 - r)^2}\, g_0$
Solar pressure	$\approx 6.\ 10^{-5}\, g_0$
J_2	$\approx \frac{1.23\ 10^{-10}}{(1 - r)^4}\, g_0$

Table 5: Approximate range of each acceleration source.
(r is the distance between the solar sail and the Moon)

This study of the various accelerations is going to help us choose a dynamical model for the intercept part of the trajectory. Out of the five

sources of acceleration, we are only keeping three into account. We decided to neglect the Sun's gravity gradient since its magnitude is low all along the path from the Earth to the Moon. We will also neglect the acceleration due to the J_2 term. For the latter, the approximation is valid at high altitude above the Earth, whereas it is not so accurate around a low perigee. However our planar model is already a source of approximation and taking the oblateness in consideration in this "high" part of the trajectory would not be in agreement with the degree of accuracy that is defined by the planar model.

Figure 6 shows the range of each kind of acceleration as functions of the distance between the solar sail and the Earth.

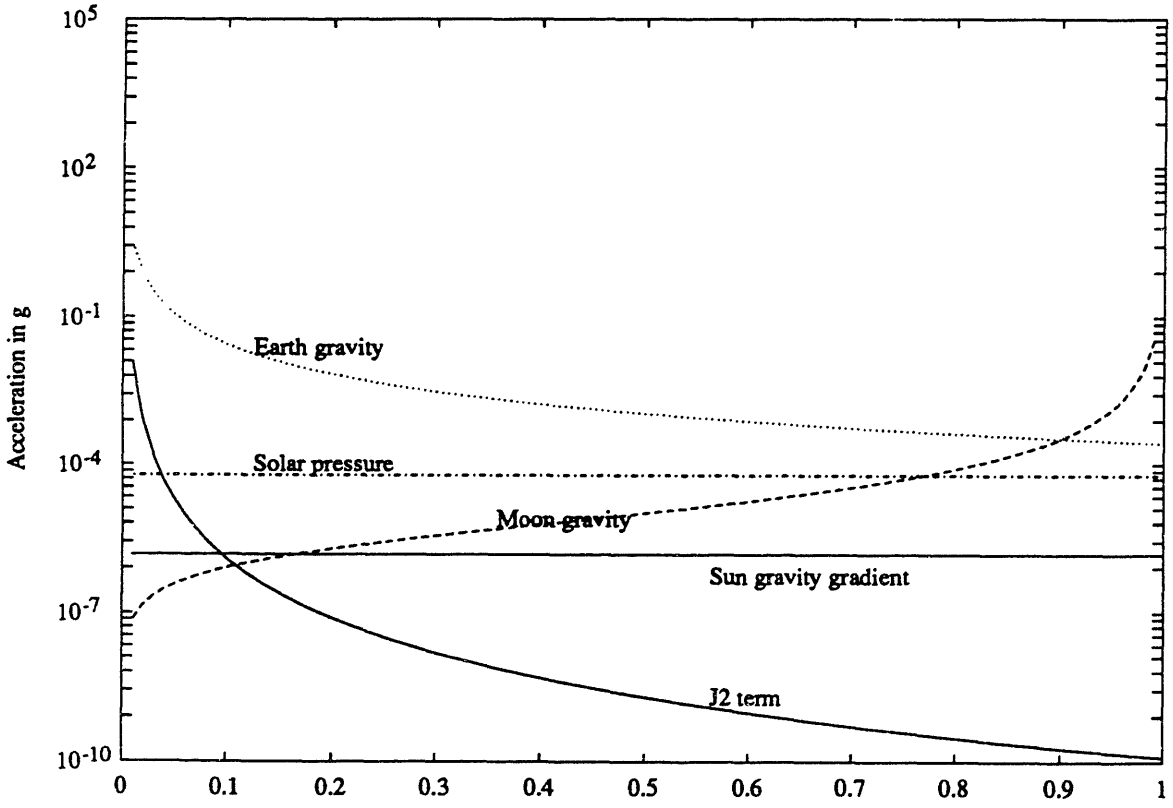

Figure 6: Acceleration sources vs distance from the Earth (in Earth-Moon distance)

Our model of the dynamics needs to be relevant for orbits with semi major axis larger than 50% of the Earth-Moon distance (384,400 km). Figure 6 shows that it is acceptable to neglect the Sun gravity gradient and the effect of the J_2 term at such altitudes. Eventually, our model of the solar sail motion includes the Earth's attraction, the Moon's attraction (with its two terms) and the acceleration due to solar pressure.

$$\frac{d^2 (\underline{r}_{SS} - \underline{r}_E)}{dt^2} = - \mu_E \frac{\underline{r}_{SS} - \underline{r}_E}{|| \underline{r}_{SS} - \underline{r}_E ||^3} - \mu_M \left(\frac{\underline{r}_{SS} - \underline{r}_M}{|| \underline{r}_{SS} - \underline{r}_M ||^3} - \frac{\underline{r}_E - \underline{r}_M}{|| \underline{r}_E - \underline{r}_M ||^3} \right)$$

$$+ u_{Max} \cos^2\theta \, \hat{\underline{u}}(\theta) \qquad (4.10)$$

It can be written in terms of the position vector of the solar sail with respect to the Earth: $\underline{r} = \underline{r}_{SS} - \underline{r}_E$.

$$\frac{d^2 \underline{r}}{dt^2} = - \mu_E \frac{\underline{r}}{|| \underline{r} ||^3} - \mu_M \left(\frac{\underline{r} + \underline{r}_E - \underline{r}_M}{|| \underline{r} + \underline{r}_E - \underline{r}_M ||^3} - \frac{\underline{r}_E - \underline{r}_M}{|| \underline{r}_E - \underline{r}_M ||^3} \right)$$

$$+ u_{Max} \cos^2\theta \, \hat{\underline{u}}(\theta) \qquad (4.11)$$

4.3. Formulation of the minimum time intercept problem

The general problem can be stated as follows:

1/ given an initial orbit and a position on this orbit.

2/ given the model of the solar sail dynamics.

3/ given a desired final position: $\underline{r}(t_f) = \underline{r}_f$.

4/ given the initial positions of the Sun and of the Moon.

find the control law θ(t) for t0<t<tf that minimizes the time tf to reach our final desired position.

Through-out this study, our desired final position is going to be a given location behind the Moon: behind meaning that the sail cannot be seen from the Earth.

In order to find a solution to this problem, the optimal control theory and the calculus of variations will be used (formulations and derivations of the optimal control law will be in agreement with the Minimum Principle). As a result, we are going to be faced with a two-point-boundary-value-problem (TPBVP), that must be solved numerically.

For a complete derivation of the necessary conditions for optimality of the control law we will use as a reference: Applied Optimal Control by Bryson & Ho, and more precisely: their minimum-time section (see reference [32]).

Our state vector is composed of the position and velocity vectors of the solar sail in an Earth centered inertial frame. The dynamics of the solar sail can be formulated by:

$$\frac{d}{dt}\begin{bmatrix}\underline{r}\\ \underline{v}\end{bmatrix} = \begin{bmatrix}\underline{v}\\ \underline{f}(\underline{r},\theta,t)\end{bmatrix} \tag{4.12}$$

$$\underline{f}(\underline{r},\theta,t)) = -\mu_E \frac{\underline{r}}{||\underline{r}||^3} - \mu_M\left(\frac{\underline{v}}{||\underline{v}||^3} - \frac{\underline{r}_E - \underline{r}_M}{||\underline{r}_E - \underline{r}_M||^3}\right) + u_{Max}\cos^2\theta\ \hat{\underline{u}}(\theta)$$

$$\underline{Y} = \underline{r} + \underline{r}_E - \underline{r}_M$$

Our criterion to be minimized is: $J = \int_{t_0}^{t_f} 1 \, dt$ •13•

Hence we have defined the Hamiltonian of the problem:

$$H = 1 + \underline{\lambda}_r^T \underline{v} + \underline{\lambda}_v^T \underline{f}(\underline{r},\theta,t)) \qquad \bullet 14 \bullet$$

Where: $\underline{\lambda}_r$ is the costate of the position vector.

$\underline{\lambda}_v$ is the costate of the velocity vector, it is often called the primer vector (see reference •r4.3•) and bears a very important property as it will be seen when deriving the optimal setting of the sail.

4.3.1 Optimal setting of the sail

The optimality of the angle θ is provided by the following relation:

$$\theta opt = \underset{-\frac{\pi}{2} < \theta < \frac{\pi}{2}}{\text{Arg Min}} \{ H(\underline{r},\theta,t) \} \qquad \bullet 15 \bullet$$

The constraint $-\frac{\pi}{2} < \theta < \frac{\pi}{2}$ accounts for the requirement that the sail must always be oriented so that the reflecting side is towards the solar radiation and thus, no thrust can be applied towards the Sun.

A necessary condition is that:

$$\frac{\partial H}{\partial \theta}(\theta opt) = 0 \qquad \bullet 16 \bullet$$

The only part of the Hamiltonian that depends on the angle θ is:

$$\tilde{H}(\theta) = \underline{\lambda_V}^T \; u_{Max} \cos^2\theta \; \underline{u}(\theta)$$

This expression shows the general result about the primer vector $\underline{\lambda_V}$: θ must be chosen so as to maximize the projection of the thrust on - $\underline{\lambda_V}$.

$$\theta opt = \underset{-\frac{\pi}{2} < \theta < \frac{\pi}{2}}{Arg\ Max} \left\{ - \cos^2\theta \; \underline{\lambda_V}^T \; \underline{u}(\theta) \right\} \qquad (4.17)$$

θ denotes the angle between the Sun to solar sail direction and the thrust vector. Let us define ζ as the angle between the Sun to solar sail line and the primer vector $\underline{\lambda_V}$.

$$\tilde{H}(\theta) = u_{Max} \cos^2\theta \; (\cos\zeta \cos\theta + \sin\zeta \sin\theta) \qquad (4.18)$$

The extreme values $\theta = \pm\frac{\pi}{2}$ are to be avoided since they define settings of the sail that provide no thrust because the sail is only "showing its edge" to the Sun. The following derivation is quite similar to the one that was done in the first part, but the final expression is going to be slightly different.

$$\left\{ \frac{\partial H}{\partial \theta} = 0 \right\} \qquad \Leftrightarrow \qquad \{ \; 2 \sin\zeta \tan^2\theta + 3 \cos\zeta \tan\theta - \sin\zeta = 0 \; \} \qquad (4.19)$$

We thus have two solutions: $\tan\theta = \dfrac{- 3 \cos\zeta \pm \sqrt{8 + \cos^2\theta}}{4 \sin\zeta}$

One is going to maximize $\tilde{H}(\theta)$ and the other one is going to minimize it. To get rid of the indetermination, let us consider the case where $\zeta = \frac{\pi}{2}$, then $\tan\theta = \pm\frac{\sqrt{8}}{4}$. $H(\theta)$ will be minimized if $\tan\theta = -\frac{\sqrt{8}}{4}$.

We now have a closed form expression for the optimal setting of the sail in terms of the primer vector angle ζ:

$$\theta_{opt} = -\,\mathrm{Atan}\left[\frac{3\cos\zeta + \sqrt{8 + \cos^2\zeta}}{4\sin\zeta}\right] \qquad (4.20)$$

This expression is the same as in Sauer's paper (reference [24]) and complies with the constraints: $-\frac{\pi}{2} < \theta < \frac{\pi}{2}$ because of the Atan(x) domain.

4.3.2. Dynamics of the Lagrange multipliers

The formulation of the minimization problem, involves two sets of differential equations. First, the dynamics of the state vector, which has been studied in the preceding section. Second, the dynamics of the Lagrange multiplier vector associated with the state vector.

The general expression of this set of first order differential equation is:

$$\frac{d}{dt}\left[\underline{\lambda}^T\right] = -\frac{\partial H}{\partial \underline{x}} \qquad (4.21)$$

Where: $\underline{x}$ is the state vector.

$\underline{\lambda}$ is the vector of Lagrange multipliers (or costate vector).

H is the Hamiltonian of the problem.

Here, we have:

$$\begin{cases} \frac{d}{dt}\lambda_{\underline{r}}^{T} = -\frac{\partial H}{\partial \underline{r}} \\ \frac{d}{dt}\lambda_{\underline{v}}^{T} = -\frac{\partial H}{\partial \underline{v}} \end{cases} \tag{4.22}$$

with:

$$H = 1 + \lambda_{\underline{r}}^{T}\,\underline{v} + \lambda_{\underline{v}}^{T}\,\underline{f}(\underline{r},\theta,t)) \tag{4.23}$$

from which:

$$\dot{\lambda}_{\underline{v}} = -\lambda_{\underline{r}} \tag{4.24}$$

Let us now derive the expression of $\dot{\lambda}_{\underline{r}}$.

$$\dot{\lambda}_{\underline{r}}^{T} = -\frac{\partial H}{\partial \underline{r}} = -\lambda_{\underline{v}}^{T}\frac{\partial \underline{f}(\underline{r},\theta,t)}{\partial \underline{r}} \tag{4.25}$$

$$\underline{f}(\underline{r},\theta,t) = -\mu_E\frac{\underline{r}}{||\underline{r}||^3} - \mu_M\left(\frac{\underline{y}}{||\underline{y}||^3} - \frac{\underline{r}_E - \underline{r}_M}{||\underline{r}_E - \underline{r}_M||^3}\right) + u_{Max}\cos^2\theta\,\hat{\underline{u}}(\theta)$$

Eventually, the dynamics of the Lagrange multipliers are given by:

$$\begin{cases} \dot{\lambda}_{\underline{r}} = -M\,\lambda_{\underline{v}} \\ \dot{\lambda}_{\underline{v}} = -\lambda_{\underline{r}} \end{cases}$$

$$M = \frac{\partial \underline{f}}{\partial \underline{r}} = -\mu_E\frac{r^2 I_2 - 3\,\underline{r}\,\underline{r}^T}{r^5} - \mu_M\frac{y^2 I_2 - 3\,\underline{y}\,\underline{y}^T}{y^5}$$

$\underline{y} = \underline{r} + \underline{r}_E - \underline{r}_M$: position vector with respect to the Moon.

4.3.3. Boundary conditions

At t_0: position and velocity of the solar sail are given:

$$\underline{r}(t_0) = \underline{r}_0 \quad \underline{v}(t_0) = \underline{v}_0$$

Hence, the costate vectors $\lambda_{\underline{r}}(t_0)$ and $\lambda_{\underline{v}}(t_0)$ are free .

At t_f: position is given: $\underline{r}(t_f) = (1 + \varepsilon)\,\underline{r}_{Moon}(t_f)$ with $0<\varepsilon<1$.

velocity is free.

Hence $\lambda_{\underline{v}}(t_f)$ has to be $\underline{0}$ and $\lambda_{\underline{r}}(t_f)$ is free.

Optimality condition for t_f : $H(t_f) = 0$

4.3.4. The two-point-boundary-value-problem

Given the parameters: $\underline{r}(t_0), \underline{v}(t_0)$.

Guess: $\lambda_{\underline{r}}(t_0)$, $\lambda_{\underline{v}}(t_0)$ and t_f (5 unknowns).

So that, using the dynamics:

$$\begin{cases} \dot{\underline{r}} = \underline{v} \\ \dot{\underline{v}} = \underline{f}(\underline{r}, \theta_{opt}, t) \\ \dot{\lambda}_{\underline{r}} = -M\,\lambda_{\underline{v}} \\ \dot{\lambda}_{\underline{v}} = -\lambda_{\underline{r}} \\ \theta_{opt} = -\mathrm{Atan}\left[\dfrac{3\cos\zeta + \sqrt{8 + \cos^2\zeta}}{4\sin\zeta}\right] \end{cases}$$

we reach:

$$\begin{cases} \underline{r}(t_f) = (1 + \varepsilon)\,\underline{r}_{Moon}(t_f) \\ \lambda_{\underline{v}}(t_f) = \underline{0} \\ H(t_f) = 0 \end{cases} \qquad \text{(5 equations)}$$

The general minimum time problem is thus presented as a system of five non linear equations in five unknowns, solving it produces a local-minimum-time trajectory.

CHAPTER V

FINDING A SOLUTION TO THE INTERCEPT PROBLEM

Numerical methods become necessary to solve the system of five non-linear equations that characterize the minimum time intercept problem. However, before applying a Newton-Raphson algorithm, there are several remarks that can be made and simplifications that are possible to reduce the complexity of our numerical problem.

5.1. Simplifications of the two-point-boundary-value-problem

5.1.1. Scaling of the Lagrange multipliers

Based on reference [32] and on a previous work on solar-sail trajectory optimization by Dr. D. Flament (reference [34]), several simplifications can be applied to the two-point-boundary-value-problem that was defined in chapter IV.

Let us consider a first guess of the five unknowns $\lambda_{\underline{r}}(t_0)$, $\lambda_{\underline{v}}(t_0)$ and t_f. This choice leads to final values $\underline{r}(t_f)$, $\underline{v}(t_f)$, $\lambda_{\underline{r}}(t_f)$ and $\lambda_{\underline{v}}(t_f)$.

Let us now consider a new guess, which differs from the first only by the fact that the Lagrange multipliers are all multiplied by a given factor k. Our new guess is now, $k\,\lambda_{\underline{r}}(t_0)$, $k\,\lambda_{\underline{v}}(t_0)$ and t_f. These initial values of the Lagrange multipliers, together with the initial values of the state: $\underline{r}(t_0)$ and $\underline{v}(t_0)$ are propagated from t_0 to t_f according to the equations of the sail's dynamics.

First remark: The sail's dynamics depend on the dynamic equations of the costate only through the formula defining the optimal setting angle: θ_{opt}.

Second remark: The determination of θ_{opt} requires only the knowledge of the direction of the primer vector $\lambda_{\underline{v}}$. The magnitude $||\lambda_{\underline{v}}||$ does not matter in the computation of θ_{opt}.

Third remark: From the two previous remarks and given the linear form of the equations of the dynamics of the Lagrange multipliers, we conclude that: guessing $k\lambda_{\underline{r}}(t_0)$ and $k\lambda_{\underline{v}}(t_0)$ is not going to change the history of the state's dynamics: $\underline{f}(\underline{r},\theta,t)$, $t_0 \le t \le t_f$. Hence, only the final values of the costate components are going to change by a factor of k, the state components at final time will be the same as with the first guess.

Given $\underline{r}(t_0)$ and $\underline{v}(t_0)$:

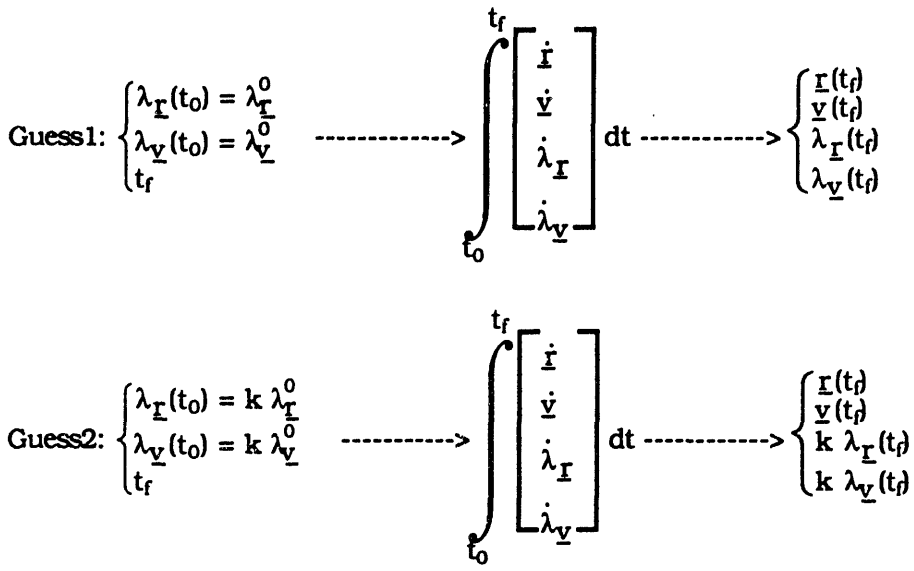

This scaling property is going to reduce the order of the system of non linear equations from 5 to 4.

5.1.2. Reducing the order of the system

Since the vector of Lagrange multipliers can be scaled, we can get rid of one component of the primer vector at initial time. Indeed, the primer vector at t_0 cannot be $\underline{0}$ since the value of the final time (which is the performance index) does obviously depend on the initial magnitude and orientation of the velocity vector (the primer vector is the costate of the velocity vector). By choosing an appropriate frame, we can make sure that the first component of the primer vector at t_0 is not equal to zero.

Instead of having the five components: $\lambda_{r_x}(t_0)$, $\lambda_{r_y}(t_0)$, $\lambda_{v_x}(t_0)$, $\lambda_{v_y}(t_0)$ and tf, we end up with the four variables to be guessed:

$$\frac{\lambda_{r_x}(t_0)}{\lambda_{v_x}(t_0)}, \frac{\lambda_{r_y}(t_0)}{\lambda_{v_x}(t_0)}, \frac{\lambda_{v_y}(t_0)}{\lambda_{v_x}(t_0)} \text{ and } t_f.$$

We can also get rid of one equation, namely $H(t_f) = 0$.

$$H(t_f) = 1 + \underline{\lambda_r}^T \underline{v}(t_f) + \underline{\lambda_v}^T \underline{f}(\underline{r},\theta,t_f) \text{ or more compactly: } H(t_f) = 1 + \underline{\Delta}^T \dot{\underline{X}}$$

If a first choice of initial Lagrange multipliers $\underline{\Delta}(t_0)$ satisfies both of the following boundary conditions:

$$\begin{cases} \underline{\lambda_v}(t_f) = \underline{0} \\ \underline{r}(t_f) = (1 + k)\, \underline{r}_{Moon}(t_f) \end{cases}$$

Then the new choice of initial costates $\frac{\underline{\Delta}(t_0)}{\kappa}$ will still bring these two equations to zero but for a particular value of κ, $H(t_f)$ will also be equal to zero. This value of κ is: $\kappa = -\left(\underline{\lambda_r}^T \underline{v}(t_f) + \underline{\lambda_v}^T \underline{f}(\underline{r},\theta,t_f) \right)$ (5.1)

The new system of non-linear equations that needs to be solved is of order 4 and can be put in the form:

$$F(\underline{\alpha}) = \underline{0}$$

$$\begin{cases} \alpha_1 = \lambda_{r_x}(t_0) \\ \alpha_2 = \lambda_{r_y}(t_0) \\ \alpha_3 = \lambda_{v_y}(t_0) \\ \alpha_4 = t_f \end{cases} \quad \text{-------F--------} > \quad \begin{cases} F_1(\underline{\alpha}) = r_x(t_f) - (1 + \varepsilon)\, r_{x_{Moon}}(t_f) \\ F_2(\underline{\alpha}) = r_y(t_f) - (1 + \varepsilon)\, r_{y_{Moon}}(t_f) \\ F_3(\underline{\alpha}) = \lambda_{v_x}(t_f) \\ F_4(\underline{\alpha}) = \lambda_{v_y}(t_f) \end{cases}$$

5.2. Looking for a sub-optimal solution

The above system of equations can be interpreted as the minimization of the norms of two vectors: $\underline{v}_1 = \underline{r}(t_f) - (1 + \varepsilon)\,\underline{r}_{Moon}(t_f)$ and $\underline{v}_2 = \lambda_{\underline{V}}(t_f)$. Minimizing each of these two vector norms defines two coupled problems. However, we are going to consider solving the intercept problem alone:

$$\underset{\underline{\alpha}}{\text{Min}} \left\{ \| \underline{r}(t_f) - (1 + \varepsilon)\,\underline{r}_{Moon}(t_f) \| \right\} \qquad (5.2)$$

What sort of a solution can we obtain when ignoring the final norm of the primer vector?

First, the trajectory that will be defined by solving this intercept problem will reach the target point behind the Moon, which is our primary goal.

Second, this trajectory is still a minimum time trajectory. If we call $\underline{v}_f$ the final velocity of the solar sail at the target point, the trajectory that we obtained, is the minimum time trajectory that leads to the target point with a final velocity $\underline{v}_f$.

Bringing $\lambda_{\underline{V}}(t_f)$ to zero will make sure that all neighboring trajectories, no matter what their final velocity $\underline{v}(t_f)$ are, require a longer flight time t_f.

The biggest asset of solving the intercept problem alone is that it brings down the system of non-linear equations to a single equation for which all the techniques of non-linear programming are available:

$$|| \underline{r}(t_f) - (1 + \varepsilon)\underline{r}_{Moon}(t_f) || = 0 \qquad (5.3)$$

5.3 Solving the simplified intercept problem

We are now faced with a single non-linear equation: $f(\underline{\alpha}) = 0$, where $\underline{\alpha}$ has four components: $\lambda_{r_x}(t_0)$, $\lambda_{r_y}(t_0)$, $\lambda_{v_y}(t_0)$ and t_f.

There are two aspects in the search of a solution α^* to this problem:

1/ A good algorithm: which means robustness and good convergence rate.

2/ A good initial guess to start the algorithm: $\underline{\alpha}_0$.

5.3.1. A good algorithm

With the appearance of a new set of Matlab functions in the frame of the "Optimization Toolbox" it has been possible to avoid coding a minimization algorithm. There are actually several kinds of algorithms devoted to non-linear unconstrained minimization. In the case of our scalar function, quasi-Newton methods are available in several Matlab routines since September 1990.

The Broyden-Fletcher-Godfarb-Shanno (BFGS) method is the best quasi-Newton method currently known and we are going to present the basics of this algorithm which has been coded in the Matlab routine fminu.m.

The BFGS method is a quasi-Newton method in the sense that every iteration of the algorithm is of the form (reference [35]):

$$X_{k+1} = X_k - \alpha_k D_k \nabla f(X_k) \tag{5.4}$$

Where f(X) is to be minimized.

For the Newton method, $D_k = [\nabla^2 f(X_k)]^{-1}$ and $\alpha_k = 1$; here D_k is an approximation of the inverse of the Hessian matrix and is updated according to the set of formula:

$$D_{k+1} = D_k + \frac{p_k p_k^T}{p_k^T p_k} - D_k \frac{q_k q_k^T}{q_k^T D_k q_k} + \tau_k v_k v_k^T \tag{5.5}$$

$$v_k = \frac{p_k}{p_k^T q_k} - \frac{D_k q_k}{\tau_k} \tag{5.6}$$

$$\tau_k = q_k^T D_k q_k \tag{5.7}$$

$$p_k = X_{k+1} - X_k \tag{5.8}$$

$$q_k = \nabla f(X_{k+1}) - \nabla f(X_k) \tag{5.9}$$

In our case, the function f does not have an analytical expression for its gradient which must be calculated through finite differences. The function f(x) is calculated according to the following description:

$\underline{r}(t_0)$ and $\underline{v}(t_0)$ are given.

$$\begin{cases} \alpha_1 = \lambda_{r_x}(t_0) \\ \alpha_2 = \lambda_{r_y}(t_0) \\ \alpha_3 = \lambda_{v_y}(t_0) \\ \alpha_4 = t_f \end{cases} \quad \text{-------->} \quad \int_{t_0}^{t_f} \begin{bmatrix} \dot{\underline{r}} \\ \dot{\underline{v}} \\ \dot{\lambda}_{\underline{r}} \\ \dot{\lambda}_{\underline{v}} \end{bmatrix} dt \quad \text{------>} \quad f(\underline{\alpha}) = \| \underline{r}(t_f) - (1 + \varepsilon)\, \underline{r}_{Moon}(t_f) \|$$

5.3.2. A good guess for the initial costate vector and the final time

To guess a good value for the four variables $\lambda_{r_x}(t_0)$, $\lambda_{r_y}(t_0)$, $\lambda_{v_y}(t_0)$ and t_f, we make various evaluations of the function $f(\underline{\alpha})$ which needs to be brought to zero.

The special form of the function makes it possible to guess by using graphical outputs. The evaluation of $f(\underline{\alpha})$ requires the numerical integration of eight first order differential equations from t_0 to t_f. The eight variables are $\underline{r}$, $\underline{v}$, $\lambda_{\underline{r}}$ and $\lambda_{\underline{v}}$ (4 two-dimensional vectors) and plotting $\underline{r}$ gives a graphical view of the trajectory.

Combined with a plot of the Moon's trajectory between t_0 and t_f, each evaluation of $f(\underline{\alpha})$ shows how changes in $\underline{\alpha}$ induce changes in the final position of the solar sail with respect to the Moon. Then, given a large value of t_f, variations on the three parameters $\alpha_1 = \lambda_{r_x}(t_0)$, $\alpha_2 = \lambda_{r_y}(t_0)$ and $\alpha_3 = \lambda_{v_y}(t_0)$ make it possible to reach a near-lunar location. Reducing

t_f until the final point of the trajectory is at the near-lunar location, enables the full starting guess of the four parameters to be optimized.

For reasons of easy graphical output and practical coding, the main routine was coded in the Matlab language. However, to increase the speed of each function evaluation (one function evaluation is equivalent to the computation of a whole trajectory), the computation of the derivatives of the state and costate was coded in C (reference [36]) and compiled to define a new Matlab function. This procedure speeded up the whole program by a factor of 60 and made each function evaluation last less than three seconds (on a Sun Sparkstation).

5.2.3. Numerical simulations of the intercept

The near lunar location that is chosen as the intercept point is 15,600 km behind the Moon's center. Several cases were solved but all were associated with the same initial elliptic orbit which characteristics are:

semi major axis: a=0.7 Earth-Moon distance.

eccentricity: e=0.7.

inclination with respect to the ecliptic: i=0.

angle between the apsidal line and the Sun radiation: α=90 deg.

Then, each case was defined by a different initial position of the Moon. Four values of the angle between the apsidal line and the Earth-Moon direction were considered: 0, 90, 180 and 270 degrees. The four

associated intercept trajectories are shown in Appendix 3. They all share the joint feature that they last less than 30 days.

Those trajectories are extremal trajectories since they are the minimum-time trajectories that lead to the required location with the final velocity that is reached. However these trajectories are not local minimum-time trajectories since the final norm of the primer vector has not been brought to zero, which means that neighboring trajectories with slightly different final velocity vectors may require less time to reach the intercept position.

We are now going to present one of those intercept trajectories and the associated initial and final values of the optimization parameters.

Initial position of the Moon.	+ 90 deg. wrt the apsidal line.		
Desired final position.	15,600 km behind the Moon.		
Optimized value of the final time.	24.19 days.		
Distance from goal at tf.	0.048 kilometers.		
Optimized value of the costate at t_0.	0.123	-0.67	-4.10

Table 6: Characteristics of the intercept trajectory (Moon(t_0)= 90deg.)

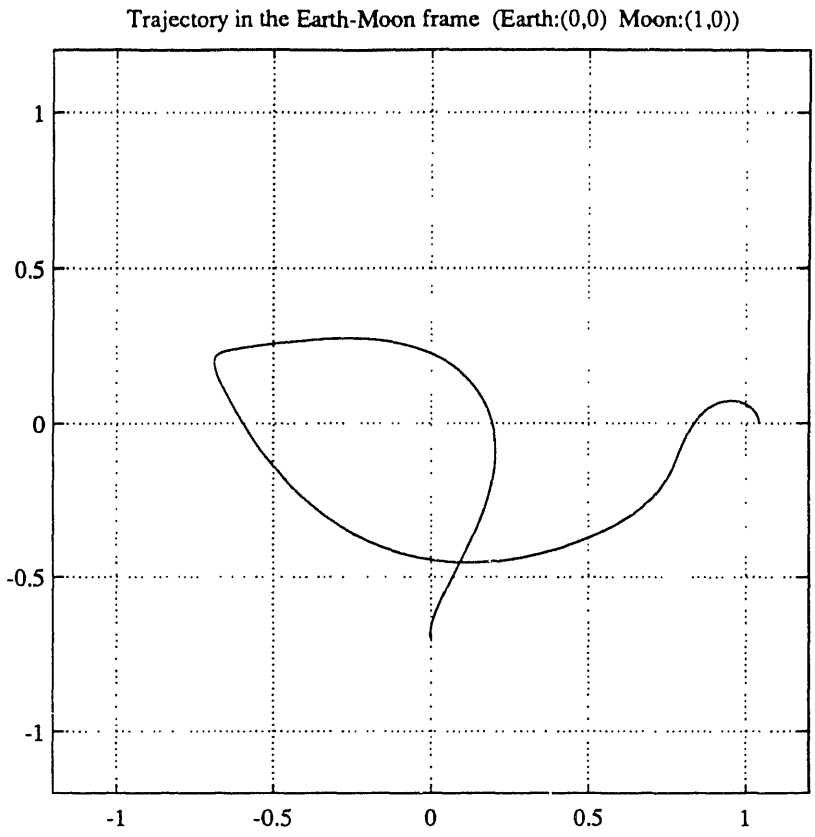
Trajectory in the Earth-Moon frame (Earth:(0,0) Moon:(1,0))
1
0.5
0
-0.5
-1
-1
-0.5
0
0.5
1

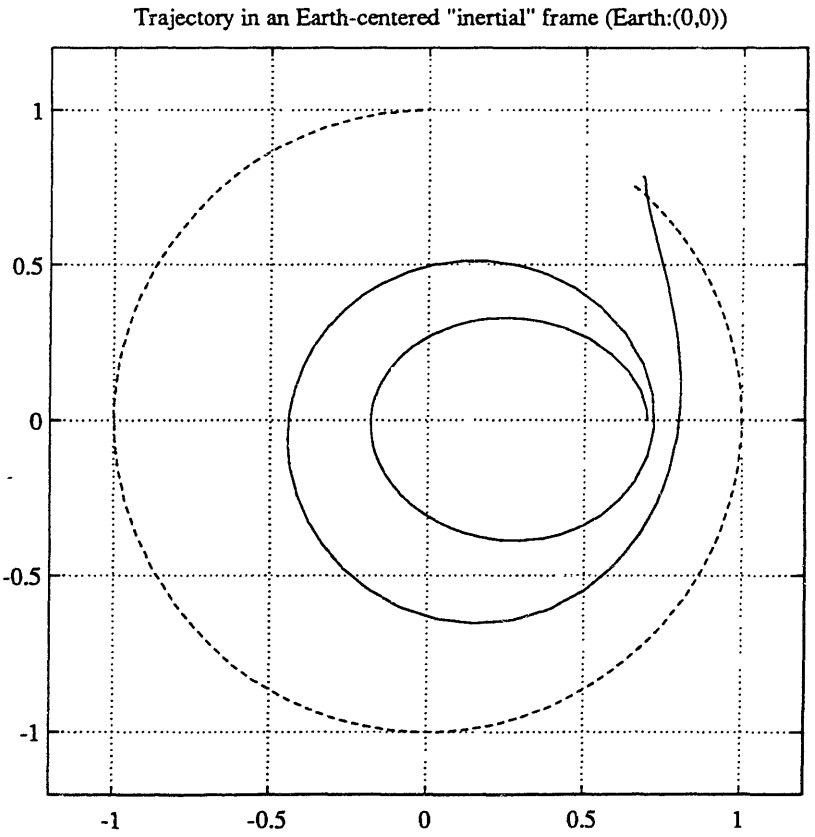
Trajectory in an Earth-centered "inertial" frame (Earth:(0,0))
1
0.5
0
-0.5
-1
-1
-0.5
0
0.5
1

EPILOGUE

CHAPTER VI

CONCLUSIONS

The simulations of the intercept phase of the trajectory bring the solar sail to its final location and bring this study to an end. One of its main feature is the fact that it dealt with both parts of the Earth-Moon "race" trajectory. Until now, most of the work done on solar sail trajectory design was focused on either the planetocentric part (see references [19], [20] and [25]) or on the interplanetary part (see references [24] and [37]). The two parts of this document intend to cover the whole length of the trajectory, from low-Earth departure (perigee at 7,500 km and apogee at 42,000 km from the Earth's center), to the near-lunar intercept point (15,600 km behind the Moon). A steering law is associated with each phase of the trajectory, and we are now going to summarize the two orientation schemes that were developed.

In the first part of the flight from GTO to approximately half of the distance to the Moon, the steering law was based upon heuristic law design: the semi major axis was increased by orientating the thrust along the velocity vector and the inclination with respect to the Ecliptic was brought to zero by orientating the thrust along the orbital kinetic momentum or its opposite in the vicinity of the nodes. In this part of the flight, an averaging technique was used for simulation. These

simulations became questionable at semi major axis of a=0.5 Earth-Moon distance when $\Delta a/a$ = 5% per orbit. A more complete study would integrate further (even from GTO) without averaging. This part of the flight (from GTO to a=0.5) requires about 160 days.

The goal of raising the semi major axis (a) will not lead to lunar intercept. For this reason, the guidance for the second phase of the flight is achieved with an optimal control formulation. For this flight portion, from an elliptical orbit with e=0.7 and a=0.7 Earth-Moon distance to lunar fly-by, about 1.5 revolution i.e. 30 days are necessary.

As one can notice in tables 7 and 8, there is a gap between the values of the semi major axis at the end of the first phase (a=0.5), and at the beginning of the second phase (a=0.7). The arc associated with these two values is defined by the strategy used during the first phase. However, its actual simulation requires switching back to an unaveraged formulation of the sail's dynamics since the validity of the averaging methods is no longer guaranteed with such values of the semi major axis (see table 1).

PART 1	
GOAL	Increase the semi major axis and decrease the inclination with respect to the Moon's orbital plane.
STRATEGY	Maximize the thrust along: H in the vicinity of the descending node , -H in the vicinity of the descending node and V on the rest of the orbit.
FEATURES	Uses averaging methods, lasts 160 days, $a(t_0) = 0.065$, $a_f = 0.5$
BASED ON	Variational equations of the orbital elements.

Table 7: Characteristics of the first part of the trajectory design.
H denotes the orbital kinetic momentum and V the sail's velocity vector

PART 2	
GOAL	Reach a given location behind the Moon
STRATEGY	Maximize the thrust along the opposite of the primer vector.
FEATURES	Lasts less than 30 days, $a(t_0) = 0.7$, final position: less than 1 km from goal.
BASED ON	Optimal control theory, non-linear programming.

Table 8: Characteristics of the second part of the trajectory design.

Recommendations for further study.

Several aspects of the trajectory design can be improved.

In the frame of the first part, where the sail's trajectory goes through fast revolutions about the Earth, the rate of change of the angle defining the sail's orientation is quite high, which is not practically acceptable. It is interesting to consider the orientation history provided by the strategy developed in part 1 and to constrain it so that the precession rate of the thrust axis would always remain between realistic values. First ideas and issues concerning this problem are presented in appendix D.

For the intercept part, some improvement could be done in order to solve the full two-point-boundary-value-problem. It would then be possible to consider locally minimum-time trajectories instead of extremal trajectories which satisfy all but one of the optimality conditions (necessary conditions for stationary value of the performance index). Several approaches are possible. The two-point-boundary-value-problem is in the form:

$$f_1(\alpha_1, \alpha_2, \alpha_3, \alpha_4) = 0$$

$$f_2(\alpha_1, \alpha_2, \alpha_3, \alpha_4) = 0$$

Where α_1, α_2 and α_3 are the unknowns initial values of the costate, α_4 is the unknown final time t_f, f_1 is the distance from the desired final position at t_f and f_2 is the norm of the primer vector at t_f. The first

technique that has been tried was to minimize a combination of the two functions that need to be brought to zero. In this case, convergence of the BFGS algorithm was hard to obtain and other possibilities were considered. f_1 and f_2 are actually the norms of two two-component vectors so that instead of having two equations in four unknowns, a system of four equations in four unknowns could be defined by trying to bring each component of the two vectors to zero. This would allow a Newton-Raphson approach or a least square minimization approach. On the other hand, keeping only two equations allows us to consider one of the equations as an equality constraint in the minimization problem defined by the other equation.

However, one problem emerged with these new minimization problems: particular initial values of the costate are defined by the minimization algorithms and lure the sail into crashing on the Moon's surface. For this reason, one of the interesting feature of Breakwell's approach in reference [18] is to consider a new two-point-boundary-value-problem. It is then intended to generate two different arcs of trajectory, one being simulated forward from the given initial sail's position and another one starting from the desired final intercept location, running backwards in time. Both arcs are then modified until the state and costate components match at an intermediate location.

Finally, in the frame of a race to the Moon, the time optimization of the entire trajectory is desirable.

APPENDICES

APPENDIX A

SIMULATIONS OF THE "INCREASING ENERGY STRATEGY"

This appendix presents different trajectory simulations generated with the "increasing energy strategy" and associated with various initial orientations of the apsidal line.

All simulations were performed with a Runge-Kutta-Fehlberg integrator provided by Matlab, but the averaging methods were coded in the C language thus improving by an estimated factor of 300 the speed of the simulation program. Defining new Matlab functions coded in C enabled writing a relatively concise and simple code.

The following simulations are associated with orientations of the apsidal line of 0, 45, 90, 135, 180, 225, 270 and 315 degrees (the angle that is considered here is the angle α defined in figure 4).

-Time histories of the orbital elements show that some particular initial orientations of the apsidal line (180-270 degrees) bring about large eccentricity increases and enable little semi major axis increase,in comparison with the "best" cases (0-90 degrees).

Projections of the initial, intermediate and final trajectories on the ecliptic

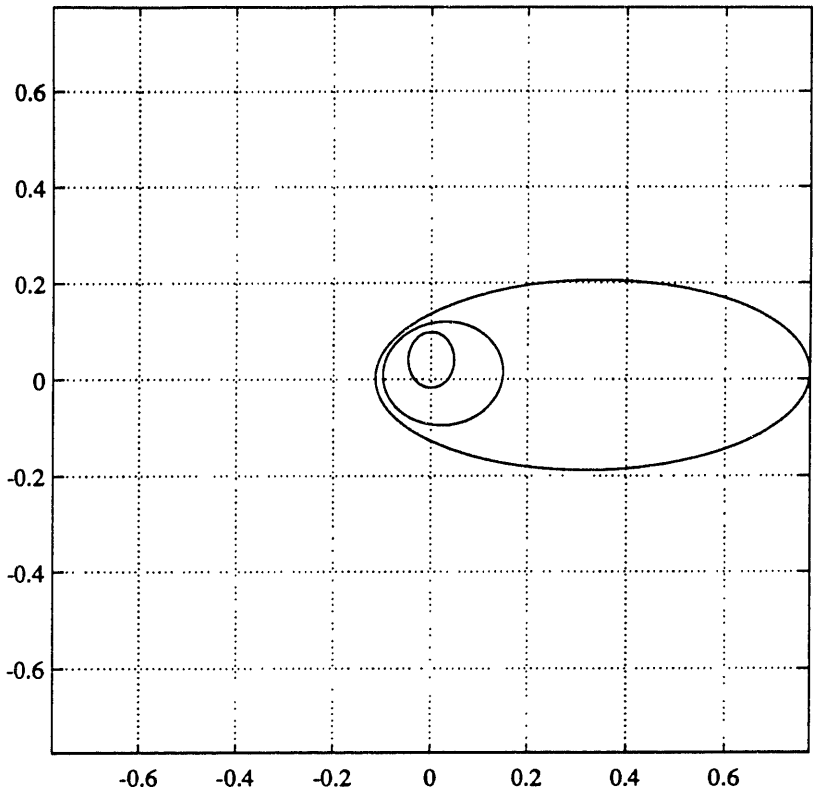

ORBITAL ELEMENTS

	INITIAL VALUES	FINAL VALUES
Semi major axis	0.065	0.444
Excentricity	0.7	0.743

The following elements are referenced to the Ecliptic:

Inclination	28	48.5
Ascending node	0	-0.2934
Argument of perigee	-90	-177.4

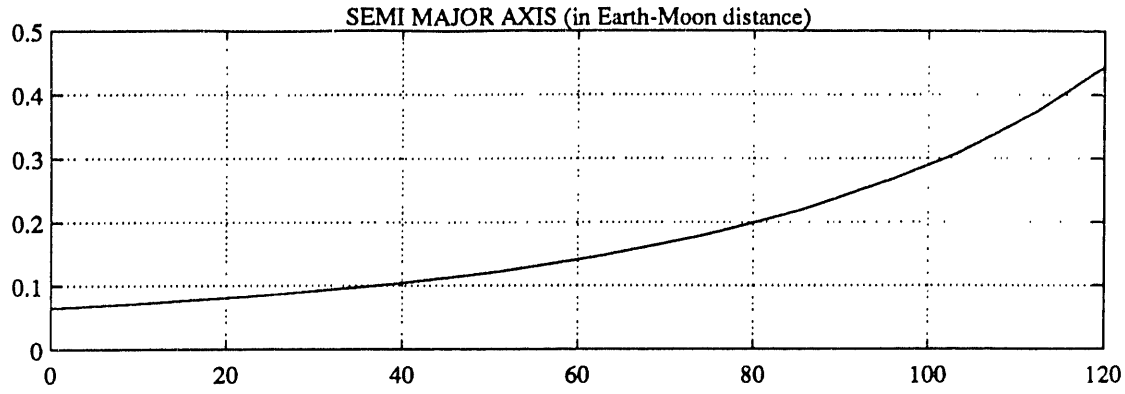
SEMI MAJOR AXIS (in Earth-Moon distance)
0.5
0.4
0.3
0.2
0.1
0
0
20
40
60
80
100
120

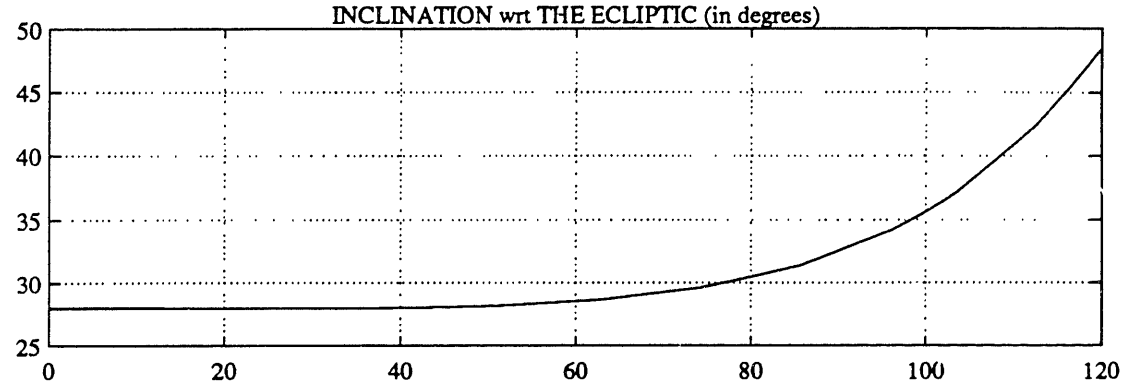
INCLINATION wrt THE ECLIPTIC (in degrees)
50
45
40
35
30
25
0
20
40
60
80
100
120

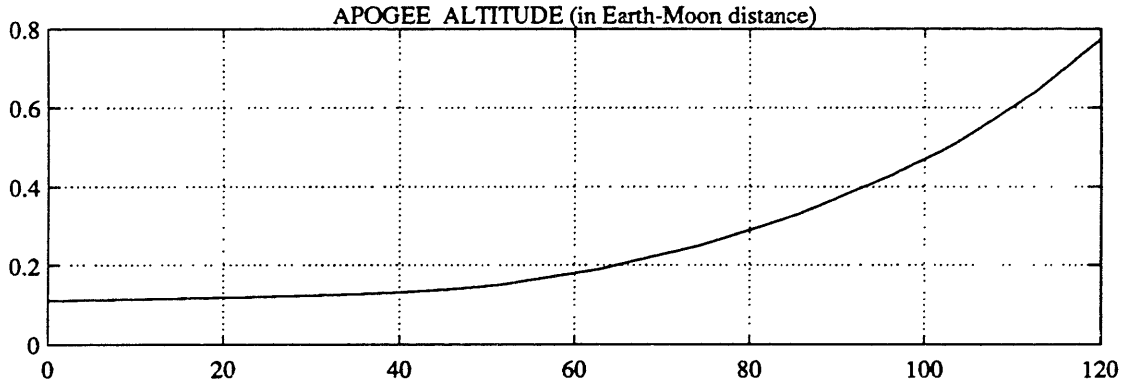
APOGEE ALTITUDE (in Earth-Moon distance)
0.8
0.6
0.4
0.2
0
0
20
40
60
80
100
120

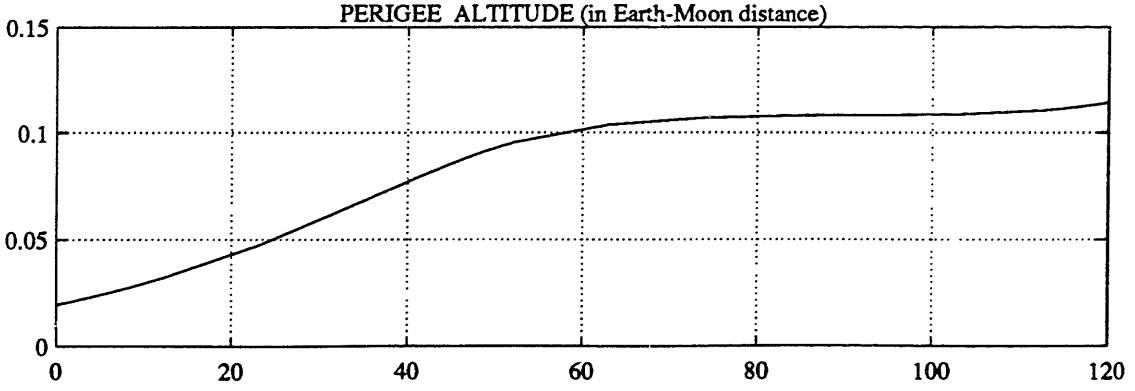
PERIGEE ALTITUDE (in Earth-Moon distance)
0.15
0.1
0.05
0
0
20
40
60
80
100
120

Projections of the initial, intermediate and final trajectories on the ecliptic

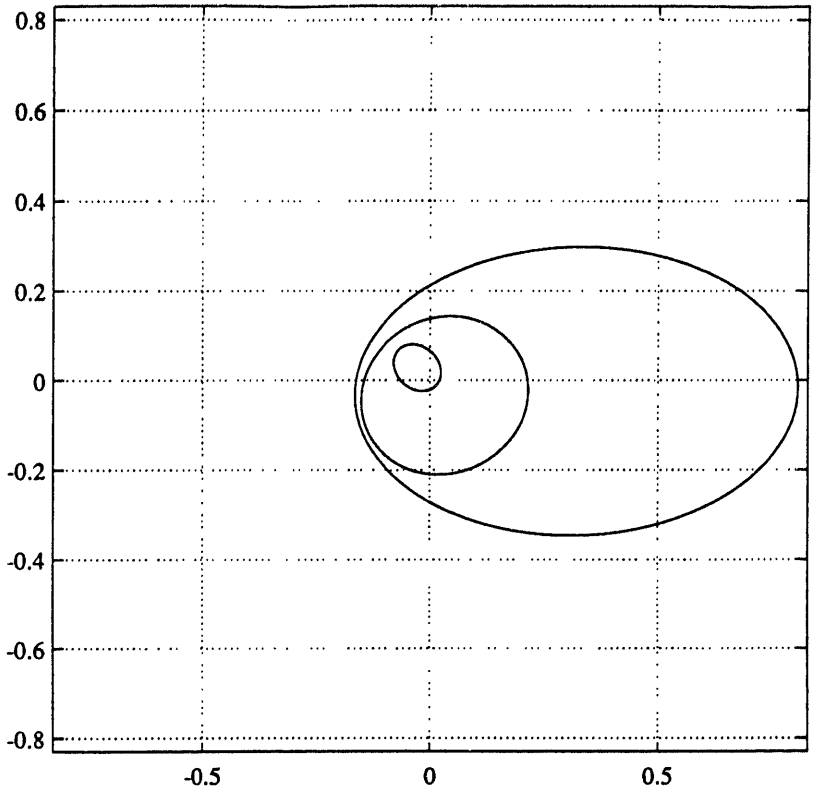

ORBITAL ELEMENTS

	INITIAL VALUES	FINAL VALUES
Semi major axis	0.065	0.4983
Excentricity	0.7	0.6648

The following elements are referenced to the Ecliptic:

Inclination	28	32.14
Ascending node	45	18.64
Argument of perigee	-90	153.4

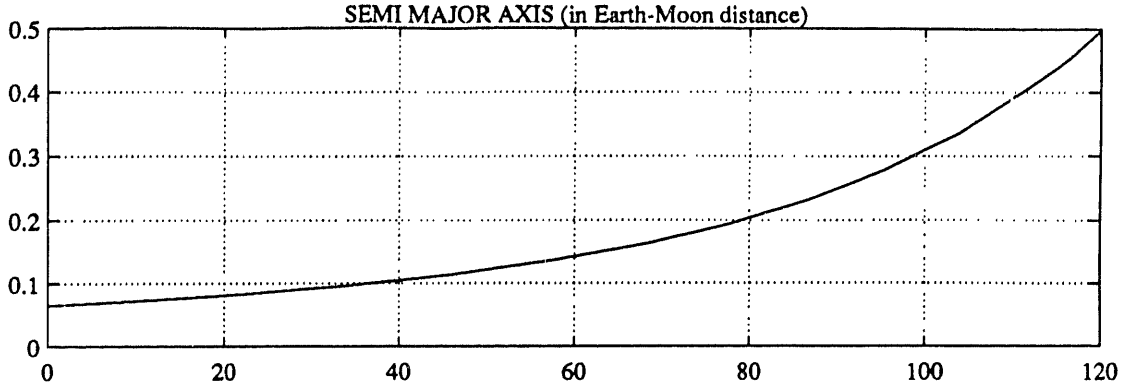
SEMI MAJOR AXIS (in Earth-Moon distance)
0.5
0.4
0.3
0.2
0.1
0
0
20
40
60
80
100
120

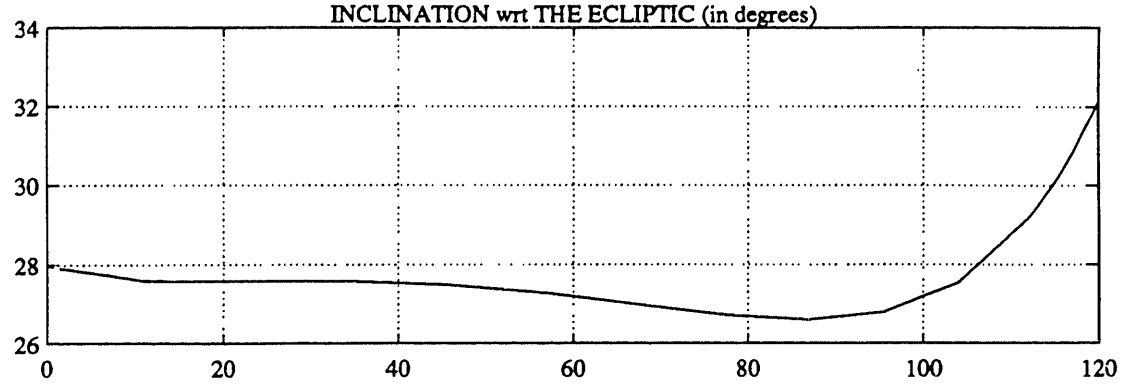
INCLINATION wrt THE ECLIPTIC (in degrees)
34
32
30
28
26
0
20
40
60
80
100
120

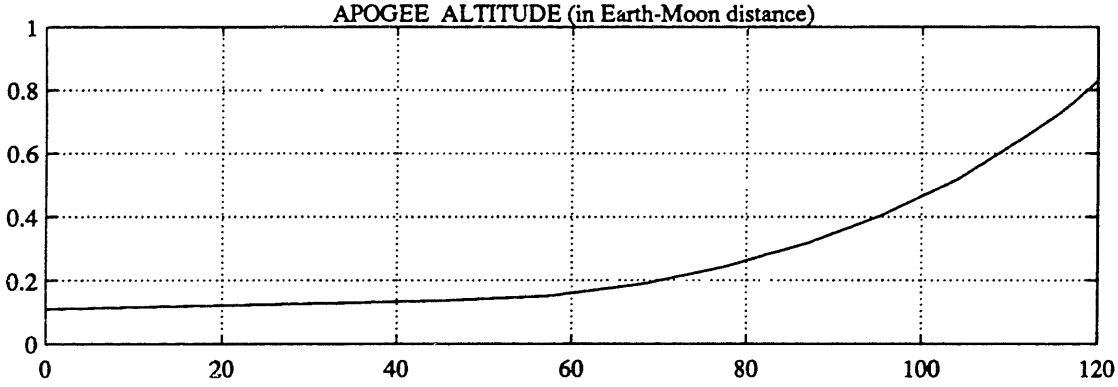
APOGEE ALTITUDE (in Earth-Moon distance)
1
0.8
0.6
0.4
0.2
0
0
20
40
60
80
100
120

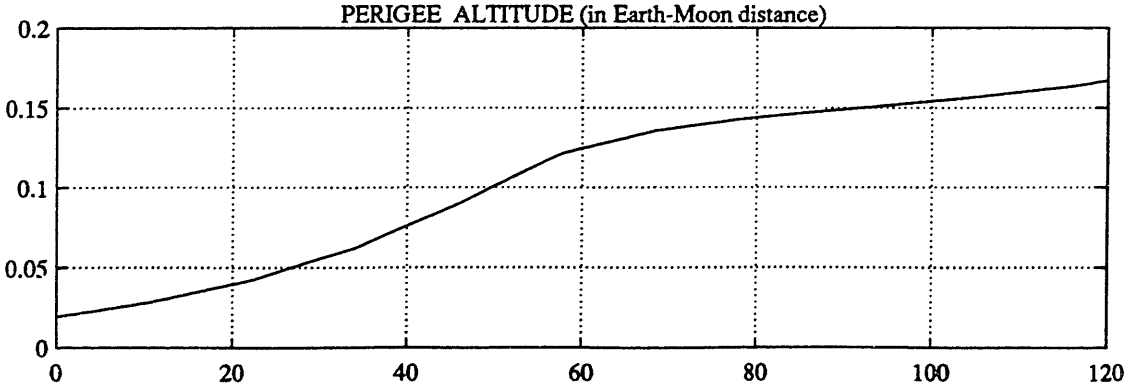
PERIGEE ALTITUDE (in Earth-Moon distance)
0.2
0.15
0.1
0.05
0
0
20
40
60
80
100
120

Projections of the initial, intermediate and final trajectories on the ecliptic

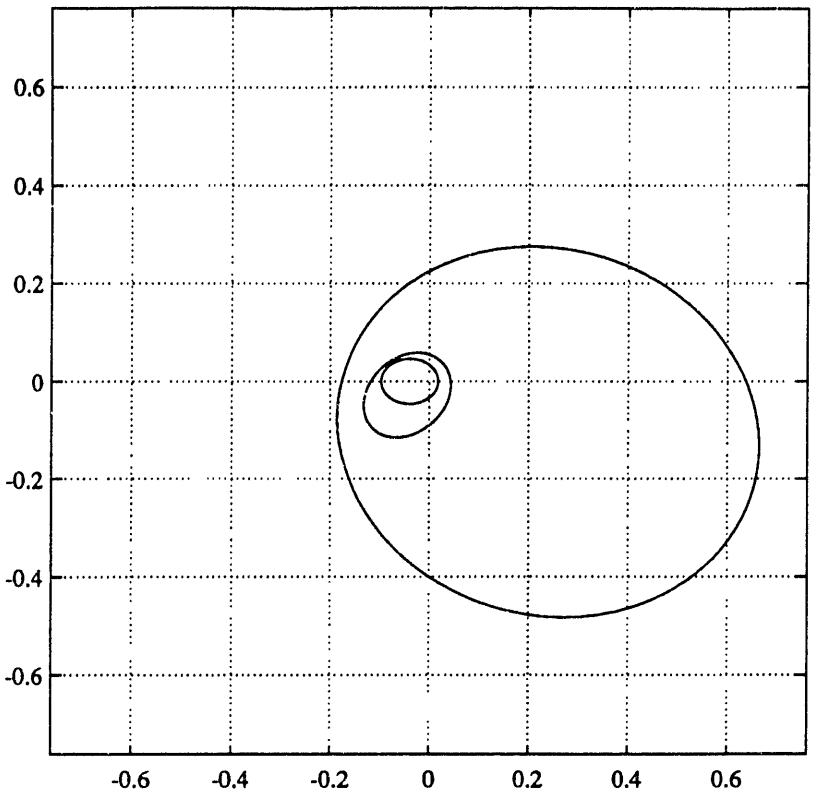

ORBITAL ELEMENTS

	INITIAL VALUES	FINAL VALUES
Semi major axis	0.065	0.4735
Excentricity	0.7	0.6067

The following elements are referenced to the Ecliptic:

Inclination	28	25.51
Ascending node	90	55.23
Argument of perigee	-90	100.2

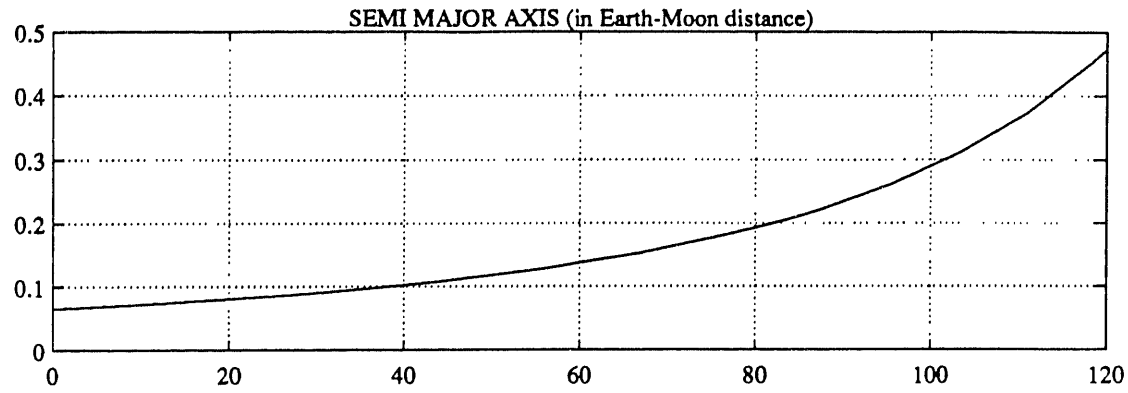
SEMI MAJOR AXIS (in Earth-Moon distance)
0.5
0.4
0.3
0.2
0.1
0
0
20
40
60
80
100
120

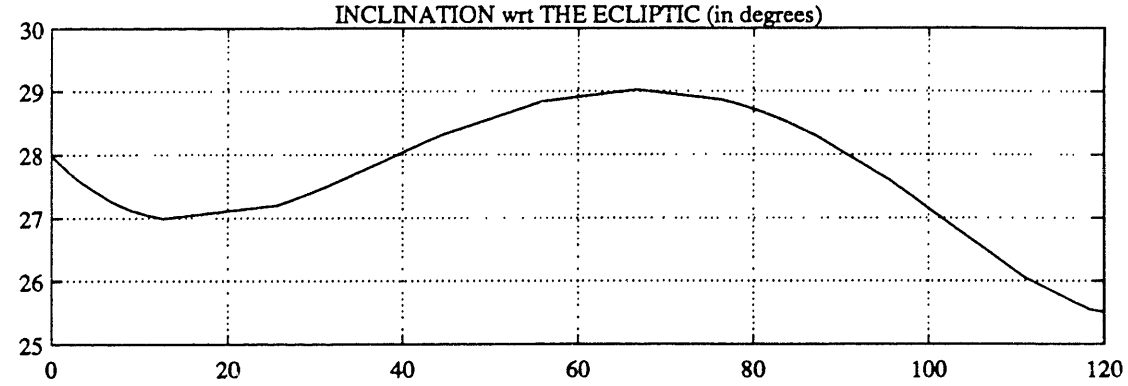
INCLINATION wrt THE ECLIPTIC (in degrees)
30
29
28
27
26
25
0
20
40
60
80
100
120

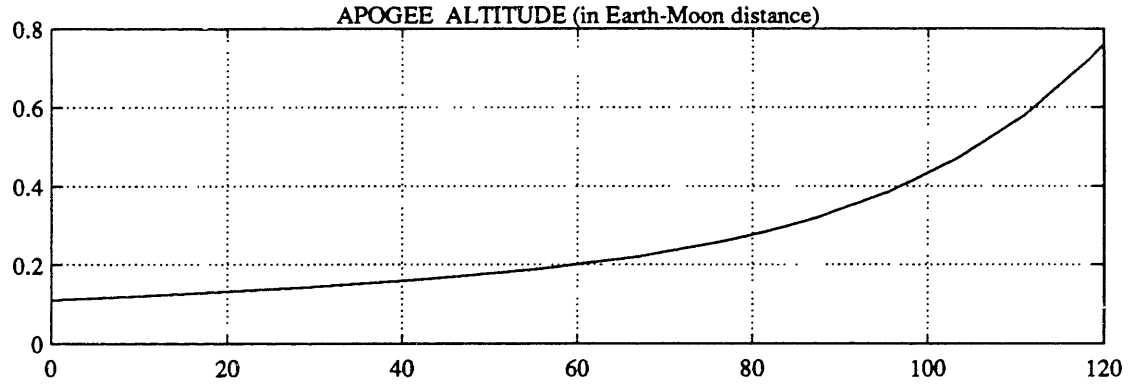
APOGEE ALTITUDE (in Earth-Moon distance)
0.8
0.6
0.4
0.2
0
0
20
40
60
80
100
120

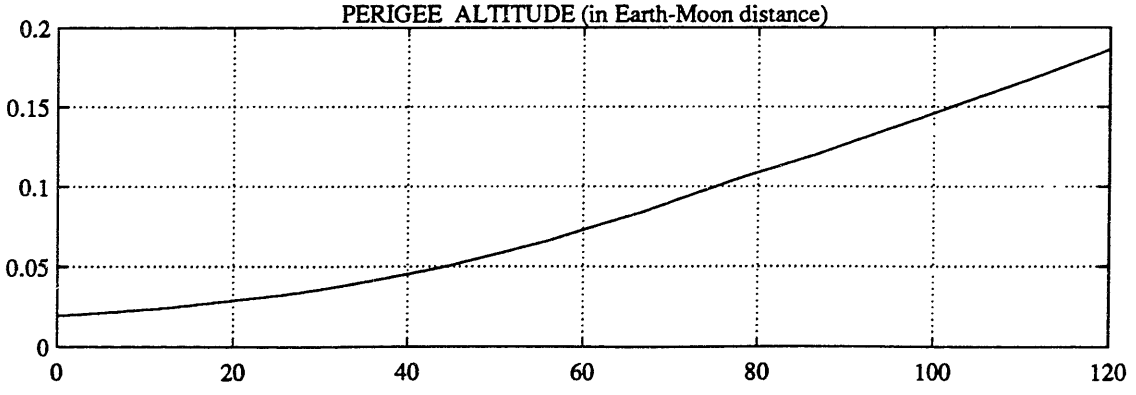
PERIGEE ALTITUDE (in Earth-Moon distance)
0.2
0.15
0.1
0.05
0
0
20
40
60
80
100
120

Projections of the initial, intermediate and final trajectories on the ecliptic

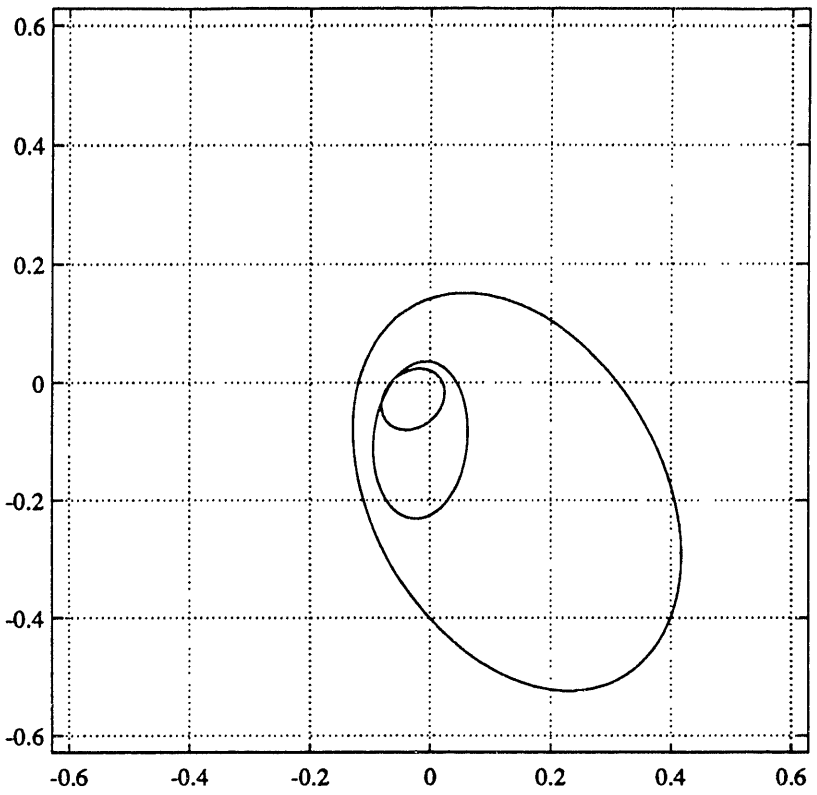

ORBITAL ELEMENTS

	INITIAL VALUES	FINAL VALUES
Semi major axis	0.065	0.3772
Excentricity	0.7	0.6654

The following elements are referenced to the Ecliptic:

Inclination	28	34.73
Ascending node	135	95.66
Argument of perigee	-90	37.28

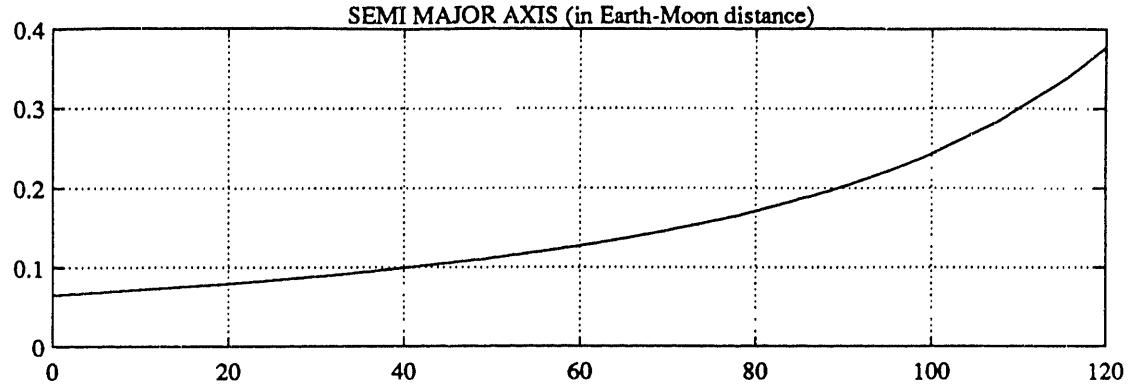
SEMI MAJOR AXIS (in Earth-Moon distance)
0.4
0.3
0.2
0.1
0
0
20
40
60
80
100
120

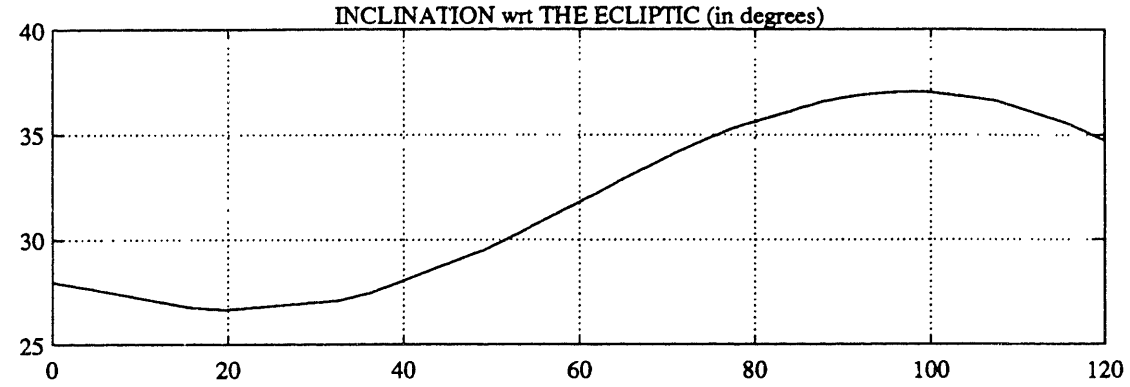
INCLINATION wrt THE ECLIPTIC (in degrees)
40
35
30
25
0
20
40
60
80
100
120

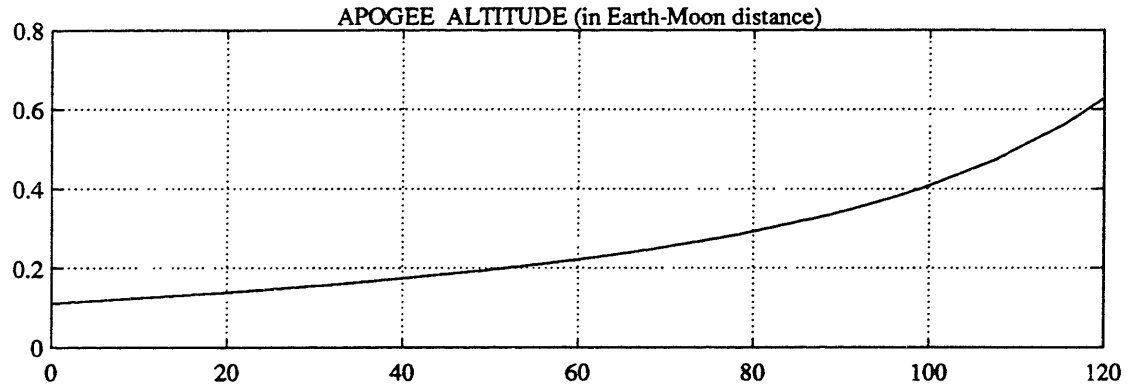
APOGEE ALTITUDE (in Earth-Moon distance)
0.8
0.6
0.4
0.2
0
0
20
40
60
80
100
120

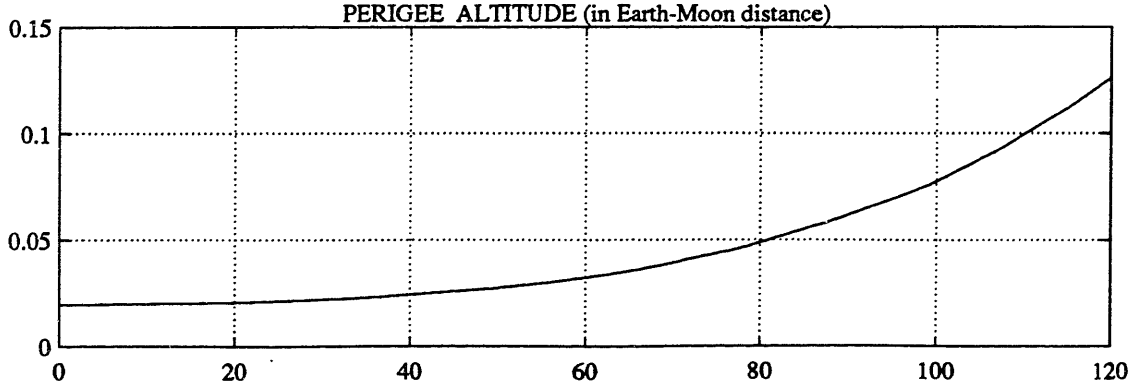
PERIGEE ALTITUDE (in Earth-Moon distance)
0.15
0.1
0.05
0
0
20
40
60
80
100
120

Projections of the initial, intermediate and final trajectories on the ecliptic

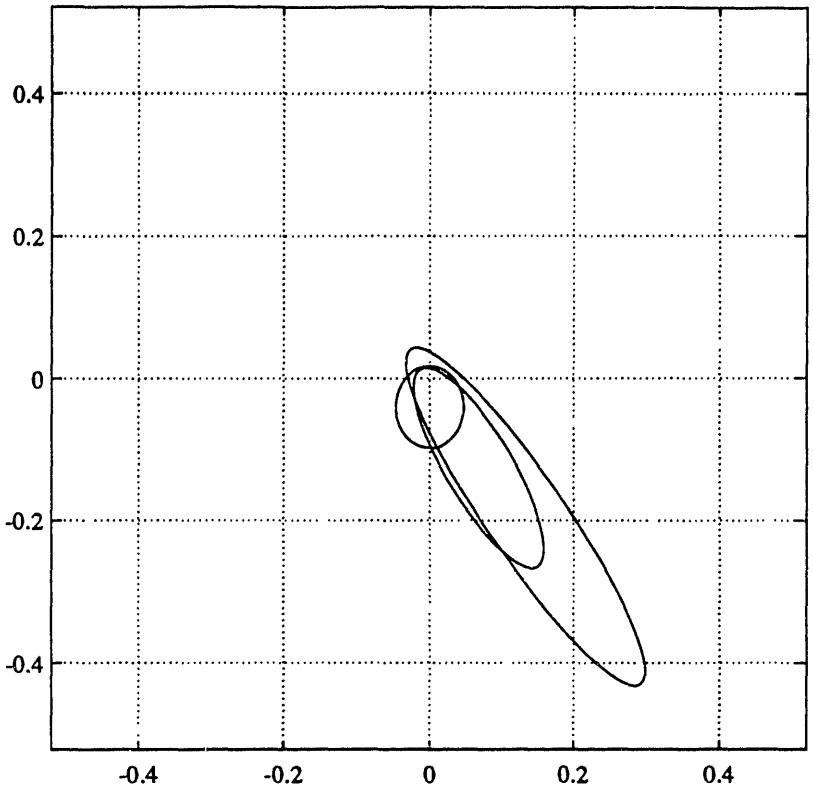

ORBITAL ELEMENTS

	INITIAL VALUES	FINAL VALUES
Semi major axis	0.065	0.2842
Excentricity	0.7	0.8291

The following elements are referenced to the Ecliptic:

Inclination	28	69.55
Ascending node	180	123.3
Argument of perigee	-90	3.191

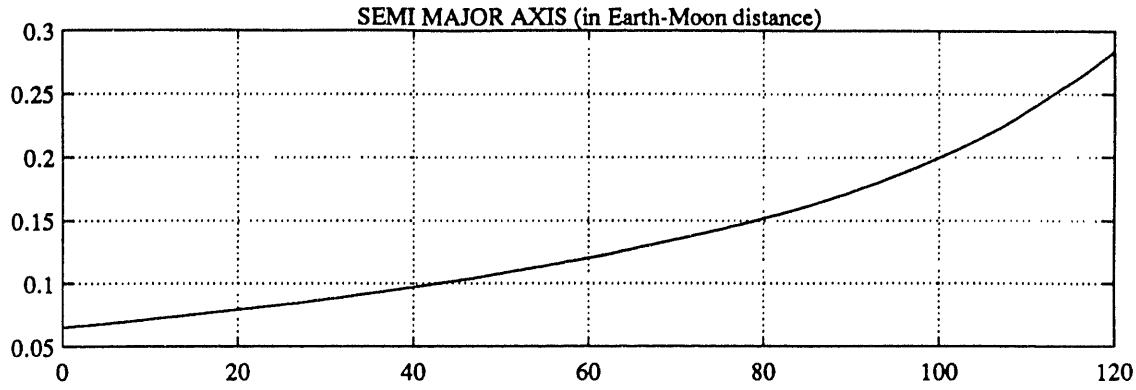
SEMI MAJOR AXIS (in Earth-Moon distance)
0.3
0.25
0.2
0.15
0.1
0.05
0
20
40
60
80
100
120

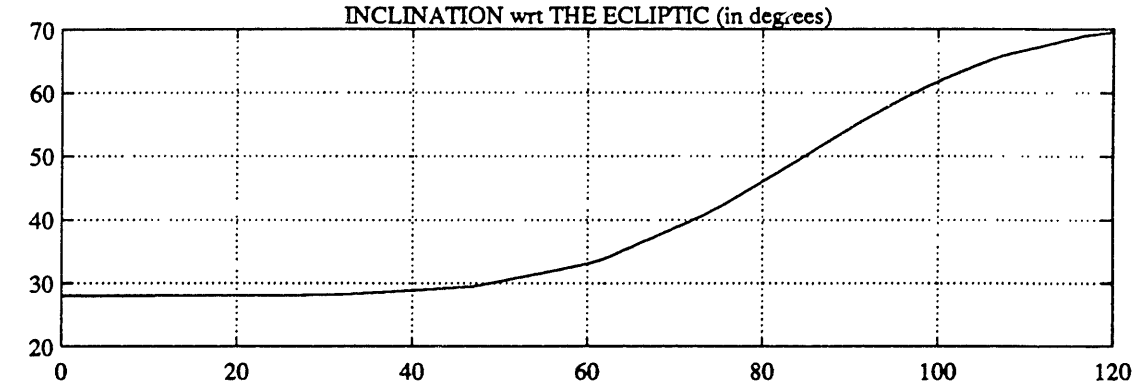
INCLINATION wrt THE ECLIPTIC (in degrees)
70
60
50
40
30
20
0
20
40
60
80
100
120

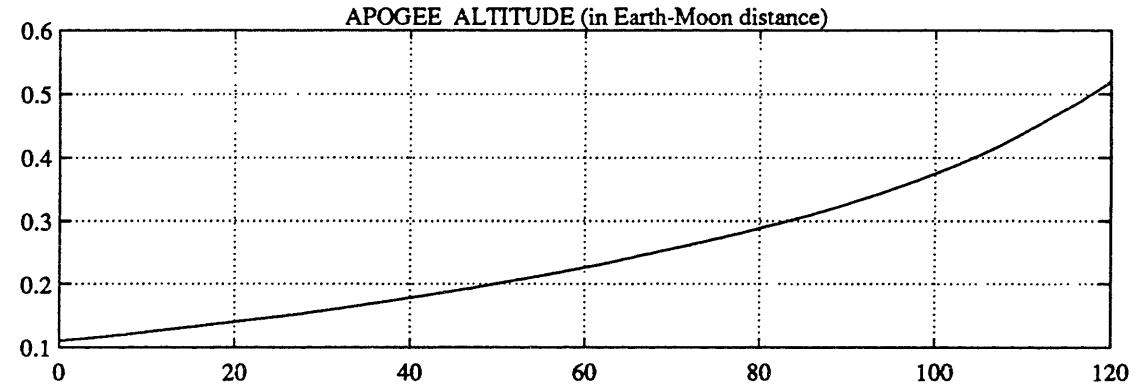
APOGEE ALTITUDE (in Earth-Moon distance)
0.6
0.5
0.4
0.3
0.2
0.1
0
20
40
60
80
100
120

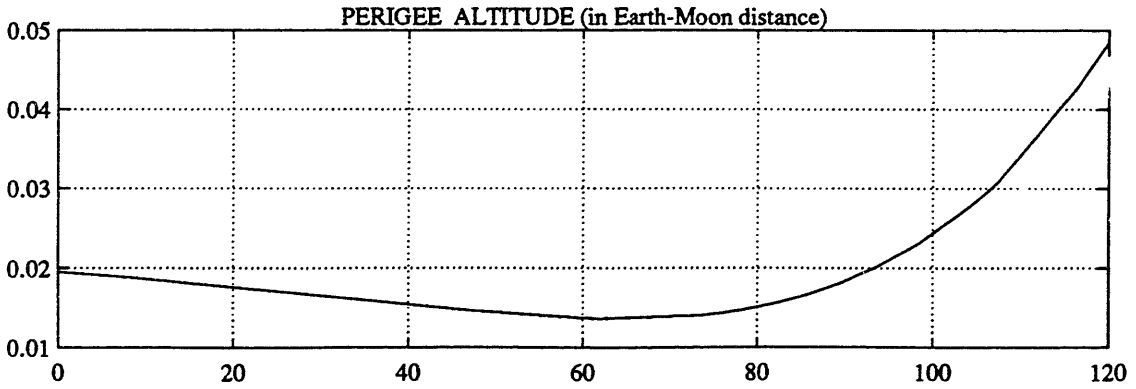
PERIGEE ALTITUDE (in Earth-Moon distance)
0.05
0.04
0.03
0.02
0.01
0
20
40
60
80
100
120

Projections of the initial, intermediate and final trajectories on the ecliptic

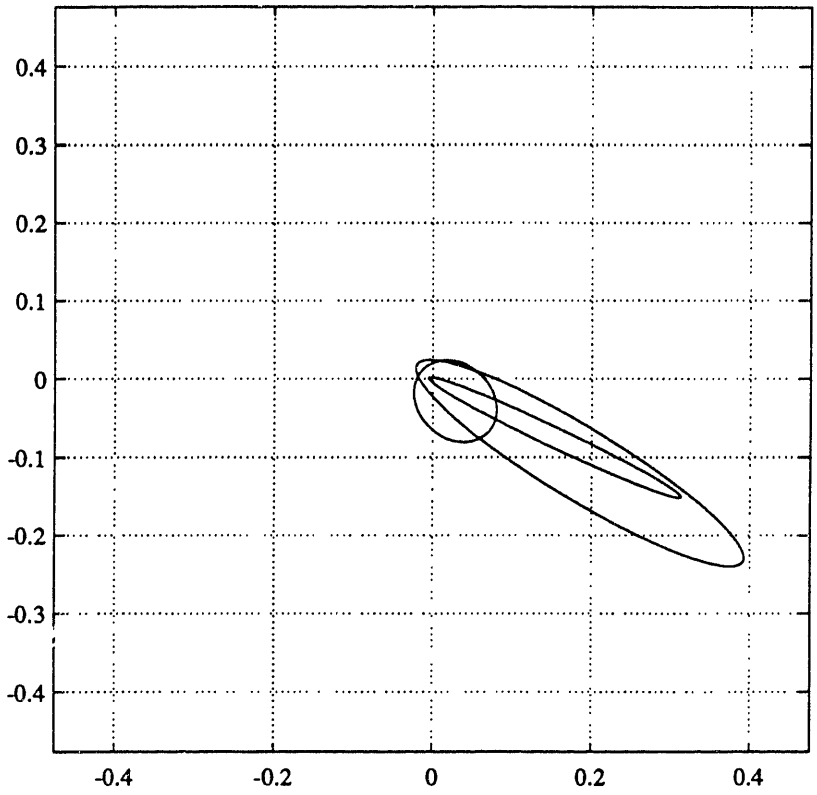

ORBITAL ELEMENTS

	INITIAL VALUES	FINAL VALUES
Semi major axis	0.065	0.2506
Excentricity	0.7	0.8973

The following elements are referenced to the Ecliptic:

Inclination	28	113.3
Ascending node	-135	-217.9
Argument of perigee	-90	-18.82

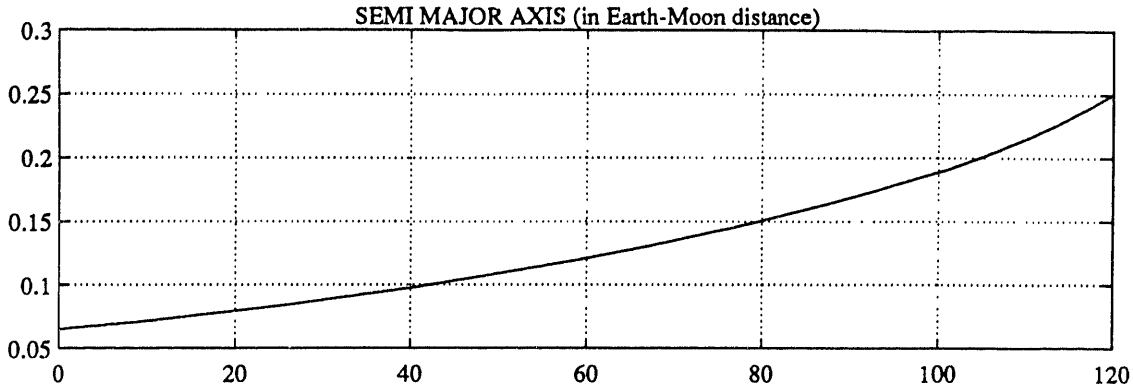
SEMI MAJOR AXIS (in Earth-Moon distance)
0.3
0.25
0.2
0.15
0.1
0.05
0
20
40
60
80
100
120

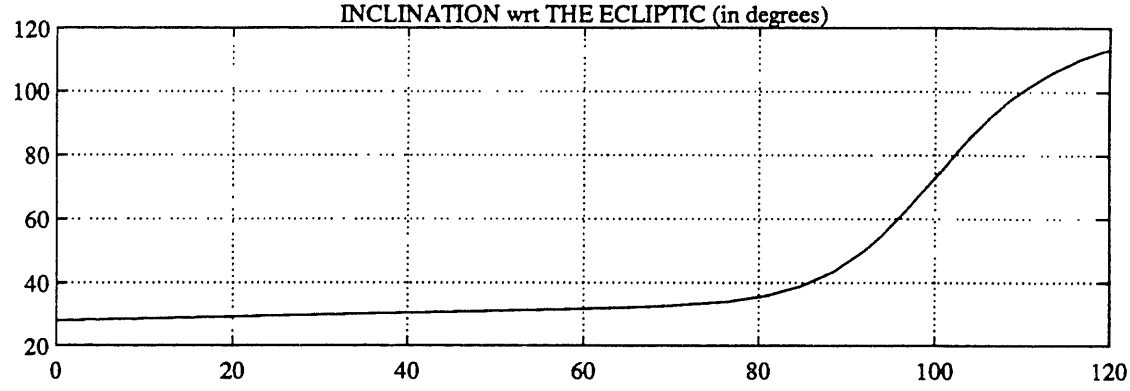
INCLINATION wrt THE ECLIPTIC (in degrees)
120
100
80
60
40
20
0
20
40
60
80
100
120

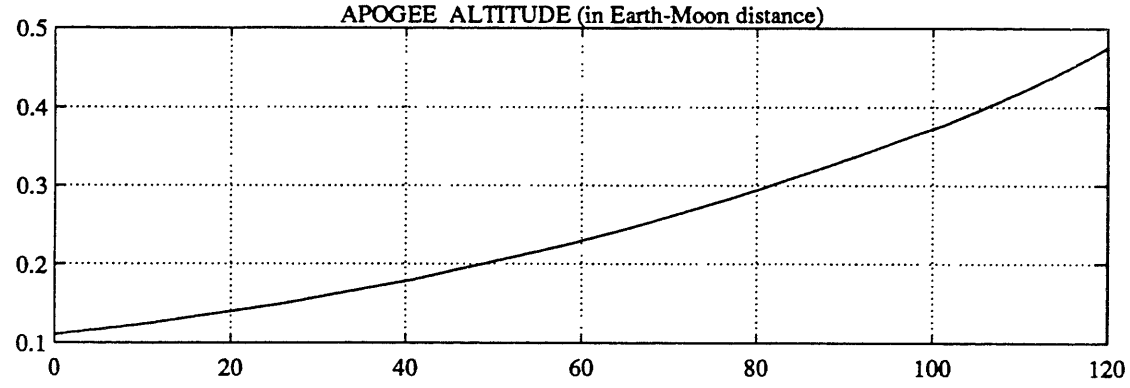
APOGEE ALTITUDE (in Earth-Moon distance)
0.5
0.4
0.3
0.2
0.1
0
20
40
60
80
100
120

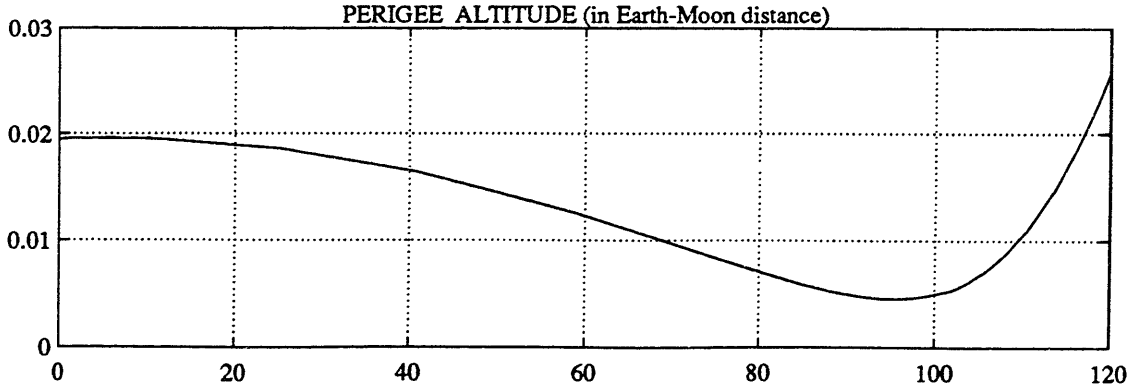
PERIGEE ALTITUDE (in Earth-Moon distance)
0.03
0.02
0.01
0
0
20
40
60
80
100
120

Projections of the initial, intermediate and final trajectories on the ecliptic

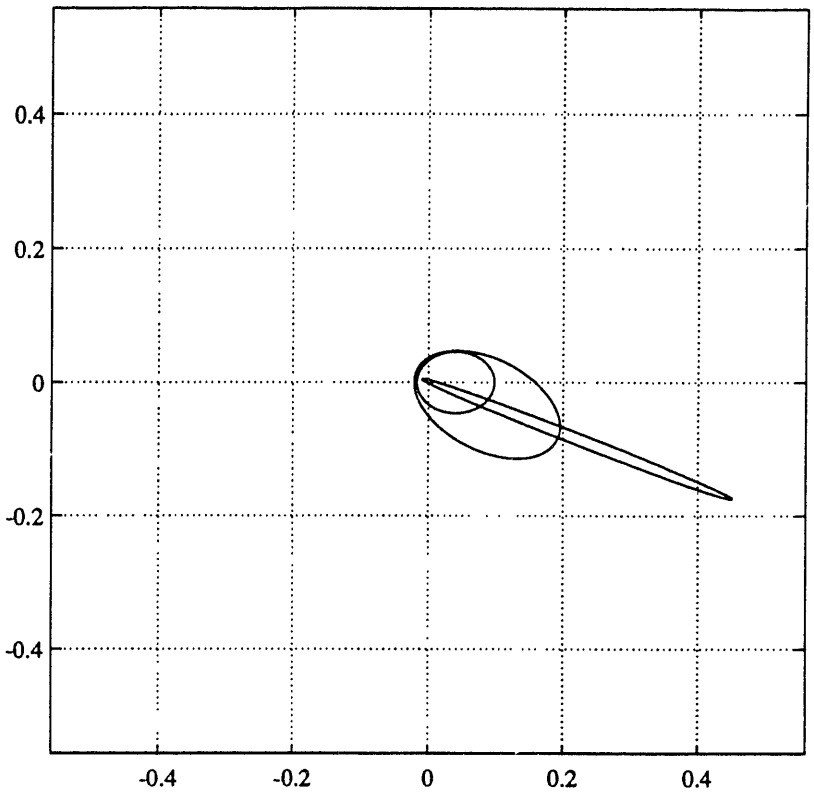

ORBITAL ELEMENTS

	INITIAL VALUES	FINAL VALUES
Semi major axis	0.065	0.2838
Excentricity	0.7	0.9669

The following elements are referenced to the Ecliptic:

Inclination	28	84.02
Ascending node	-90	-24.59
Argument of perigee	-90	-149.3

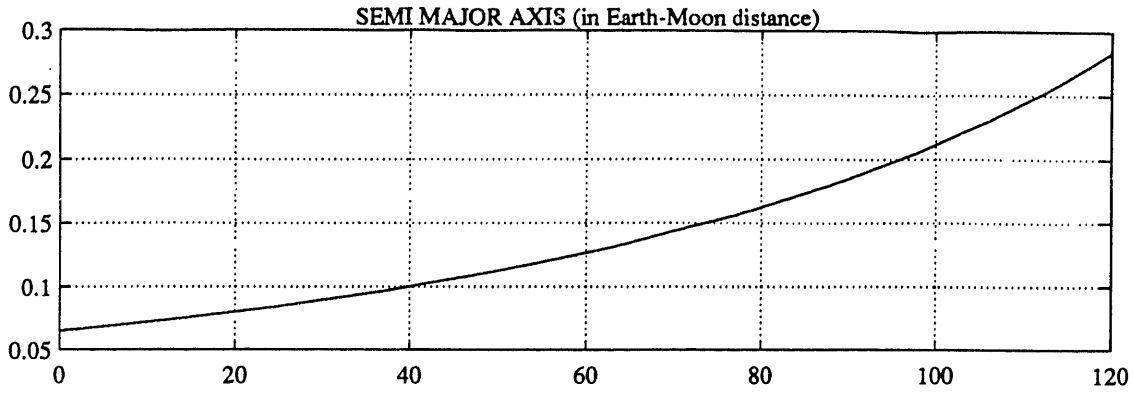
SEMI MAJOR AXIS (in Earth-Moon distance)
0.3
0.25
0.2
0.15
0.1
0.05
0
20
40
60
80
100
120

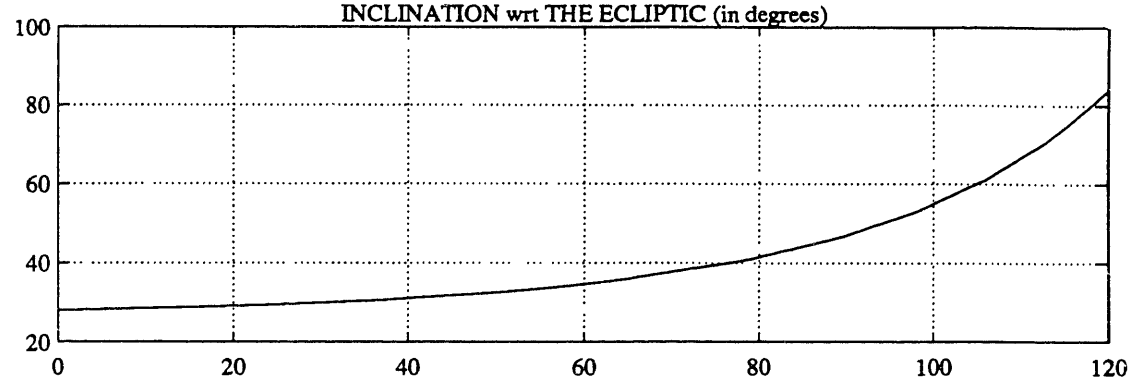
INCLINATION wrt THE ECLIPTIC (in degrees)
100
80
60
40
20
0
20
40
60
80
100
120

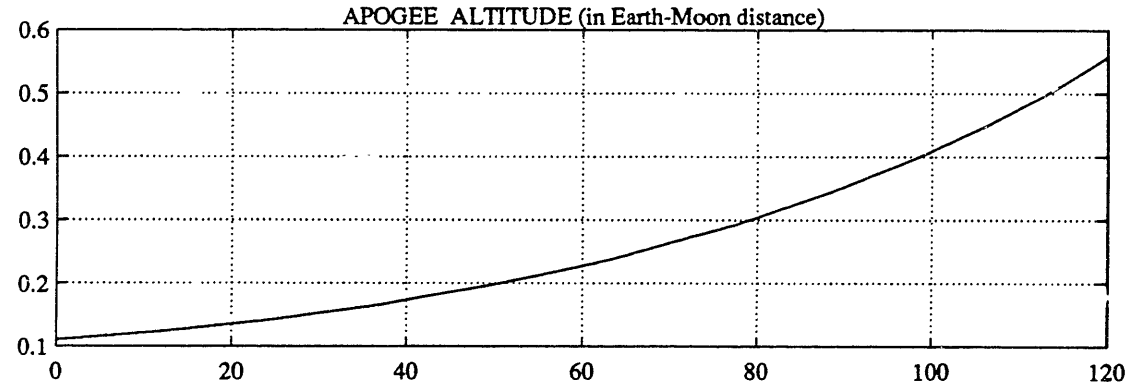
APOGEE ALTITUDE (in Earth-Moon distance)
0.6
0.5
0.4
0.3
0.2
0.1
0
20
40
60
80
100
120

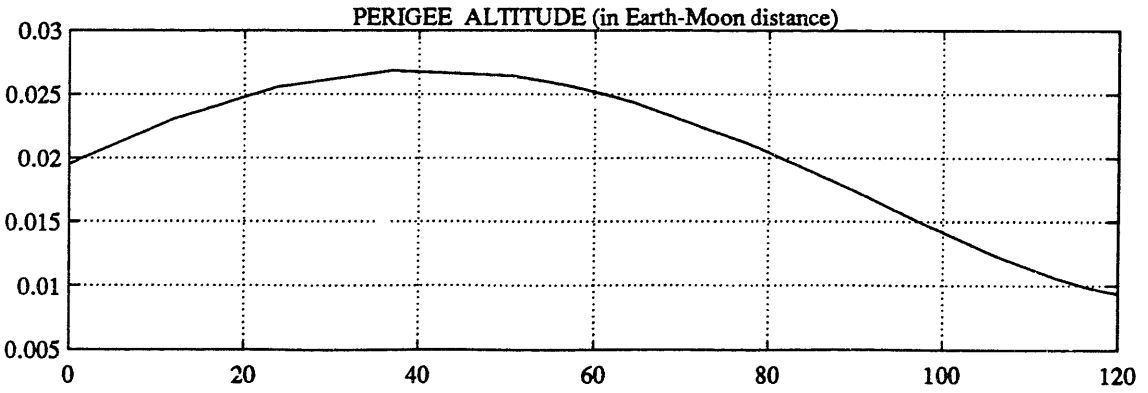
PERIGEE ALTITUDE (in Earth-Moon distance)
0.03
0.025
0.02
0.015
0.01
0.005
0
20
40
60
80
100
120

Projections of the initial, intermediate and final trajectories on the ecliptic

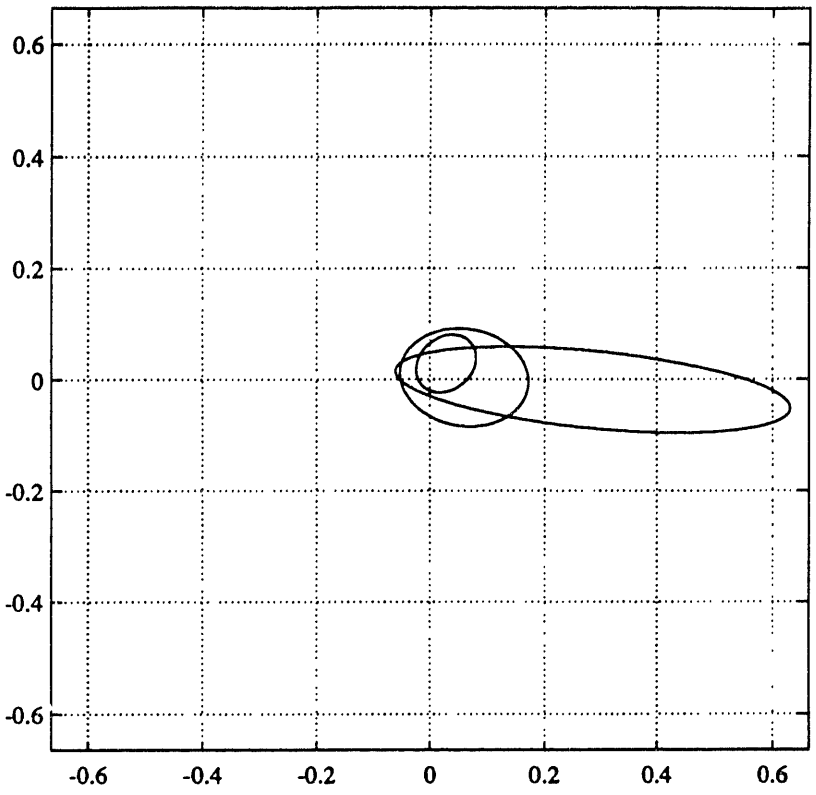

ORBITAL ELEMENTS

	INITIAL VALUES	FINAL VALUES
Semi major axis	0.065	0.3617
Excentricity	0.7	0.8368

The following elements are referenced to the Ecliptic:

Inclination	28	70.31
Ascending node	-45	-10.8
Argument of perigee	-90	-159.7

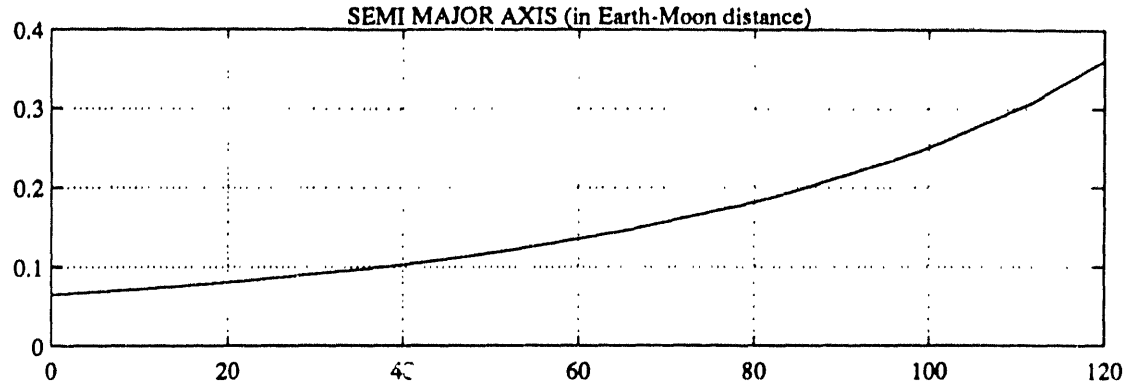
SEMI MAJOR AXIS (in Earth-Moon distance)
0.4
0.3
0.2
0.1
0
0
20
60
80
100
120

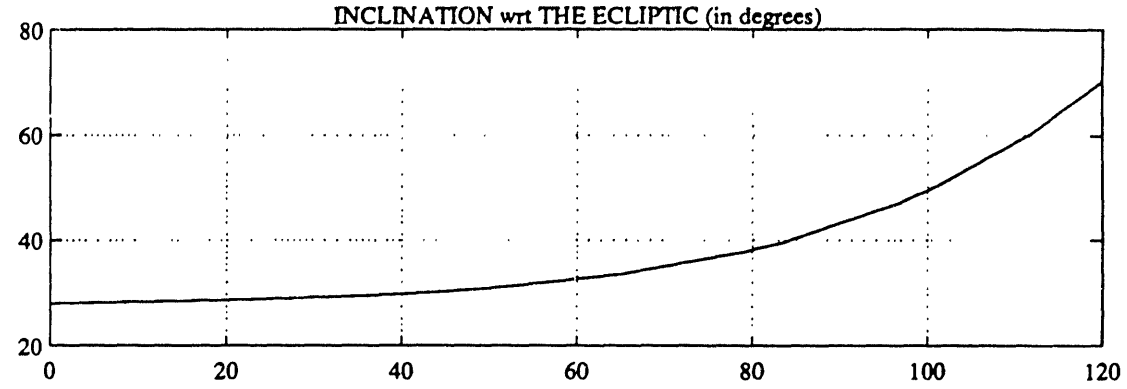
INCLINATION wrt THE ECLIPTIC (in degrees)
80
60
40
20
0
20
40
60
80
100
120

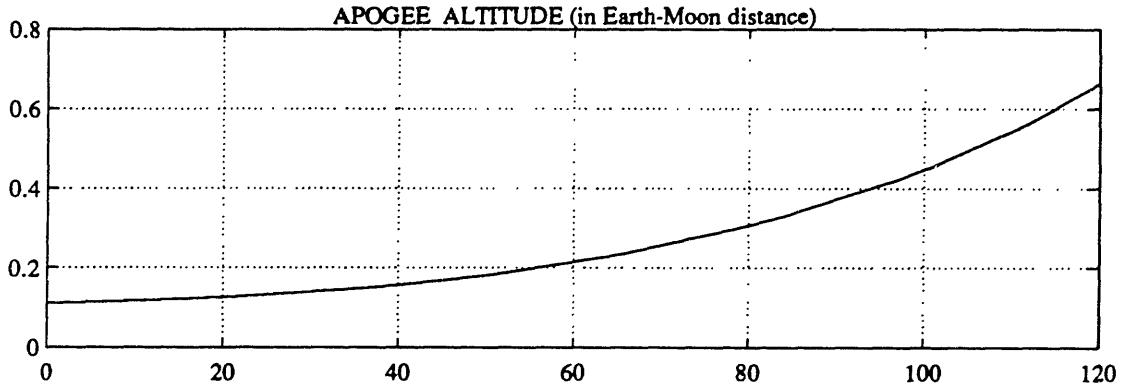
APOGEE ALTITUDE (in Earth-Moon distance)
0.8
0.6
0.4
0.2
0
0
20
40
60
80
100
120

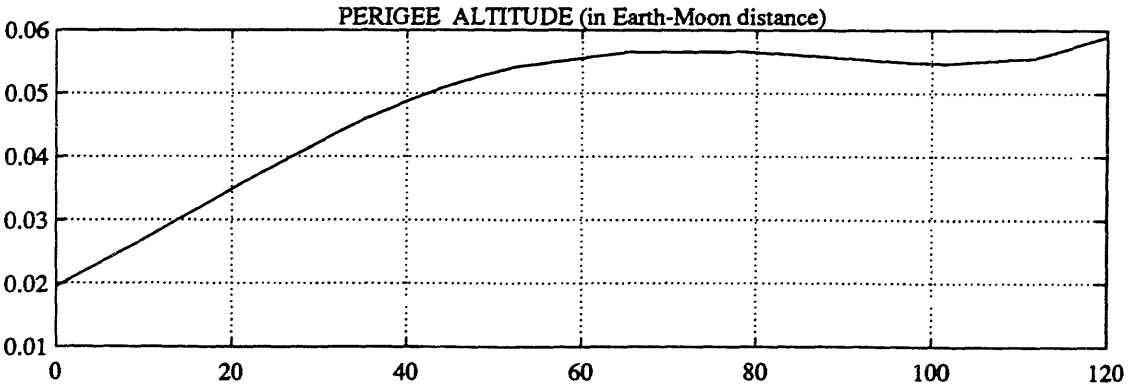
PERIGEE ALTITUDE (in Earth-Moon distance)
0.06
0.05
0.04
0.03
0.02
0.01
0
20
40
60
80
100
120

APPENDIX B

SIMULATIONS OF THE "GENERAL STRATEGY"

The trajectories presented in this appendix show the performances of the "general strategy". This strategy intends to increase the semi major axis and decrease the inclination with respect to the Moon's orbital plane. Three different initial orientations of the apsidal line are considered: 45, 90 and 135 degrees with respect to the initial Sun direction. These orientations proved to be the most efficient ones according to the results presented in appendix 1.

In each of these cases, the inclination with respect to the Moon's orbital plane is brought back to zero and the semi major axis increases as shown on the time histories of the orbital elements. The semi major increase provided by the "general strategy" enable reaching high-Earth orbits (a=0.4 Earth-Moon distance).

Each initial orientation of the apsidal line defines a different case for which one needs to define the region around the nodes of the sail's trajectory where the inclination control is to be applied.

Projections of the initial, intermediate and final trajectories on the equatorial plane

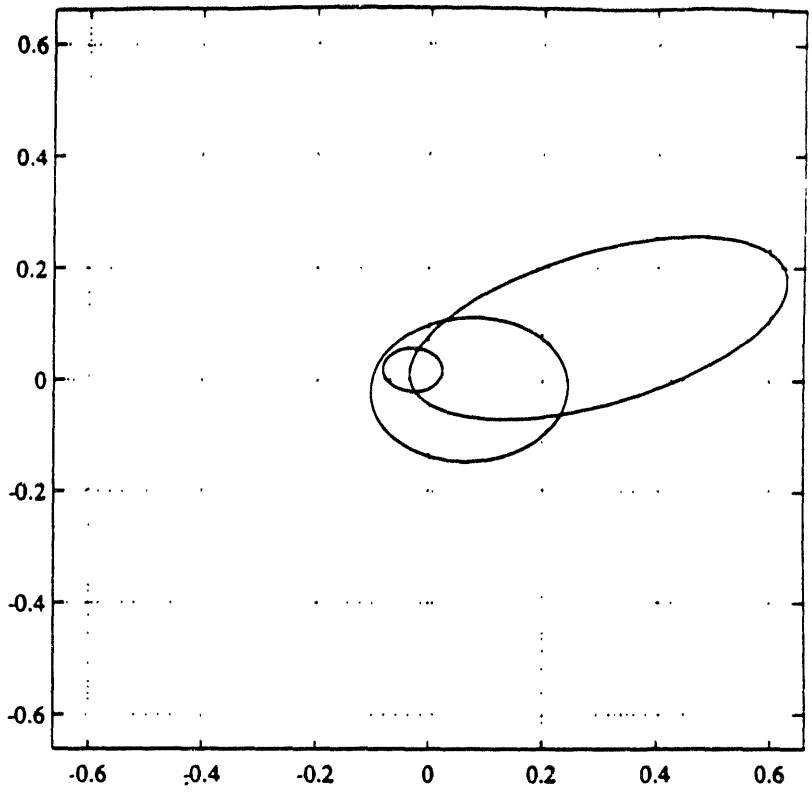

ORBITAL ELEMENTS

	INITIAL VALUES	FINAL VALUES
Semi major axis	0.065	0.3472
Excentricity	0.7	0.9065

The following elements are referenced to the Ecliptic:

Inclination	28	0.141
Ascending node	45	35.38
Argument of perigee	-90	163.2

Inclination control if: $a < 0.2$ and theta < 30 degrees, or

$a > 0.2$ and theta < 18 degrees

where theta is the sail's angular position with respect to the nearest node.

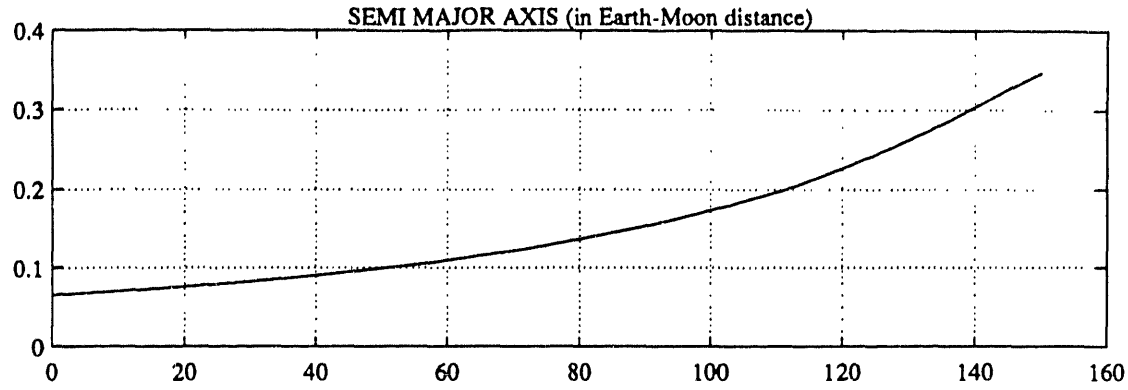
SEMI MAJOR AXIS (in Earth-Moon distance)
0.4
0.3
0.2
0.1
0
0
20
40
60
80
100
120
140
160

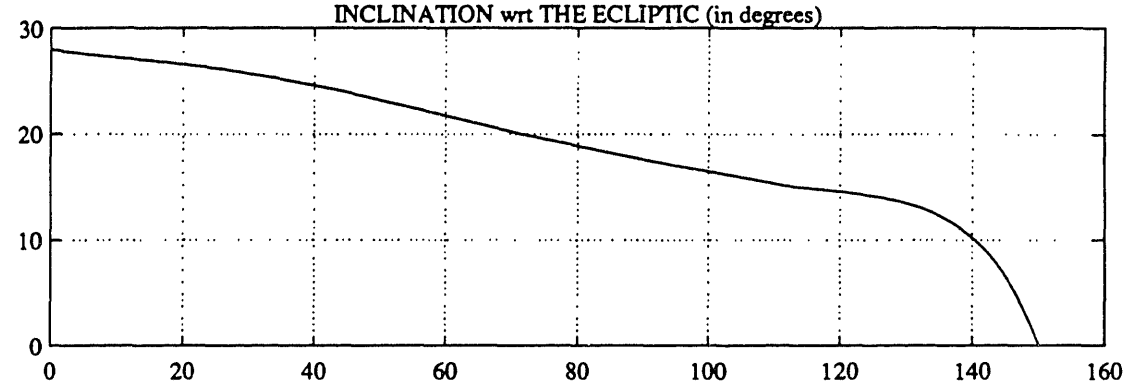
INCLINATION wrt THE ECLIPTIC (in degrees)
30
20
10
0
0
20
40
60
80
100
120
140
160

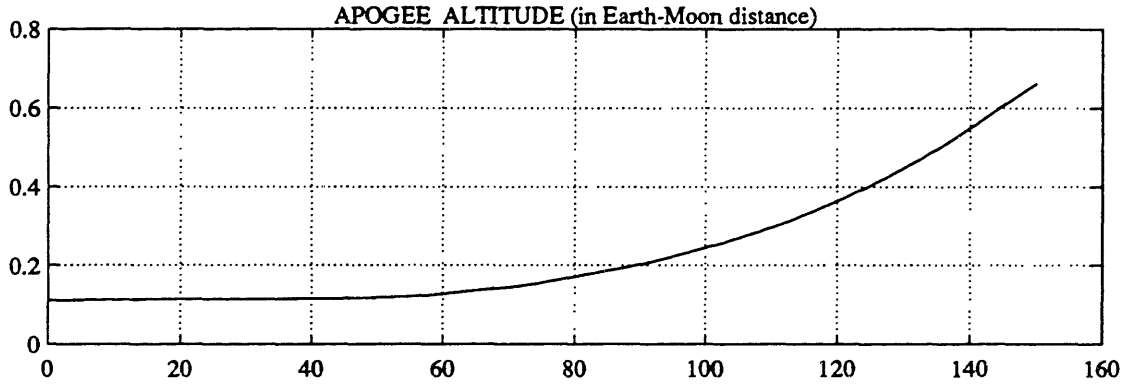
APOGEE ALTITUDE (in Earth-Moon distance)
0.8
0.6
0.4
0.2
0
0
20
40
60
80
100
120
140
160

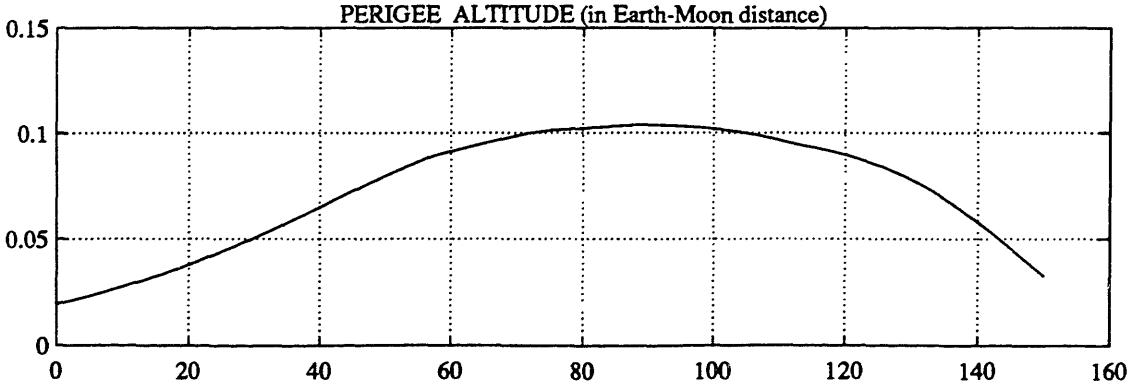
PERIGEE ALTITUDE (in Earth-Moon distance)
0.15
0.1
0.05
0
0
20
40
60
80
100
120
140
160

Projections of the initial, intermediate and final trajectories on the ecliptic

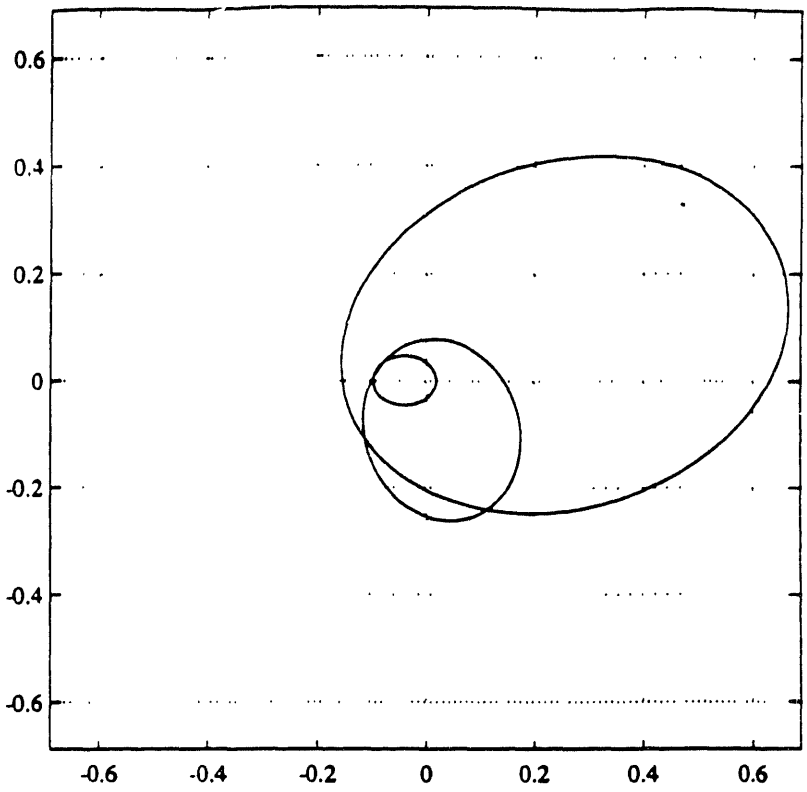

ORBITAL ELEMENTS

	INITIAL VALUES	FINAL VALUES
Semi major axis	0.065	0.4197
Excentricity	0.7	0.6397

The following elements are referenced to the Ecliptic:

Inclination	28	0.004816
Ascending node	90	47.5
Argument of perigee	-90	150.8

Inclination control if: $a < 0.2$ and theta < 30 degrees, or

$a > 0.2$ and theta <18 degrees

where theta is the sail's angular position with respect to the nearest node.

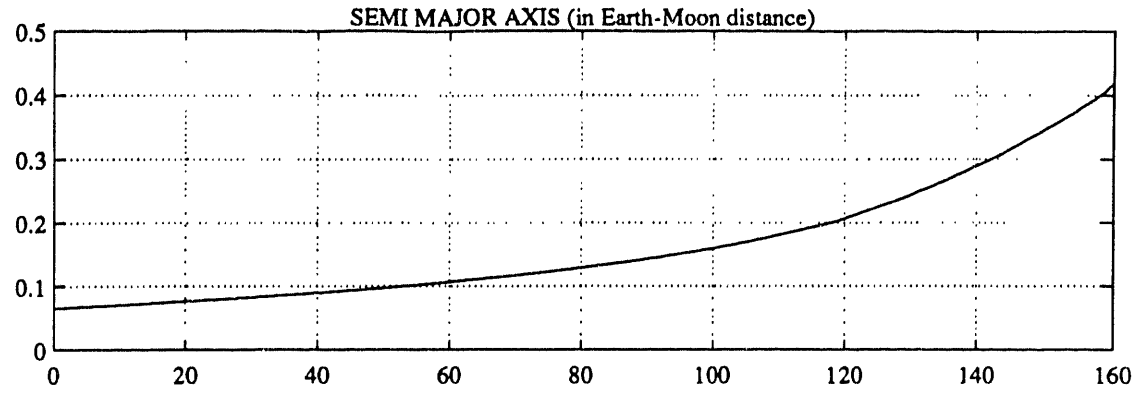
SEMI MAJOR AXIS (in Earth-Moon distance)
0.5
0.4
0.3
0.2
0.1
0
0
20
40
60
80
100
120
140
160

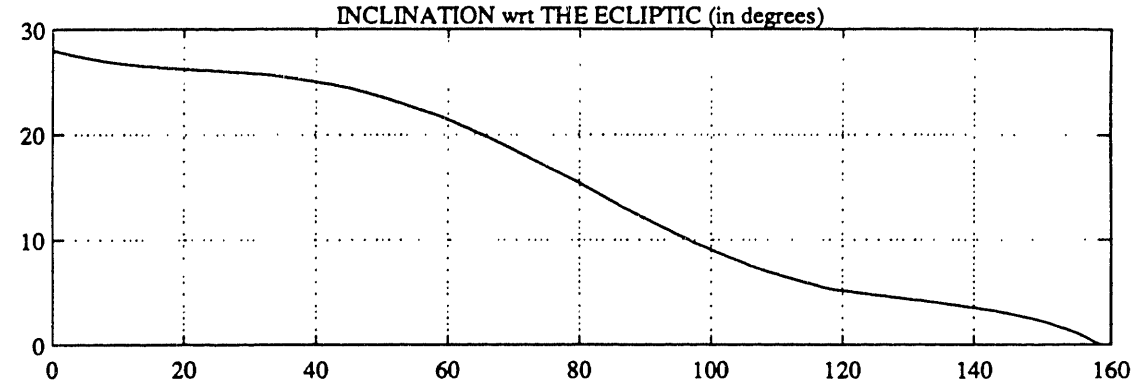
INCLINATION wrt THE ECLIPTIC (in degrees)
30
20
10
0
0
20
40
60
80
100
120
140
160

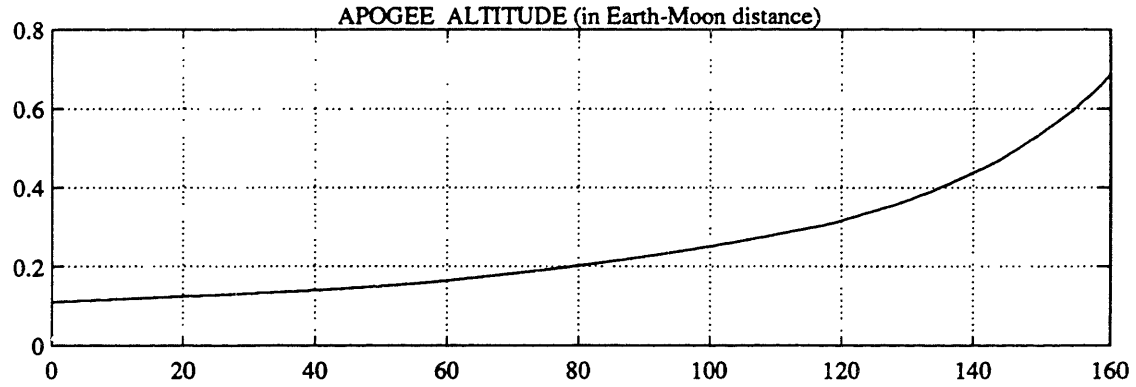
APOGEE ALTITUDE (in Earth-Moon distance)
0.8
0.6
0.4
0.2
0
0
20
40
60
80
100
120
140
160

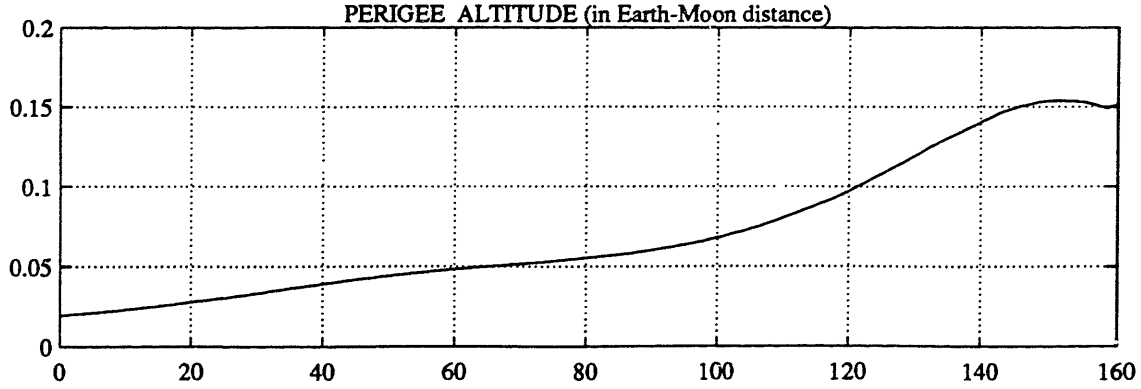
PERIGEE ALTITUDE (in Earth-Moon distance)
0.2
0.15
0.1
0.05
0
0
20
40
60
80
100
120
140
160

Projections of the initial, intermediate and final trajectories on the ecliptic

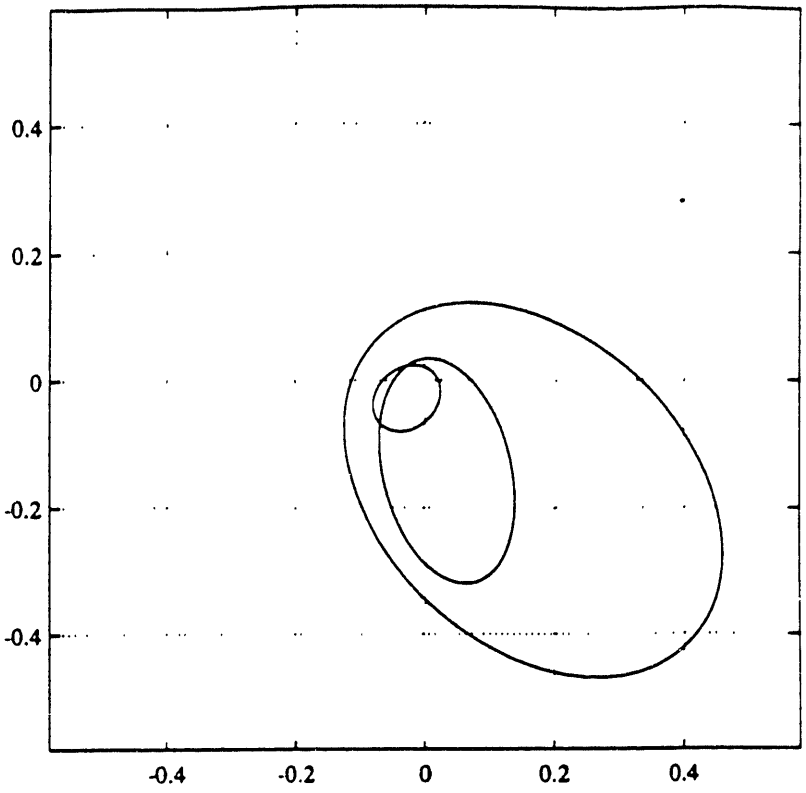

ORBITAL ELEMENTS

	INITIAL VALUES	FINAL VALUES
Semi major axis	0.065	0.3401
Excentricity	0.7	0.7099

The following elements are referenced to the Ecliptic:

Inclination	28	0.04233
Ascending node	135	56.95
Argument of perigee	-90	77.1

Inclination control if: $a > 0.1$ and theta < 18 degrees

where theta is the sail's angular position with respect to the nearest node.

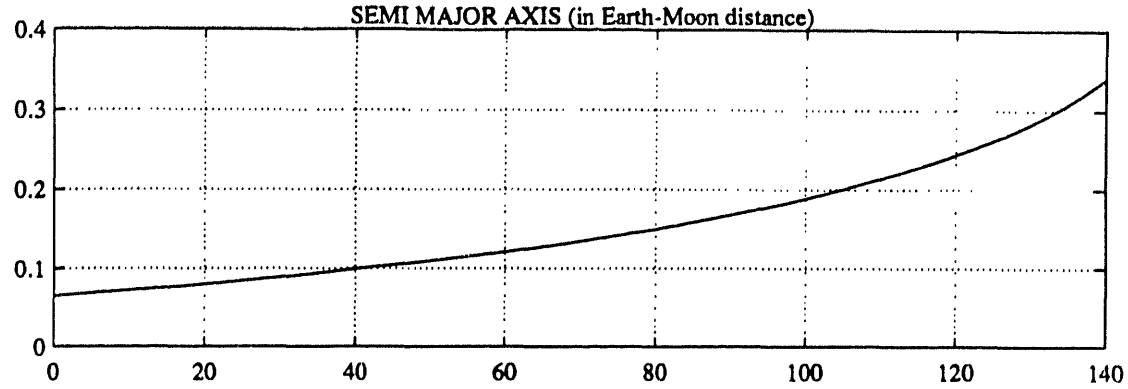
SEMI MAJOR AXIS (in Earth-Moon distance)
0.4
0.3
0.2
0.1
0
0
20
40
60
80
100
120
140

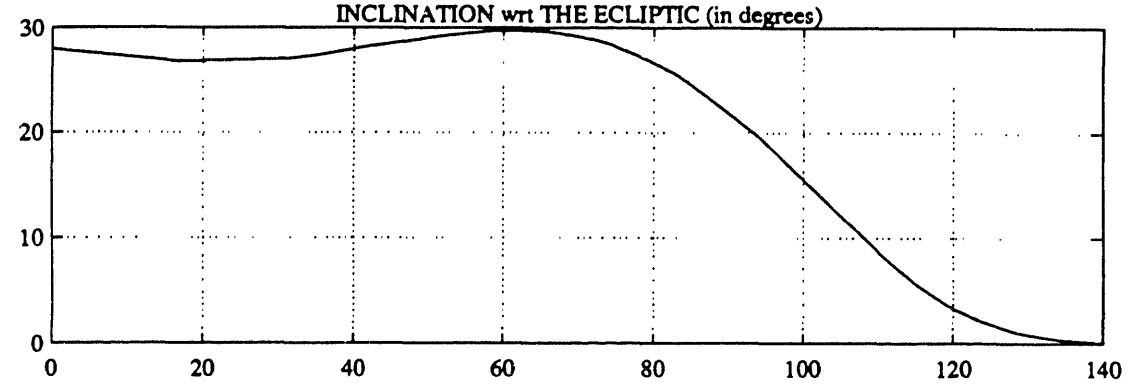
INCLINATION wrt THE ECLIPTIC (in degrees)
30
20
10
0
0
20
40
60
80
100
120
140

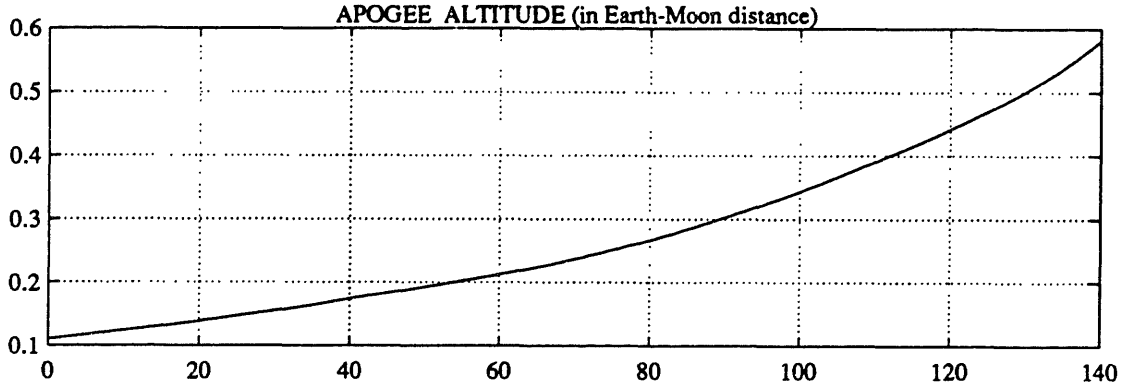
APOGEE ALTITUDE (in Earth-Moon distance)
0.6
0.5
0.4
0.3
0.2
0.1
0
20
40
60
80
100
120
140

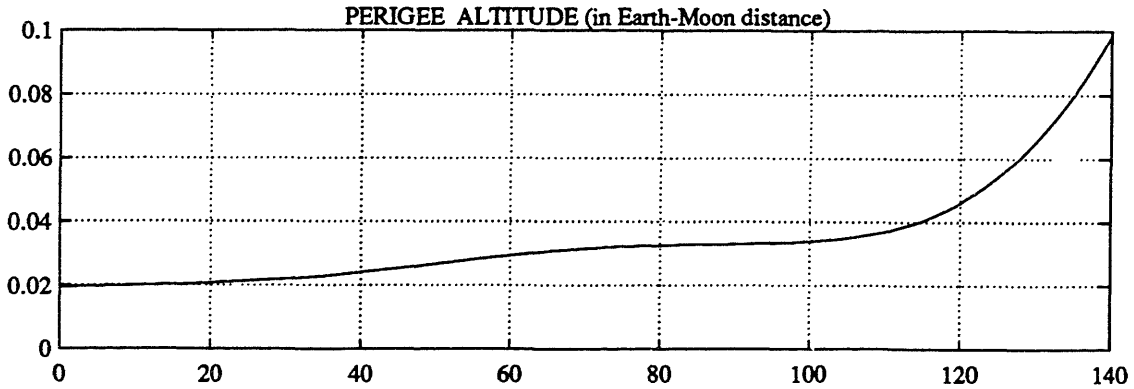
PERIGEE ALTITUDE (in Earth-Moon distance)
0.1
0.08
0.06
0.04
0.02
0
0
20
40
60
80
100
120
140

APPENDIX C

SIMULATIONS OF THE INTERCEPT PHASE

In this appendix, the second part of the trajectory is presented. An initial high orbit is chosen (a=0.7, e=0.7 for the semi major axis and the eccentricity). The initial point of this arc of trajectory is at apogee, and the Sun initial position is always chosen to be towards the negative y-axis of the trajectory plots thus making an initial angle of -90 degrees with the apsidal line.

Three cases are presented, each case is associated with a different initial position of the Moon with respect to the apsidal line of the sail's initial orbit. For each case a table gives the characteristics of the intercept trajectory.

Initial position of the Moon.	0 deg. wrt the apsidal line.		
Desired final position.	15,600 km behind the Moon.		
Optimized value of the final time.	27.69 days		
Distance from goal at tf.	0.015 km		
Optimized value of the costate at t_0.	0.918	-3.97	23.01

Table 9: Characteristics of the intercept trajectory (Moon(t_0)=0 deg.)

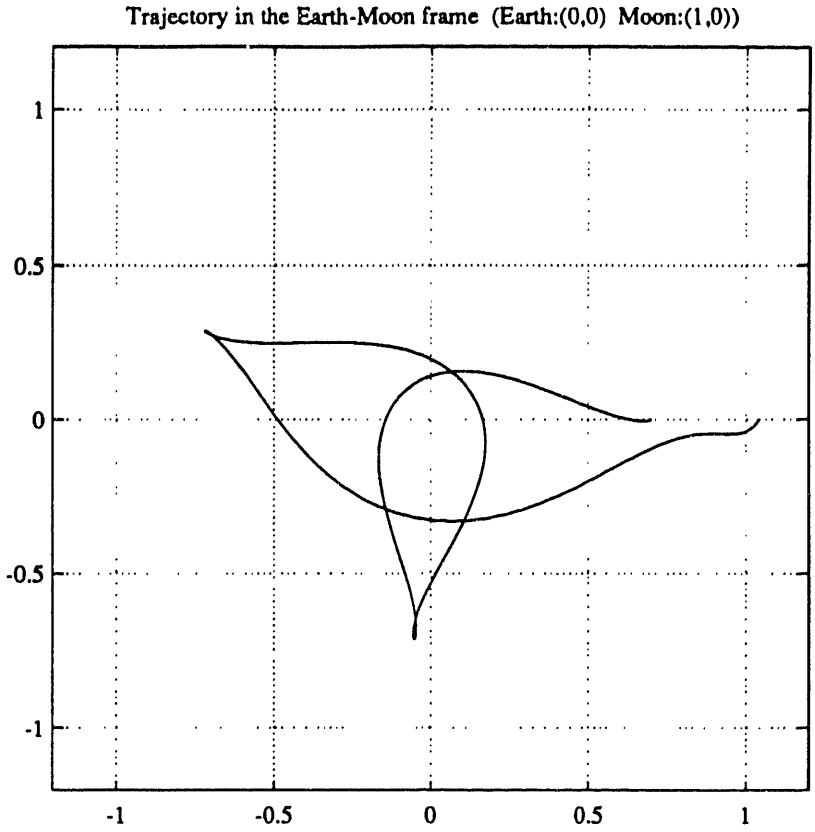
Trajectory in the Earth-Moon frame (Earth:(0,0) Moon:(1,0))
1
0.5
0
-0.5
-1
-1
-0.5
0
0.5
1

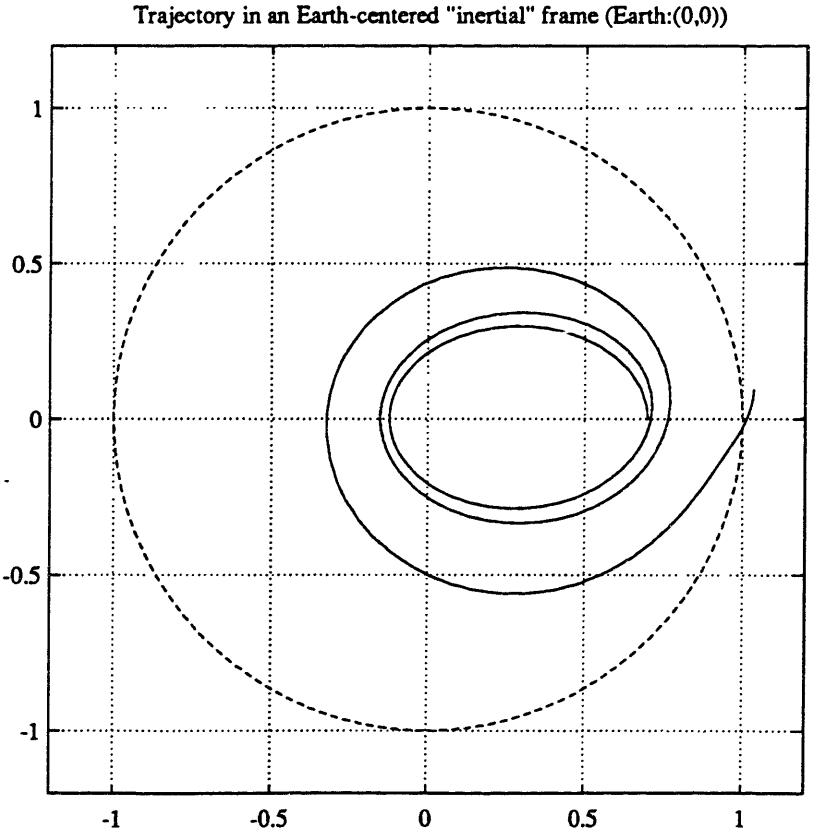
Trajectory in an Earth-centered "inertial" frame (Earth:(0,0))
1
0.5
0
-0.5
-1
-1
-0.5
0
0.5
1

Initial position of the Moon.	180 deg. wrt the apsidal line.		
Desired final position.	15,600 km behind the Moon.		
Optimized value of the final time.	27.33 days		
Distance from goal at tf.	0.04 km		
Optimized value of the costate at t_0.	-1.01	-1.03	1.771

Table 10: Characteristics of the intercept trajectory (Moon(t_0)=+90 deg.)

Trajectory in the Earth-Moon frame (Earth:(0,0) Moon:(1,0))

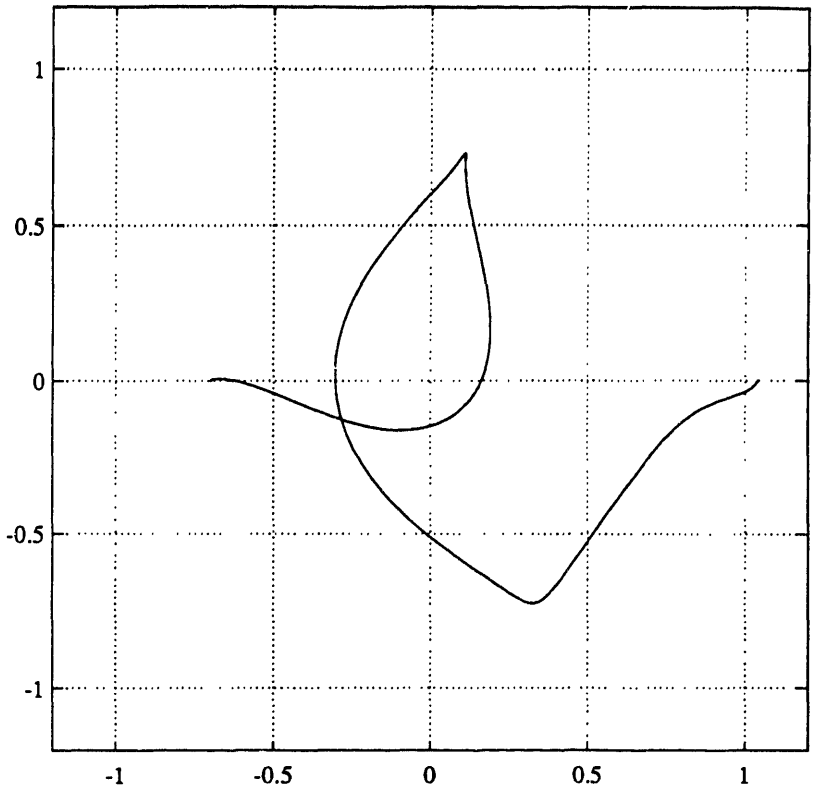

Trajectory in an Earth-centered "inertial" frame (Earth:(0,0))

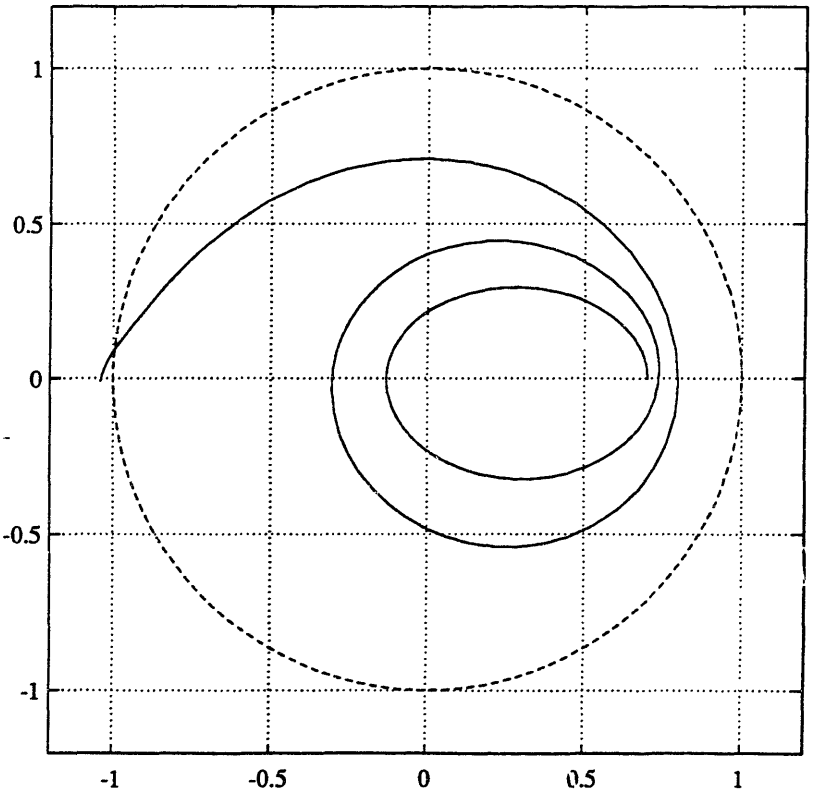

Initial position of the Moon.	270 deg. wrt the apsidal line.		
Desired final position.	15,600 km behind the Moon.		
Optimized value of the final time.	29.7 days		
Distance from goal at tf.	0.014 km		
Optimized value of the costate at t_0.	0.132	0.045	4.85

Table 12: Characteristics of the intercept trajectory (Moon(t_0)=270deg.)

Trajectory in the Earth-Moon frame (Earth:(0,0) Moon:(1,0))

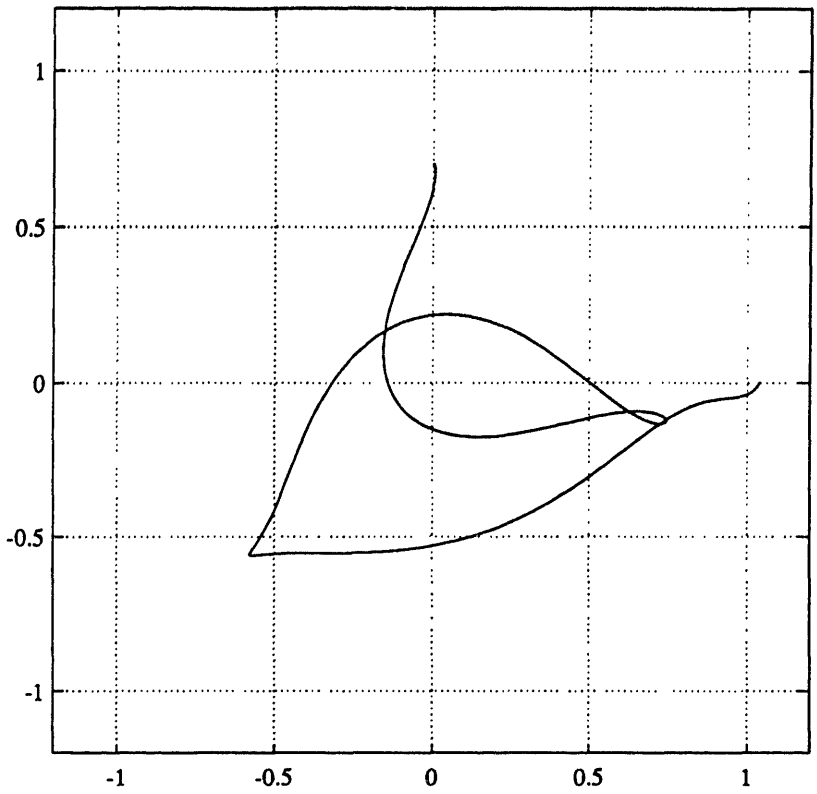

Trajectory in an Earth-centered "inertial" frame (Earth:(0,0))

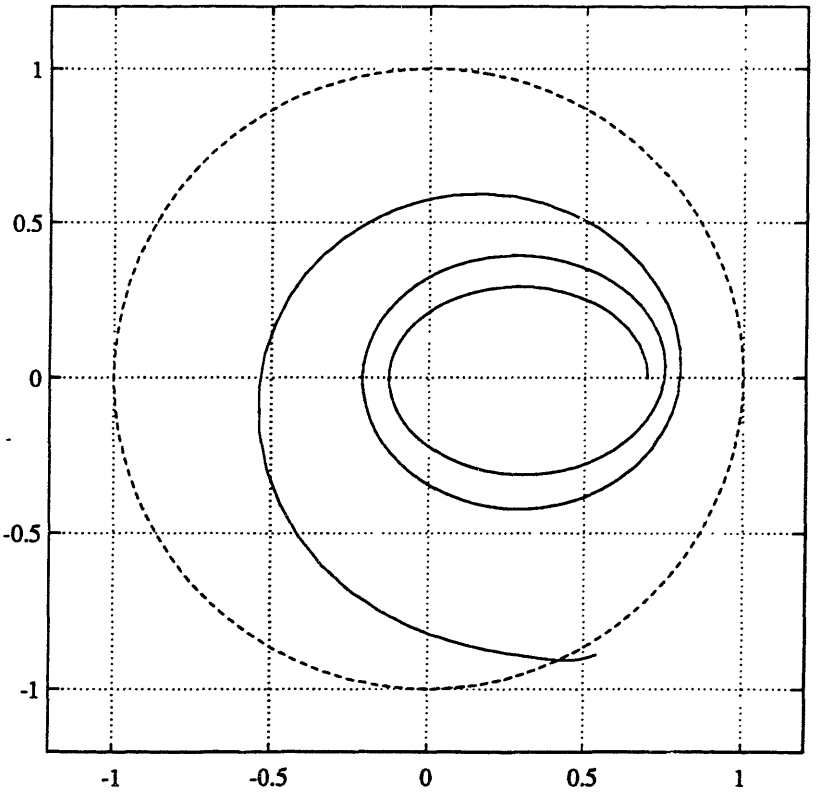

APPENDIX D

PRECESSION RATE CONSTRAINT

This appendix presents a first approach to the problem raised by the impossibility of rotating the thrust vector arbitrarily fast. Various heliogyro designs were studied by Blomquist in reference [8] and show that the precession rate is bounded and must usually remain smaller than 500 degrees per day.

To investigate the importance of this constraint, we will only consider the planar case in which the sail, the Earth and the Sun are in the same plane and for which it is intended to increase the semi major axis. In that case, the "optimal" sail orientation is defined by maximizing the component of the thrust along the velocity vector. The limitation on the thrust vector precession rate prevents from following the "optimal" sail orientation scheme in two particular situations.

The first of these situations happens when the velocity vector is changing direction so fast that the thrust vector cannot follow it. This occurs when the orbit is low and especially in the vicinity of the perigee. The lower the perigee altitude, the larger the arc along which the "optimal" orientation law cannot be applied. Hence, the maximum

precession rate required by the "optimal" orientation law, as well as the length of the arc on which this law cannot be applied are decreasing functions of the semi major axis and increasing functions of the eccentricity.

The other situation where boundedness of the precession rate prevents the application of the "optimal" orientation law is defined as follows. In the planar case, once per orbit, the velocity vector points towards the Sun and obliges the thrust vector to achieve an instantaneous 180 degree flip in order to keep on maximizing the thrust component along the velocity vector. If one does not use both sides of the sail this requires that the precession rate be infinite. This happens regardless of the values of the eccentricity and of the semi major axis. It should be noted that for the three dimensional problem, there will still be an instantaneous flip required by the "optimal" orientation law. It will take place when the component of the velocity vector that lies in the ecliptic points towards the Sun, but due to the orbit inclination with respect to the ecliptic, the flip will require an instantaneous change of less than 180 degrees.

These considerations are going to define requirements for the initial orbit of the solar sail. In order to achieve the 180 degree flip without losing too much performance on the semi major axis increase, it is desirable to have the flip taking place in the vicinity of the apogee. Indeed, the time required to perform the flip is only specified by the maximum precession rate available (e.g. 500 degree/day enables a 180

degree flip in 8.6 hours). Hence, it is best to schedule the flip where the rate of change of the semi major axis is minimum, which happens to be at apogee. The best orientation of the initial orbit would be such that during the first days of the trajectory the velocity vector at apogee would be pointing towards the Sun.

The maximum precession rate available is also going to define a lower bound on the initial perigee altitude in order to decrease as much as possible the length of the orbital arc around the perigee where the precession rate required by the "optimal" orientation law cannot be achieved.

Table 13 summarizes the approximate required rates. We can see that a sail capable of a thrust vector precession rate of 500 degrees per day will be severely handicapped in the highly elliptical GTO and not at all constrained with an initial GEO.

Three kinds of precession rates are given for three different orbits. The rate at perigee is an approximation of the maximum rate required when the sail passes at perigee. It is given as half of the angular rate of the sail on its orbit (rate at perigee= $\frac{1}{2}\dot{\theta} = \frac{1}{2}\frac{\sqrt{\mu\, a\,(1-e^2)}}{a^2\,(1-e)^2}$).

On the other hand, the rates presented for the flip at apogee are calculated by dividing 180 degrees by the time required to fly a 40 or 60 degree arc of orbit centered on the apogee.

Orbit	GTO: a=0.065 and e=0.7	GEO: a=0.11 and e=0	e=0.7 and a=0.13
Rate at perigee	3140 deg/day	180 deg/day	1100 deg/day
Flip at apogee (40 degrees)	707 deg/day	1620 deg/day	250 deg/day
Flip at apogee (60 degrees)	309 deg/day	1080 deg/day	110 deg/day

Table 13 : Required precession rates for GTO, GEO and higher orbits.

The following plots show the time histories of several parameter for the third orbit (a=0.13 and e=0.7), one can notice both the peek of the precession rate and the flip of the cone angle.

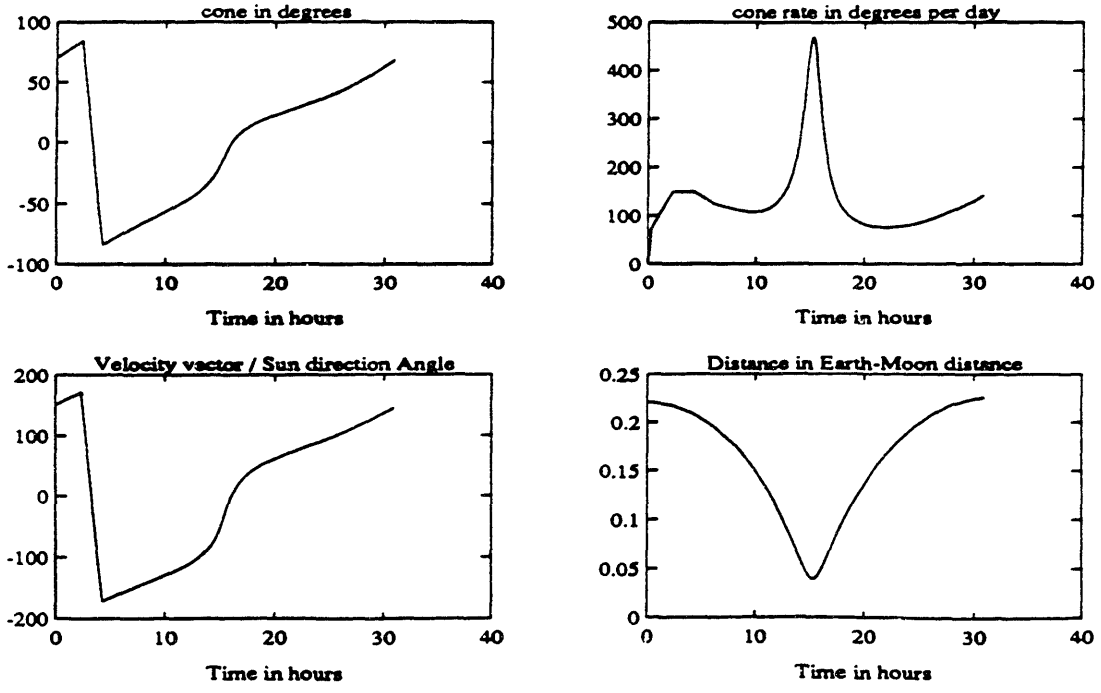

REFERENCES.

Chapter I.

1. Tsander, K., "From A Scientific Heritage", NASA TTF-541, 1967 (quoting a 1924 report by the author).

2. Tsiolkovsky, K, E., "Extension Of Man Into Outer Space", 1921. (cf. also, Tsiolkovsky, K. E., Symposium Jet Propulsion, No 2, United Scientific and Technical Presses (NTI), 1936 [in Russian]).

3. Wright, J. and Warmke, J., "Solar Sailing Mission Applications", AIAA/AAS Astrodynamics Conference, August 1976, Paper No 76-808.

4. Friedman, L., Starsailing: Solar Sails And Interstellar Travel, John Wiley & Sons, Inc., New York, 1988.

5. Friedman, L., "Solar Sailing - The Concept Made Realistic", Jet Propulsion Laboratory California Institute of Technology Pasadena, California.
MacNeal, R., Schwendler Corp., Los Angeles, California.

6. Foundation News, "Solar Sailing For The Quincentenary", Winter 1989 issue, World Space Foundation, P.O. Box Y, South Pasadena, California 91031 USA.

7. Euroavia Presentation of ISY'92, Munich Germany, "The Earth-Moon Race Between Solar Sails", Presentation by G. Pignolet, January 25, 1991.

8. Blomquist, R. S., Design Study Of A Solid-State Heliogyro Solar Sail, CSDL report T-1064,1990.

9. Sackett, L. L., Optimal Solar Sail Planetocentric Trajectories, CSDL report R-1113, September 1977.

10. McInnes, C., "On The Crest Of A Sunbeam", New Scientist 5 January 1991.

11. McInnes, C., "Exotic Solar Sail Trajectories", Dept. Of Physics and Astronomy, University of Glasgow, Glasgow G12 8QQ, Scotland , June 1990.

12. McInnes, C. and Simmons, J. F. L., "Halo Orbits For Solar Sails - Dynamics And Applications", 19 June 1989

13. McInnes, C. and Simmons, J. F. L., "Solar Sail Halo Orbits I: - Heliocentric Case", University of Glasgow G12 8QQ, Scotland, to be published in Journal of Spacecraft and Rockets.

14. McInnes, C. and Simmons, J. F. L., "Solar Sail Halo Orbits II: - Geocentric Case", University of Glasgow G12 8QQ, Scotland, to be published in Journal of Spacecraft and Rockets.

15. MacNeal, R. H., "Structural Dynamics Of The Heliogyro", NASA-CR-1754A, 1971.

16. Breakwell, J. V and Rauch, H. E., "Asymptotic Matching In Power-Limited Interplanetary Transfers", Space Flight Mechanics Specialist Symposium, AAS Science and Technology Series, Vol 11, 1967.

17. Golan, O. M. and Breakwell, J. V., "Minimum Fuel Trajectories For A Low-Thrust Power-Limited Mission To The Moon And To Lagrange Points L4 And L5", AAS/AIAA Astrodynamics Specialist Conference, Stowe, Vermont, August 1989, Paper No 89-351.

18. Golan, O. M. and Breakwell, J. V. , "Minimum Fuel Lunar Trajectories For A Low-Thrust Power-Limited Spacecraft", Astrodynamics Specialist Conference, Portland, Oregon, August 20-22 1990, Paper No 90-2975.

Chapter II.

19. Fimple, W. R., "Generalized Three-Dimensional Trajectory Analysis Of Planetary Escape By Solar Sail", ARS Journal, Volume 32, June 1962, pp. 883-887.

20. Sands, N.,"Escape From Planetary Gravitational Fields By Use Of Solar Sails", ARS Journal, Volume 31, April 1961, pp. 527-531.

21. Uphoff, C., "Escape From Elliptic Orbits By Solar Sail", Jet Propulsion Laboratory Interoffice Memorandum, March 23, 1977.

22. Cavoti, C. R., "Numerical Solutions On The Astronautical Problem Of Thrust Vector Control For Optimum Solar Sail Transfer", Paper No 2627-62, General Electric Company, Valley Forge, Penn, November 13-18 1962.

23. Zhukov, A. N. and Lebedev, V. N., "Variational Problem Of Transfer Between Heliocentric Orbits By Means Of A Solar Sail", Cosmic Research, Volume 2 , 1964, pp. 41-44.

24. Sauer, C. G., "Optimum Solar Sail Interplanetary Trajectories", AIAA/AAS Astrodynamics Conference, San Diego, California, August, 1976, Paper No 76-792.

25. Sackett, L. L. and Edelbaum, T. M.,"Optimal Solar Sail Spiral To Escape", AAS/AIAA Astrodynamics Conference, September 1977.

26. Cefola, P. J., "Equinoctial Orbit Elements - Application To Artificial Satellite Orbits", AIAA Paper No 72-937, AIAA/AAS Astrodynamics Conference, Palo Alto, California, September 11-12 1972.

27. Uphoff, C., "Numerical Averaging In Orbit Prediction", AIAA Journal , Vol. 11, No 11, pp. 1512-1516, 1972.

28. Velez, C. E. and Fuchs A. J., "A Review Of Averaging Techniques And Their Application To Orbit Determination Systems", AIAA 12th Aerospace Sciences Meeting, Washington, D.C., January 30 -February 1, 1974, Paper No 74-171.

29. Press, W. H., Numerical Recipes In C: the art of scientific computing, New York: Cambridge University Press, 1988.

Chapter III

30. Miller, J. S., Trajectory and Guidance Theory For A Low-Thrust Lunar Reconnaissance Vehicle, Report T-292, MIT Instrumentation Laboratory, Cambridge, Mass., 1961.

31. Battin, R. H., Astronautical Guidance, McGraw-Hill, New-York, 1964.

Chapter IV

32. Bryson, A. E. and Ho, Y., Applied Optimal Control, pp. 71-86, Hemisphere Publishing Corporation, 1975.

33. Lawden, D. F., Optimal Trajectories For Space Navigation, pp. 54-60, London Butterworths, 1963.

Chapter V

34. Flament, D., Optimisation De Trajectoire Terre-Lune Pour Une Voile Solaire, Thèse de Docteur Ingénieur, I.D.N., January 31, 1986.

35. Bertsekas, D., Lecture Notes On Non-Linear Programming For MIT Course 6.252 , to be published.

36. Kernighan, B.W. and Ritchie D. M., The C Programming Language, Second Edition, Prentice Hall, Englewood Cliffs, New Jersey 07632, 1988.

37. Jayraman, T. S., "Time-Optimal Transfer Trajectory For Solar Sail Spacecraft", Journal Of Guidance And Control, Vol.3 No 6, pp. 536-542, Nov-Dec 1980.